SYNTHESIS AND PROPERTIES OF NOVEL TYPES OF GLYCOPOLYMERS

KOHJI OHNO

1998

SYNTHESIS AND PROPERTIES OF NOVEL TYPES OF GLYCOPOLYMERS

KOHJI OHNO

1998

Contents

General Introduction

1. Biological Importance of Glycopolymers

It is recognized today that carbohydrates represent the third important class of informational biomolecules after proteins and nucleic acids.[1] They play roles as informational biomolecules in plants, animals, and micro-organisms. The term "glycobiology" has been coined to cope with the rapidly rising interest in carbohydrate science,[2–4] and it primarily deals with studies on carbohydrate–protein interactions. To understand the mechanisms of these interactions, one has to use structurally homogeneous carbohydrate ligands.[1b] It is, however, very difficult to obtain ligands with desired structures from natural sources because of their structural complexity and heterogeneity. A powerful alternative is to prepare synthetic glycoconjugates which contain carbohydrate residues representing the essential structural features involved in the binding of ligands by proteins.[5–7] A newer term "neoglycoconjugates" is now widely accepted to designate seminatural and nonnatural carbohydrate-containing substances.[8,9] There are a lot of virtues in neoglycoconjugates:[10] (1) they contain carbohydrate groups of known structure and assured purity; (2) they can be prepared in a larger quantity than the corresponding isolated natural materials; and (3) they provide multivalency which may enhance the binding of the target carbohydrates. Many subtle differentiations of carbohydrate recognition can be magnified by using polyvalent carbohydrate ligands, which frequently perform better than naturally available substances.

A glycopolymer, or a polymer consisting of a chemically and biologically stable backbone and a hydrophilic mono- or oligosaccharide in the side chains, is one of neoglycoconjugates.[11,12] Ever since glycopolymers were first developed by Horejsi et al,[13] they have attracted increasing interest because of their advantageous physicochemical and structural properties. As mentioned above, the density of carbohydrate moieties in a glycoconjugate strongly affects the specific interaction between saccharide residues and its receptors. Particularly, the phenomenon that the binding affinity is drastically enhanced by multivalent carbohydrate ligands is called a "glycoside cluster effect".[10c–f] Therefore, the molecular design of glycopolymers for an increased spatial density of carbohydrate moieties is very important, and ligands with a high density of carbohydrate residues, which can be obtained by well-designed polymerizations of polymerizable glycosides, are extremely interesting materials not only as biomimetic models of glycoconjugates but also for therapeutic or diagnostic purposes

in biomedical fields.

2. Backgrounds and Purposes of This Thesis

In view of the importance of glycopolymers, it is of great significance to develop the science and technology of glycopolymers into higher possible achievements. Along this line is the goal of this thesis. The author would like to contribute to this rapidly growing area specifically from the two main aspects described below:

2-1. Preparation of Novel Glycolipids and Investigation of the Biological Functions of the Carbohydrates Anchored on the Surfaces of Model Lipid Membranes

There are a number of interactions between various (macro)molecules mediated by carbohydrates in living bodies. Most of those interactions occur at specific fields of interfaces between, e.g., two lipid layers or a lipid layer and a liquid phase.[14] It is well known that various cell surfaces are decorated with complex carbohydrate molecules such as oligosaccharide and glycoconjugates.[15] For example, as shown in Figure 1, the outer membrane of Gram-negative

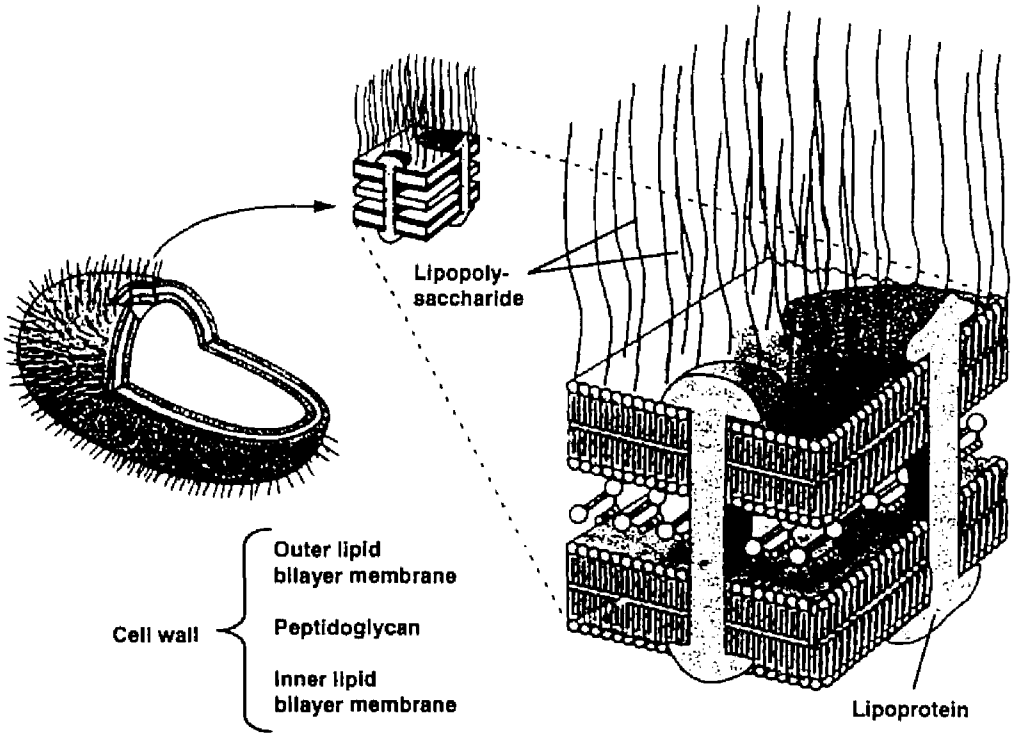

Figure 1. The structure of the cell wall and membrane in Gram-negative bacteria: Lipopolysaccharides coat the outer membrane of Gram-negative bacteria where their lipid portion is embedded and is linked to a complex polysaccharide.[16]

bacteria is coated with a highly complex lipopolysaccharide, which consists of a lipid group (anchored in the outer membrane) connected to a long polysaccharide chain of many different and characteristic repeating units. The repeating units determine the antigenicity of the bacteria; that is, the animal immune system recognizes those carbohydrate molecules as foreign substances and produces antibodies against them.[17]

Despite that the actual carbohydrates in living bodies play important roles at cell surfaces, model experiments on the interactions between glycopolymers and proteins, e.g., lectins or enzymes, have been carried out mostly in a *bulk* solution (without interfaces). In Part I of this thesis, the author pays a special attention to the biological functions of the glycopolymers and/or oligomers anchored on *lipid membrane surfaces*. Thus, subjects of this Part include the preparation of novel glycolipids with sugar-carrying polymer (or oligomer) chains as hydrophilic groups (like the lipopolysaccharide of Gram-negative bacteria), and the investigation of functions of the carbohydrate chains on the surfaces of liposomes as cell models made of the artificial glycolipids and phospholipids.

2-2. Precision Synthesis of New Types of Glycopolymers by Controlled/"Living" Radical Polymerization

During the course of the above-mentioned study, the author recognized the importance of developing model polymers or systems with well-controlled, well-defined structures. Introduction of new and well-defined model polymers or systems that had never been prepared and studied before was believed to develop the science and technology of glycopolymers into a newer stage.

In the past, several types of glycopolymers were synthesized by conventional free radical polymerizations of vinyl monomers with pendent saccharide residues.[11] Advantages of the free radical method over other polymerization techniques may be that it is applicable to a large variety of monomers and that it is basically free from cumbersome procedures, including the perfect removal of water and other impurities and the protection of reactive pendent groups. Moreover, free radical polymerization can be run even in an aqueous medium. Therefore, the radical polymerization technique has been used in most cases for the synthesis of glycopolymers. On the contrary, a clear disadvantage of the conventional radical polymerization is the poor control of macromolecular structures: for example, it is difficult to precisely control, e.g., degree of polymerization, polydispersity, end functionality, and chain architecture, because of unavoidable termination between growing radicals. For this reason, the

synthesis of well-defined, low-polydispersity glycopolymers has been achieved only via elaborate and rather demanding processes based on cationic polymerization,[18] ring-opening methathesis polymerization,[19] and ring-opening polymerization of *N*-carboxylic acid anhydrides.[20] The development of polymerization techniques which provide well-defined glycopolymers by simpler and more robust procedures has been waited for.

Under these circumstances, the author was interested in controlled/"living" free radical polymerization, which has been rapidly developing in recent years.[21] This method retains the advantages of the conventional free radical method, i.e., the simplicity, versatility, and roubustness, and yet allows fine control of polymerization and polymer structure owing to the living mechanism.[22] In Part II of this thesis, the author has applied the controlled/"living" free radial polymerization to the synthesis of new glycopolymers.

3. Outline of This Thesis

As mentioned above, this thesis consists of two parts; Part I (Chapters 1–3) describes the properties of novel sugar-carrying amphiphiles prepared with a lipophilic azo-type radical initiator (Figure 2), and Part II (Chapters 4–7) deals with the synthesis of well-defined glycopolymers by controlled/"living" free radical polymerizations.

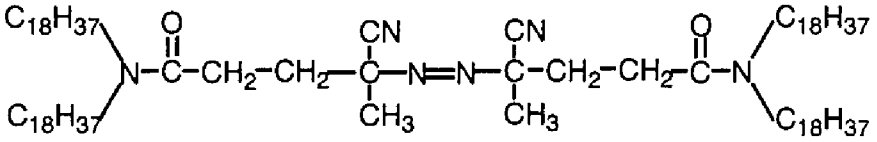

Figure 2. Chemical structure of a lipophilic radical initiator, DODA-501.

In **Chapter 1**, a glucose-carrying monomer, 2-(methacryloyloxy)ethyl-α-*D*-glucopyranoside (MEGlc, Figure 3a), is polymerized with a lipophilic radical initiator (DODA-501, Figure 2) to obtain a novel glycolipid with a glucose-carrying polymer moiety as a hydrophilic group. As a model system of the specific binding of cells to the surfaces with high affinities, the interaction of sugar residues of the amphiphile with a lectin at liquid–lipid and solid–lipid interfaces is investigated mainly by the multiple internal reflection fluorescence (MIRF) method.

In **Chapter 2**, a galactose-carrying monomer, 2-(methacryloyloxy)ethyl-β-*D*-

galactopyranoside (MEGal, Figure 3b), is polymerized in a similar way to prepare a lipid that carries many galactose residues. Furthermore, a liposome decorated with many galactose residues is prepared by mixing of the galactose-carrying amphiphile and a phospholipid. Association processes between the galactose-carrying liposomes and amino group-carrying liposomes are investigated, as a model system of cell–cell interactions.

In **Chapter 3**, the interaction of the galactose-carrying liposome described in Chapter 2 with a enzyme is kinetically investigated, for a basic understanding of the catalytic behavior of enzyme to a carbohydrate chain as a substrate on the membrane surface.

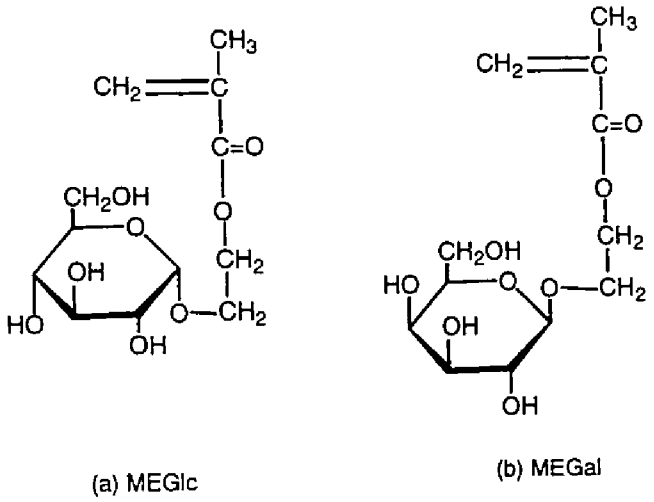

Figure 3. Chemical structures of (a) MEGlc and (b) MEGal.

In **Chapter 4**, sugar-carrying styrenic monomers, *N*-(*p*-vinylbenzyl)-[*O*-*β*-D-galactopyranosyl-(1→4)]-D-gluconamide (VLA, Figure 4a) and its acetylated derivative (Ac-VLA, Figure 4b), are polymerized by the nitroxide-mediated free radical polymerization technique. The careful and unique design of experimental conditions for obtaining well-defined polymers is described on the basis of a kinetics study on the polymerization.

In **Chapter 5**, the nitroxide-mediated free radical polymerization will be applied to precisely polymerize a sugar-carrying acrylate, 3-*O*-acryloyl-1,2:5,6-di-*O*-isoprpylidene-D-glucofuranose (AIpGlc, Figure 4c). The synthesis of low-polydispersity homopolymers with pendent sugar residues as well as of well-defined amphiphilic diblock copolymers with the glycopolymer segments is described.

In **Chapter 6**, controlled free radical polymerization of a sugar-carrying methacrylate monomer, 3-*O*-methacryloyl-1,2:5,6-di-*O*-isoprpylidene-D-glucofuranose (MAIpGlc, Figure 4d), is carried out by the atom transfer radical polymerization (ATRP) technique with an alkyl halide/copper-complex system. By the same method, an amphiphilic diblock copolymer is also synthesized by sequential addition of the two monomers (styrene and MAIpGlc) and the subsequent acidolysis of the PMAIpGlc segment.

In **Chapter 7**, by making full use of the advantage of the nitroxide-mediated polymerization, capable of effectively introducing functional groups to polymer chain ends, a synthetic route is explored to a novel artificial glycolipid with a well-defined glycopolymer as the hydrophilic group.

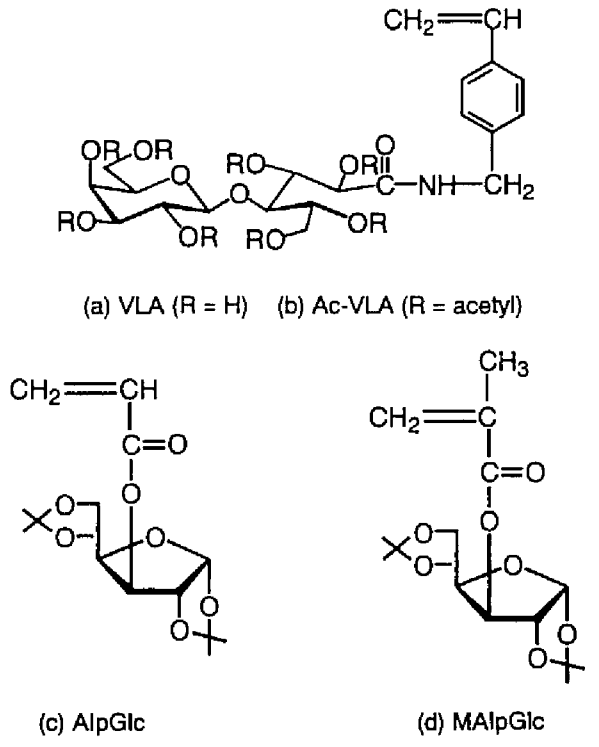

Figure 4. Chemical structures of (a) VLA, (b) Ac-VLA, (c) AIpGlc, and (d) MAIpGlc.

References

(1) (a) Fukuda, M., Hindsgaul, O., Eds. *Molecular Glycobiology*; Oxford University Press: New York, 1994. (b) Lennarz, W. L., Hart, G. W., Eds. *Methods in Enzymology*; Academic Press: San Diego, CA, 1994; Vol. 230.

(2) (a) Sharon, N.; Lis, H. *Science* **1989**, *246*, 227. (b) Springer, T. A. *Nature* **1990**, *346*, 425. (c) Lasky, L. A. *Science* **1992**, *258*, 964. (d) Mizuochi, T.; Matthews, T. J.; Kato, M.; Hamako, J.; Titani, K.; Solomon, J.; Feizi, T. *J. Biol. Chem.* **1990**, *265*, 8519.

(3) (a) Phillips, M. L.; Nudelman, E.; Gaeta, F. C. A. *Science* **1990**, *250*, 1130. (b) Berg, E. L.; Robinson, M. K.; Mansson, O. *J. Biol. Chem.* **1991**, *266*, 14869. (c) Majuri, M. L.; Mattila, P.; Renkonen, R. *Biochem. Biophys. Res. Commun.* **1992**, *182*, 1376.

(4) (a) Wasley, L. C.; Timony, G.; Murtha, P.; Stoudemire, J.; Dorner, A. J.; Caro, J.; Krieger, M.; Kaufman, B. J. *Blood* **1991**, *77*, 2624. (b) Higuchi, M.; Oh-eda, M.; Kuboniwa, H.; Tomonoh, K.; Shimonaka, Y.; Ochi, N. *J. Biol. Chem.* **1992**, *267*, 7703.

(5) (a) Bichler, J.; Baynes, J. W.; Thorpe, S. R. *Biochem. J.* **1993**, *296*, 771. (b) Needham, L. K.; Schnaar, R. L. *J. Cell Biol.* **1993**, *121*, 397. (c) Roy, R.; Tropper, F. D.; Romanowska, A. *Bioconjugate Chem.* **1992**, *3*, 256. (d) Kallin, E.; Lönn, H.; Norberg, T. *Glycoconjugate J.* **1988**, *5*, 145.

(6) (a) Pohlentz, G.; Schlemm, S.; Egge, H. *Eur. J. Biochem.* **1992**, *203*, 387. (b) Hasegawa, A.; Fushimi, K.; Ishida, H.; Kiso, M. *J. Carbohydr. Chem.* **1993**, *12*, 1203. (c) Roy, R.; Andersson, F. O.; Letellier, M. *Tetrahedron Lett.* **1992**, *33*, 6053. (d) Hanisch, F.-G.; Chai, W.; Rosankiewicz, J. R.; Lawson, A. M.; Stoll, M. S.; Feizi, T. *Eur. J. Biochem.* **1993**, *217*, 645.

(7) (a) Zanta, M.-A.; Boussif, O.; Adib, A.; Behr, J.-P. *Bioconjugate Chem.* **1997**, *8*, 839. (b) Braunmühl, V.; Jonas, G.; Stadler, R. *Macromolecules* **1995**, *28*, 17.

(8) (a) Lee, R. T.; Lee, Y. C. *Biochemistry* **1980**, *19*, 156. (b) Lee, Y. C., Lee R. T., Eds. *Neoglycoconjugates: Preparation and Applications*; Academic Press: San Diego, CA, 1994. (c) Lee, Y. C., Lee, R. T., Eds. *Methods in Enzymology*; Academic Press: San Diego, CA, 1994; Vol. 242. (d) Lee, Y. C., Lee, R. T., Eds. *Methods in Enzymology*; Academic Press: San Diego, CA, 1994; Vol. 247.

(9) (a) Jennings, H. J.; Roy, R.; Gamian, A. U.S. Patent 4727136, 1988. (b) Kudo, M.; Todo, A.; Ikekubo, K.; Hino, M. *Am. J. Gastroenterol.* **1992**, *87*, 865. (c) Gabius, S.; Joshi, S. S.; Gabius, H.-J.; Sharp, J. G. *Anticancer Res.* **1991**, *11*, 793. (d) Schnaar, R. L. U.S.

Patent 5192508, 1993. (e) Ouchi, T.; Kobayashi, H.; Hirai, K.; Ohya, Y. In *Polymeric Delivery Systems, Properties and Applications*; EI-Nokaly, M. A., Piatt, D. M., Charpentier, B. A., Eds.,; American Chemical Society, Washington, DC, 1993; p 382. (f) Wu, G. Y.; Wu, C. H. *J. Biol. Chem.* **1992**, *267*, 12436.

(10) (a) Lee, Y. C.; Stowell, C. P.; Krantz, M. J. *Biochemistry* **1976**, *15*, 3956. (b) Krantz, M. J.; Holtzman, N. A.; Stowell, C. P.; Lee, Y. C. *Biochemistry* **1976**, *15*, 39633. (c) Lee, Y. C.; Townsend, R. R.; Hardy, M. R.; Loenngren, J.; Arnarp, J.; Haraldsson, M.; Loenn, H. *J. Biol. Chem.* **1983**, *258*, 199. (d) Lee, R. T.; Lee, Y. C. *Glycoconjugate J.* **1987**, *4*, 316. (e) Lee, Y. C. *FASEB J.* **1992**, *6*, 3193. (f) Lee, R. T.; Lee, Y. C. In *Neoglycoconjugate: Preparation and Application*; Lee, Y. C., Lee, R. T., Eds.,; Academic Press, San Diego, CA, 1994; p 23.

(11) For recent review, see: (a) Wulff, G.; Schmid, J.; Venhoff, T. *Macromol. Chem. Phys.* **1996**, *197*, 259. (b) Miyata, T.; Nakamae, K. *Trends Polym. Sci.*, **1997**, *5*, 198.

(12) (a) Kallin, E.; Lönn, H.; Norberg, T.; Elofsson, M. *J. Carbohydr. Chem.* **1989**, *8*, 597. (b) Kobayashi, K.; Kobayashi, A.; Tobe, S.; Akaike, T. In *Neoglycoconjugate: Preparation and Application*; Lee, Y. C., Lee, R. T., Eds.,; Academic Press, San Diego, CA, 1994; p 261. (c) Kobayashi, K.; Akaike, T.; Usui, T. In *Methods in Enzymology*; Lee, Y. C., Lee, R. T., Eds.; Academic Press: San Diego, CA, 1994; Vol. 242, p 226. (d) Nishimura, S.-I.; Matsuoka, K.; Furuike, T.; Nishi, N.; Tokura, S.; Nagami, S.; Murayama, S; Kurita, K. *Macromolecules* **1994**, *27*, 157. (e) Roy, R.; Tropper, F. D.; Romanowska, A. *Bioconjugate Chem.* **1992**, *3*, 256. (f) Roy, R.; Andersson, F. O.; Harms, G.; Kelm, S.; Schauer, R. *Angew. Chem., Int. Ed. Engl.* **1992**, *31*, 1478. (g) Spaltenstein, A.; Whitesides, G. M. *J. Am. Chem. Soc.* **1991**, *113*, 686.

(13) (a) Horejsi, V.; Kocourek, J. *Biochim. Biophys. Acta* **1973**, *297*, 346. (b) Horejsi, V.; Smolek, P.; Kocourek, J. *Biochim. Biophys. Acta* **1973**, *297*, 346.

(14) (a) Fukuda, M. In *Molecular Glycobiology*; Fukuda, M., Hindsgaul, O., Eds.; Oxford University Press: New York, 1994; p 1. (b) Lowe, J. B. In *Molecular Glycobiology*; Fukuda, M., Hindsgaul, O., Eds.; Oxford University Press: New York, 1994; p 163.

(15) (a) Hakomori, S. *Ann. Rev. Biochem.* **1981**, *50*, 733. (b) Hakomori, S. *Ann. Rev. Immuno.* **1984**, *2*, 103.

(16) Garrett, R. H.; Grisham, C. *Biochemistry*; Saunders College Publishing, Fort Worth, 1995.

(17) Voet, D.; Voet J. G. *Biochemistry*; John Wiley & Sons, New York, 1995; Second Ed., Chap. 10, p 268.

(18) (a) Yamada, K.; Yamaoka, K.; Minoda, M.; Miyamoto, T. *J. Polym. Sci., Part A: Polym. Chem.* **1997**, *35*, 255. (b) Yamada, K.; Minoda, M.; Miyamoto, T. *J. Polym. Sci., Part A: Polym. Chem.* **1997**, *35*, 751.

(19) Fraser, C.; Grubbs, R. H. *Macromolecules* **1995**, *28*, 7248.

(20) (a) Aoi, K.; Suzuki, H.; Okada, M. *Macromolecules* **1992**, *25*, 7073. (b) Aoi, K.; Tsutsumiuchi, K.; Okada, M. *Macromolecules* **1994**, *27*, 875.

(21) For recent reviews, see: (a) Moad, G.; Rizzardo, E.; Solomon, D. H. In *Comprehensive Polymer Science*; Eastmond, G. C., Ledwith, A., Russo, S., Sigwalt, P., Eds.: Pergamon: London, 1989; Vol. 3, p 141. (b) Georges, M. K.; Veregin, R. P. N.; Kazmaier, P. M.; Hamer, G. K. *Trends Polym. Sci.* **1994**, *2*, 66. (c) Matyjaszewski, K.; Gaynor, S.; Greszta, D.; Mardare, D.; Shigemoto, T. *J. Phys. Org. Chem.* **1995**, *8*, 306. (d) Moad, G.; Solomon, D. H. *The Chemistry of Free Radical Polymerization*; Pergamon: Oxford, U. K., 1995; p 335 (e) Davis, T. P.; Haddleton, D. M. In *New Methods of Polymer Synthesis*; Ebdon, J. R., Eastmond, G. C., Eds.; Blackie: Glasgow, U. K., 1995; Vol. 2, p 1. (f) Hawker, C. J. *Trends Polym. Sci.* **1996**, *4*, 183. (g) Sawamoto, M.; Kamigaito, M. In *Polymer Synthesis*; Materials Science and Technology Series; VCH: Deerfield Beach, FL (in press). (h) Matyjaszewski, K., Ed. Controlled Radical Polymerization; ACS Symposium Series No. 685; American Chemical Society, Washington, DC, 1998. (i) Colombani, D. *Prog. Polym. Sci.* **1997**, *22*, 1649.

(22) (a) Fukuda, T.; Terauchi, T.; Goto, A.; Ohno, K.; Tsujii, Y.; Miyamoto, T.; Kobatake, S.; Yamada, B. *Macromolecules* **1996**, *29*, 6393. (b) Fukuda, T.; Goto, K.; Ohno, K.; Tsujii, Y. In *Controlled Radical Polymerization*; ACS Symposium Series No. 685; Matyjaszewski, K., Ed.: American Chemical Society, Washington, DC, 1998; Chapter 11. (c) Greszta, D.; Matyjaszewski, K. *Macromolecules* **1996**, *29*, 7661. (d) Matyjaszewski, K. *Macromol. Symp.* **1996**, *111*, 47.

Part I

Properties of Novel Sugar-Carrying Amphiphiles Prepared with a Lipophilic Azo-Type Radical Initiator

Chapter 1

Synthesis of Glucose-Carrying Amphiphiles by a Lipophilic Radical Initiator and Their Interaction with Lectin at Interfaces

1-1. Introduction

Recently molecular recognitions at interfaces such as those between two lipid bilayers, lipid bilayer and liquid phase, and lipid bilayer and solid surface have been of interest as a model system of an elementary step of various recognition phenomena in cell systems (e.g., formation of organs and tissues, and immunological protection systems). Kitano *et al.* have been studying the mutual recognition between polymerized liposomes whose surfaces are modified with complementary compounds.[1,2] In this Chapter, the author has prepared sugar-carrying lipid molecules from a lipophilic radical initiator and a sugar-carrying vinyl monomer (2-(methacryloyloxy)ethyl-α-*D*-glucopyranoside, MEGlc). By incorporating the amphiphiles into liposomes, the author could study interfacial recognition of sugar-carrying amphiphiles by a lectin using various techniques including the multiple internal reflection fluorescence (MIRF) method.[3,4,5]

The MIRF method utilizes an evanescent surface wave generated at the solid–liquid interface (Figure 1-1). The evanescent wave excites the fluorophore in the vicinity of the interface, and the emitted fluorescence comes into the waveguide. After separation from the incident light by using a dichroic mirror and a sharp cut filter, the fluorescence is detected by the photomultiplier. This method is very useful to detect processes of colloidal particles binding (proteins, liposomes, and cells, for example) to solid surfaces. Previously Kitano and co-workers examined binding processes of proteins such as human serum albumin (HSA) and human immunoglobulin G (IgG) to poly(methylmethacrylate) (PMMA) surfaces,[3] and immunological binding of anti-HSA IgG (antibody) to HSA (antigen) attached to PMMA surfaces.[4,5]

Bader *et al.* have examined interactions of a lectin (concanavalin A, Con A) with polymerized monolayers carrying sugar moieties by the MIRF method.[6] Using the MIRF method, the author has examined here very initial stages of binding processes of sugar-carrying liposomes to the PMMA surface modified with Con A, as a model system of the specific binding of cells to the surfaces with high affinities.

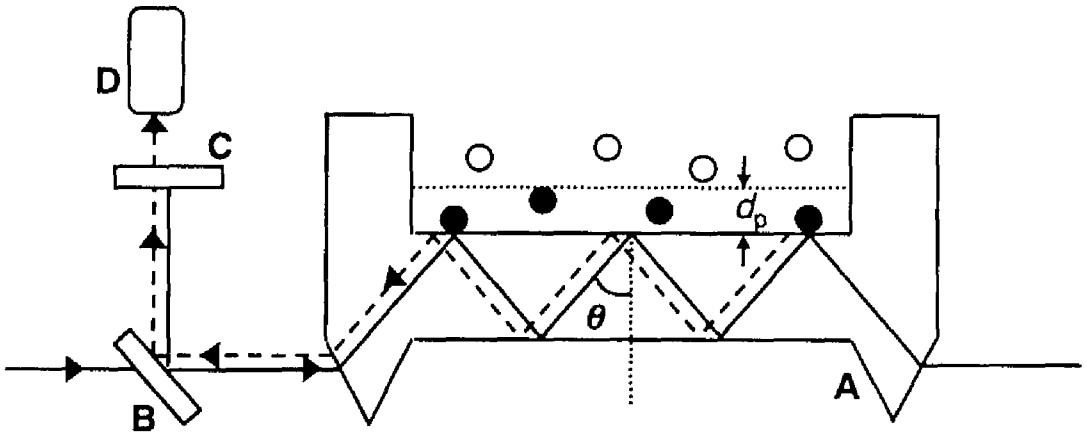

Figure 1-1. Scheme of the MIRF apparatus: (A), waveguide; (B), dichroic mirror; (C), cut filter; (D), detector. d_p, penetration depth of the evanescent wave (1500 Å in this experiment).[3] θ, angle of the incident light beam. (●), exited. (○), not exited. (—), incident light beam. (---), fluorescence.

1-2. Experimental Section

1-2-1. Materials

A glucose-carrying monomer, 2-(methacryloyloxy)ethyl-α-*D*-glucopyranoside (MEGlc, Figure 1-2b), was kindly donated by Nippon Fine Chemicals, Osaka, Japan.[7] A polymerizable lipid, bis(*trans,trans*-2,4-octadecadienoyl)phosphatidylcholine (DDPC) was kindly donated by the Japan Fat and Oil Co., Tokyo, Japan. *L*-α-Dipalmitoylphosphatidylcholine (DPPC) (> 99% by HPLC), *L*-α-dipalmitoylphosphatidylethanolamine (DPPE) and concanavalin A (Con A, from *Canavalia ensiformis*) were purchased from Sigma, St. Louis, MO, USA. Gelatin (M=10 000, PA100) was kindly donated from Nippi-Gelatin Co., Tokyo, Japan. Other reagents were commercially available. Deionized water was distilled before use.

1-2-2. Concanavalin A Labeled with Fluorescein

Concanavalin A (400 mg) was incubated with fluorescein isothiocyanate (FITC, 12 mg) in a carbonate buffer (pH 9.5, 50 mM, 10 mL) at 4 °C for 2 h. Concanavalin A modified with fluorescein (F-Con A) was separated from unreacted dye by the GPC column (Sephadex G-25, i.d. 2 x 30 cm. eluting solution, water). The F-Con A was classified by the number of fluorescein molecules bound to one Con A molecule (F/P ratio) by ion-exchange chromatography (DEAE-cellulose column, i.d. 2 x 15 cm. eluting solution, pH 7.0 phosphate

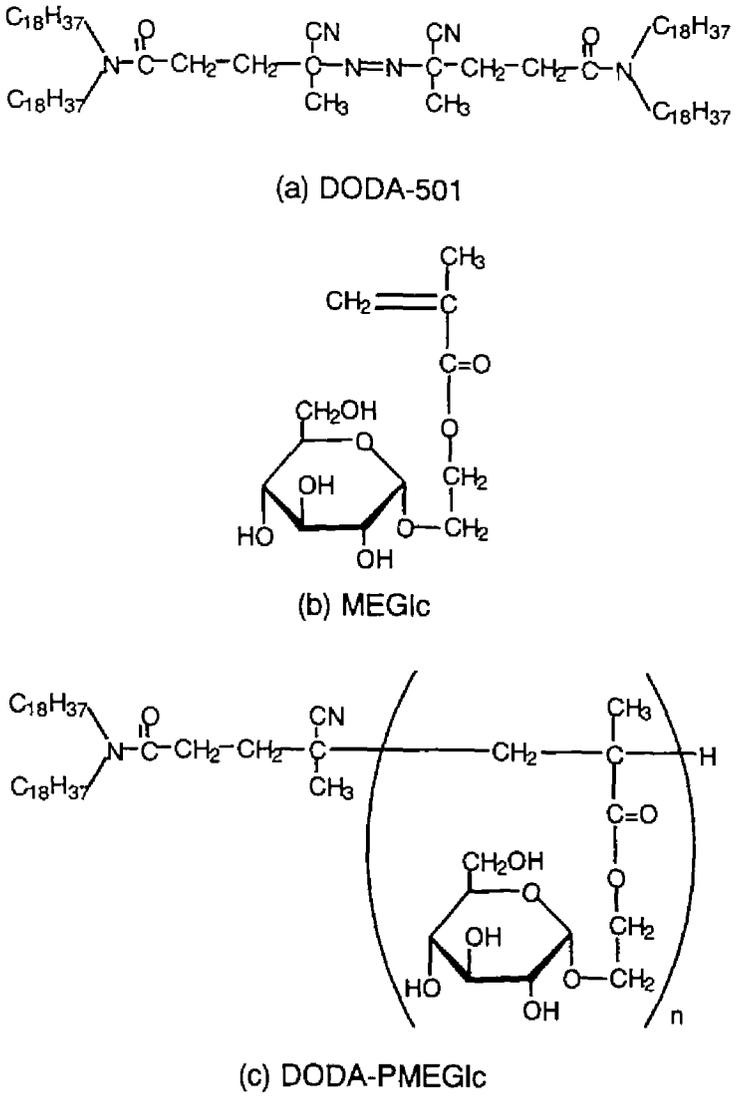

Figure 1-2. Chemical structure of DODA-501, MEGlc, and DODA-PMEGlc.

buffer (10 mM)). The F-Con A fraction with F/P ratio of 3.1 was used in this experiment.

1-2-3. Synthesis of *N*-[4,4'-Azobis(4-cyanovalerate)]-dioctadecylamide (DODA-501)[8]

DODA-501, a lipophilic radical initiator (Figure 1-2a), was prepared from disuccinimidyl 4,4'-azobis(4-cyanovalerate) (A-501) and dioctadecylamine (DODA). The $CHCl_3$ in which the DODA was dissolved was added dropwise in THF containing A-501. A solution was stirred overnight at room temperature. The product was purified by silica gel chromatography with a 3:1 *n*-hexane/ethyl acetate mixture eluent. The purified product was precipitated in acetonitrile.

1-2-4. Preparation of Sugar-Carrying Lipids

The MEGlc monomer (909 mg) and DODA-501 (400 mg) were dissolved in THF (15 mL) and

after N_2 was bubbled for several minutes, the solution mixture was incubated in a tightly sealed test tube at 70 °C for 20 h. After evaporation of the solvent *in vacuo*, the viscous oil was washed with *n*-hexane to remove unreacted initiator using a centrifugator at 10 000 rpm and 25 °C for 10 min. After decantation, the precipitate was dried *in vacuo* and dispersed in water. Polymers without lipophilic end groups were removed by the centrifugation at 10 000 rpm and 4 °C for 10 min. Finally the lipid precipitate was collected and dried *in vacuo* to give white powder (630 mg, DODA-PMEGlc, Figure 1-2c). IR: O-H stretching of galactose, 3350-3500 cm^{-1}; C≡N stretching, 2050 cm^{-1}; C=O stretching of the ester bond, 1720 cm^{-1}; C=O stretching of tertiary amide, 1630 cm^{-1}; $CH_2 \nu_{as}$, 2950 cm^{-1}; $CH_2 \nu_s$, 2870 cm^{-1}. The number-average degree of polymerization (DP) was estimated to be 83 by elemental analysis. DODA-PMEGlc (DP=83) Anal. Calcd for $C_{42}H_{82}N_2O(C_{12}H_{20}O_8)_{83}$: C, 50.08; H, 7.07; N, 0.11. Found: C, 49.61; H, 7.47; N, 0.11. Similarly, DODA-PMEGlc (DP=13, 19 mg) and DODA-PMEGlc (DP=4, 16 mg) were prepared by using 134 mg of MEGlc and 200 mg of DODA-501 and 510 mg of MEGlc and 300 mg of DODA-501, respectively. DODA-PMEGlc (DP=13) Anal. Calcd for $C_{42}H_{82}N_2O(C_{12}H_{20}O_8)_{13}$: C, 53.66; H, 7.79; N, 0.63. Found: C, 54.19; H, 7.78; N, 0.62. DODA-PMEGal (DP=4) Anal. Calcd for $C_{42}H_{82}N_2O(C_{12}H_{20}O_8)_4$: C, 60.03; H, 9.09; N, 1.56. Found: C, 59.00; H, 9.11; N, 1.59.

1-2-5. Polymerization of MEGlc

A homogeneous polymerization of MEGlc was carried out using 4,4'-azobis(4-cyanovaleric acid) (V-501, Wako Pure Chemicals, Osaka, Japan) and cysteamine hydrochloride (Cys.HCl) as initiator and chain transfer reagent, respectively, in MeOH-water (1:3). After evaporation of the solvent, the oily product was washed several times with acetone and dried *in vacuo* (PMEGlc). The number-average degree of polymerization was estimated by the conductometric titration of amino group at the end of polymers (Table 1-1).

1-2-6. Preparation of Liposomes

DPPE and DDPC (or DPPC) were dissolved in chloroform in a small round-bottomed flask. After evaporation of the solvent, the lipid thin membrane was dispersed in a *N*-(2-hydroxyethyl)piperazine-*N*'-2-ethanesulfonic acid (HEPES) buffer (pH 8.2, 10 mM) in which DODA-PMEGlc had been dispersed beforehand. The dispersion was sonicated by an ultrasonifier (Astrason W-385, Heat System-Ultrasonics, Inc., New York) for 3 min while N_2 gas was passed through the suspension. To remove large aggregates, the liposome suspension obtained was passed through a membrane filter (SLGV025LS, Millipore, pore size 0.22 μm).

Table 1-1. Preparation of MEGlc Polymers[a]

	MEGlc (mmol)	V-501 (mmol)	Cys.HCl (mmol)	yield[b] (%)	DP[c]
PMEGlc-1	8.6	0.086	0.86	71.2	9.1
PMEGlc-2	8.6	0.086	1.72	52.4	4.8
PMEGlc-3	8.6	0.086	0.60	87.9	12.9
PMEGlc-4	8.6	0.086	0.43	87.5	17.4

[a] 2.5 mL of MEOH and 7.5 mL of H_2O at 70 °C for 24 h.

[b] Relative to MEGlc.

[c] By the conductometric titration.

The hydrodynamic diameter of the liposomes was estimated by the dynamic light scattering technique (DLS-7000, Ohtsuka Electronics, Hirakata, Japan; light source, He-Ne laser 632.8 nm).

For the reproducible detection by the evanescent wave, liposomes were stabilized by the polymerization and modified with the fluorescein group as follows: The liposome consisting of DDPC, DODA-PMEGlc and DPPE (90:5:5) was passed through the filter and irradiated in a quartz cell by a UV lamp (HB-251A, Ushio, Tokyo, Japan) at room temperature for 4 h. The progress of polymerization was followed by the decrease in absorbance at 258 nm by using a UV-visible spectrophotometer (Ubest-35, Japan Spectroscopic Co., Tokyo, Japan). The polymerized liposome suspension was incubated with fluorescein isothiocyanate in a HEPES buffer (10 mM, pH 8.2) for 24 h. The liposome suspension was separated from unreacted dye by the GPC column (Sephadex G-10, i.d. 2 x 15 cm. eluting solution, pH 8.2 HEPES buffer (10 mM)). The fluorescent fraction was collected and used for the binding experiments. A polymerized liposome suspension without DODA-PMEGlc was also prepared in a similar way.

1-2-7. Characterization of Liposomes

Formation of liposomal structure was confirmed by the fluorescence dye-incorporation technique using Eosin Y as a probe[8a] (excitation at 305 nm, emission at 571 nm, FP-777, Japan Spectroscopic Co.).

1-2-8. Turbidity Measurements

The aggregation of liposomes mediated by Con A was followed by the increase in turbidity at 350 nm by using the UV-visible spectrophotometer or a stopped-flow spectrophotometer (RA-401, Ohtsuka Electronics, Hirakata, Japan). The observation cell was thermostatted at 25 °C by a Peltier device (EHC-363, Japan Spectroscopic Co.).

1-2-9. Multiple Internal Reflection Fluorescence Method[3,4,5]

Processes of the binding of sugar-carrying liposomes to the solid surface modified with concanavalin A were monitored by the multiple internal reflection fluorescence (MIRF) apparatus. The MIRF apparatus is illustrated in Figure 1-1. The light source was a 10-mW argon laser (LAI2223, Toshiba Electronics, Tokyo, Japan) operated at 488.0 nm. The excitation beam is introduced into the wave guide through the prism. The light beam strikes the interface between the wave guide and sample solution at an angle (θ) of 80° and is reflected at the interface. When the light is reflected, an evanescent surface wave is generated and penetrates into the sample solution beyond the interface. The penetration depth (d_p) of the evanescent wave calculated from Equation 1[9] is 1500 Å

$$d_p = (\lambda/n_1)/2\pi[\sin^2\theta - (n_2/n_1)^2]^{0.5} \qquad (1)$$

where n_1 and n_2 are the refractive indices of the two media, θ is the angle of the incident light beam, and λ is the wavelength of the incident light. The excitation beam is emitted inside of the wave guide with multiple reflections.

When a liposome labeled with fluorescein is adsorbed onto the surface of the wave guide modified with Con A, fluorescein is excited by the evanescent wave and emits fluorescence. The fluorescence is separated from the excitation beam using a dichroic mirror and a cutoff filter (R515, Schott) and is finally detected by a photomultiplier (R-1547, Hamamatsu Photonics, Hamamatsu, Japan).

A cuvette for the MIRF method consists of two parts, a wave guide and a cover. The wave guide with prisms is made of poly(methyl methacrylate) (PMMA). These parts are used only once. The wave guides have an intrinsic background signal due to the surface properties of the wave guide.[10] The relative fluorescence intensity corresponding to the background signal of the wave guides used here was 15 ± 1, and the author could assume that surface properties of the wave guides were constant. The surface area of the wave guide with which the sample solution can be in contact is 4 cm^2 (1 x 4 cm). The cover part with ports for injection of the

sample solutions is made of stainless steel. A silicone rubber gasket is attached to a stainless steel support to seal two parts. The total thickness of the cell is about 0.5 mm, and the total cell volume including the injection ports is about 0.25 mL.

The path of a fluorescence signal through the cutoff filter is detected by the photomultiplier and the fluorescence intensity was integrated for 1 s. A monochromator reference is also detected and the difference between the intensities of the reference signal and the fluorescence signal is calculated with a microcomputer (J-3100 GT, Toshiba Electornics, Tokyo, Japan).

1-3. Results and Discussion

1-3-1. Binding of Con A to Sugar Residues on the Liposome Surface

Mixing of a Con A solution with solutions of PMEGlc increased the turbidity quickly, and the initial slope of the turbidity change was strongly dependent on the molecular weight of PMEGlc examined (Figure 1-3a). The larger the molecular weight of PMEGlc was, the larger the rate of the turbidity change was. This turbidity change was largely reduced by the addition of α-methyl-*D*-mannopyranoside (α-Me-Man) (Figure 1-3b), which has a strong affinity with

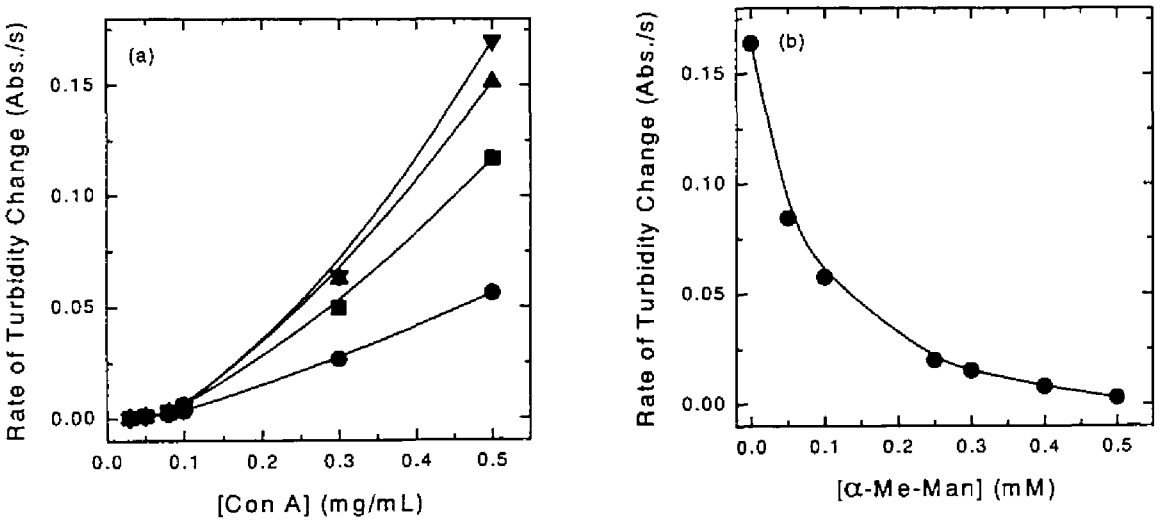

Figure 1-3. (a) Effect of concentration of Con A on the turbidity change after the addition of Con A into the PMEGlc solution: (●), DP = 4.8; (■), 9.1; (▲), 12.9; (▼), 17.4. [PMEGlc] = 50 μg/mL. (b) Inhibitory effect of α-methyl-*D*-mannopyranoside on the turbidity change. DP of PMEGlc, 17.4. [PMEGlc] = 50 μg/mL. [Con A] = 500 μg/mL. In a HEPES (10 mM, pH 7.7) buffer. [$CaCl_2$] = [$MnCl_2$] = 0.1 mM.

Con A.[11] This means that the phenomenon is due to the specific recognition of glucose residues in PMEGlc by tetrameric Con A molecules, which results in aggregation of Con A and PMEGlc molecules.

Similarly, the addition of Con A solution to the suspension of liposomes carrying oligomeric MEGlc chains on their surfaces (DODA-PMEGlc/DPPC liposome, diameter 860 Å) increased the turbidity quickly. The initial slope of the turbidity change increased with the concentration of Con A (Figure 1-4a). This turbidity change was also inhibited significantly by the addition of α-methyl-*D*-mannopyranoside (Figure 1-4b), which shows the effective recognition of sugar residues on the liposome surfaces by free Con A.

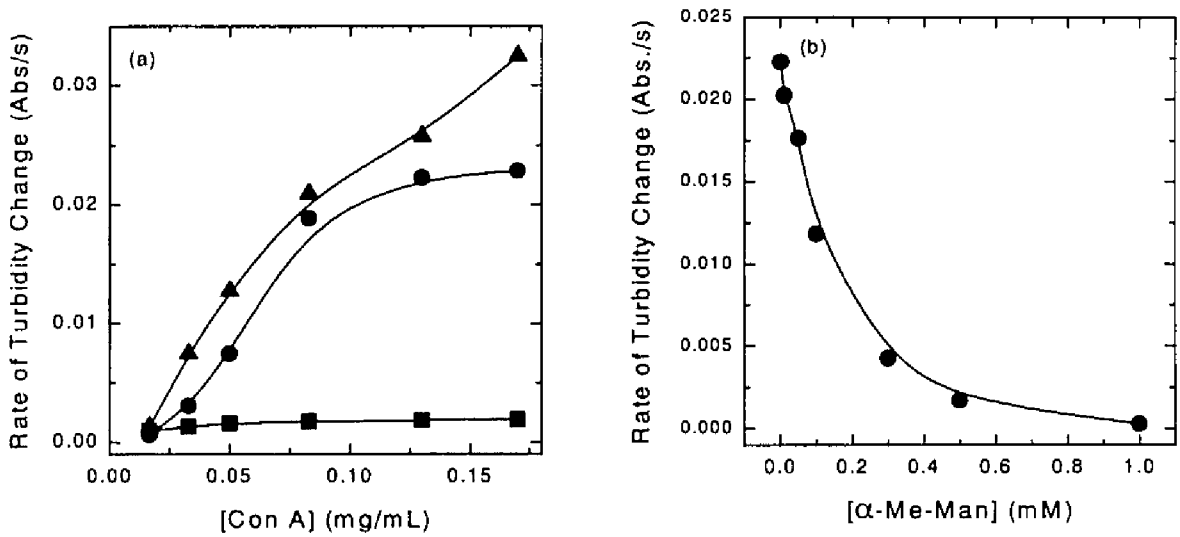

Figure 1-4. (a) Effect of concentration of Con A on the turbidity change after the addition of Con A into the liposome suspension: (▲), content of DODA-PMEGlc (DP = 83) in the liposome was 20 wt.%; (●), 12.5 wt.%; (■), 2.3 wt.%. [DODA-PMEGlc/DPPC liposome] = 50 μg/mL. (b) Inhibitory effect of a-methyl-*D*-mannopyranoside on the turbidity change. The content of DODA-PMEGlc (DP = 83) in the DODA-PMEGlc/DPPC liposome was 12.5 wt.%. [Con A] = 130 μg/mL. [liposome] = 50 μg/mL. In a HEPES (10 mM, pH 8.0) buffer. $[CaCl_2] = [MnCl_2] = 0.03$ mM.

By varying the amount of DODA-PMEGlc to be mixed with DPPC, one can examine the effect of surface concentration of sugar residues on the association by free Con A (Figure 1-5). As shown in the figure, there was no threshold value in the agglutinability of Con A, which is different from that of glycolipid-carrying liposomes.[12] Since many glucose residues are bound to one polymethacrylate chain, the lectin molecule needs not bind tightly to the

plural number of sugar-carrying lipids on one liposome surface to induce the fast aggregation. This might be the reason for the absence of the threshold value.

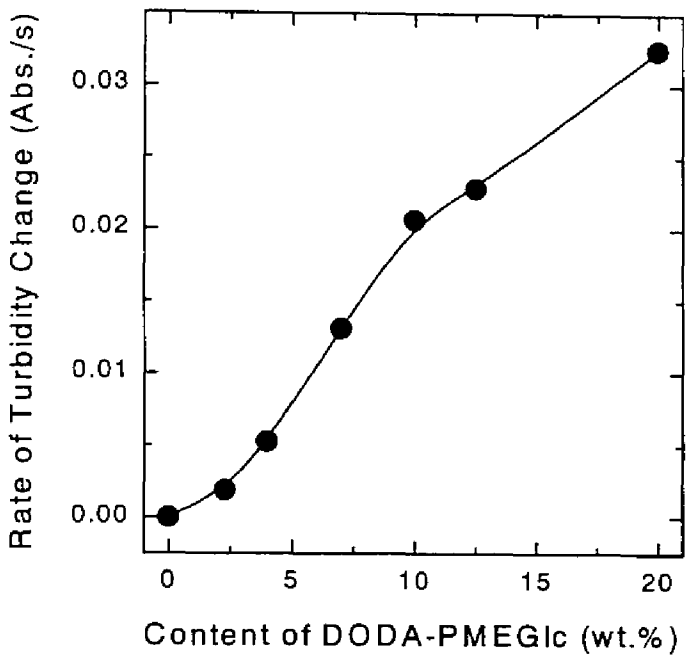

Figure 1-5. Effect of mixing ratio of DPPC and DODA-PMEGlc (DP = 83) in the liposome on the turbidity change. [Con A] = 170 μg/mL. [liposome] = 50 μg/mL. In a HEPES (10 mM, pH 8.0) buffer. [$CaCl_2$] = [$MnCl_2$] = 0.033 mM.

1-3-2. Binding of Liposomes to Con A-Carrying Cuvette

Next, the author examined binding processes of DODA-PMEGlc/DDPC(polymerized) liposomes (diameter 860 Å) to the poly(methyl methacrylate) (PMMA) surface modified with Con A. After incubation of Con A solution (5 mg/mL) in the PMMA cuvette for 3 h at pH 7.0 (10 mM HEPES, containing 0.2 mM $CaCl_2$ and 0.2 mM $MnCl_2$), the cuvette was washed well with the HEPES buffer and used in the MIRF experiment. The adsorbed Con A molecules could not be removed by repeated washings with the buffer.

When the suspension of liposomes carrying both sugar residues and fluorescein groups was injected into the cuvette, the fluorescence intensity increased rapidly and leveled off (Figure 1-6, curve 1). After the injection of the liposome modified with fluorescein groups but without sugar groups, on the contrary, there was no significant increase in fluorescence intensity (Figure 1-6, curve 2), except an initial abrupt jump due to the fluorescence

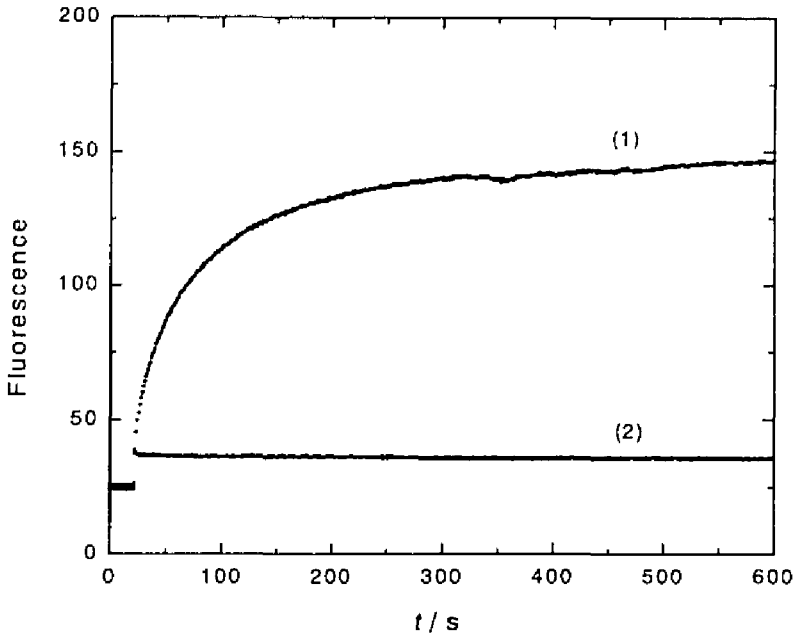

Figure 1-6. Typical profile of the increase in fluorescence intensity by the addition of sugar-carrying liposome: (1) [DODA-PMEGlc (DP = 83)/DDPC (polymerized) liposome] = 400 μg/mL; (2) [DDPC liposome] = 100 μg/mL. In a HEPES (10 mM, pH 8.2) buffer. Twenty seconds after the onset of the measurement the liposome suspension was injected.

background of bulk solution.

Furthermore, when the liposome suspension above the cuvette surface was removed and a solution of α-Me-Man (100 mM) was injected, the liposome was very slowly desorbed due to the competition of α-Me-Man with the sugar-carrying liposome to bind the Con A-carrying surface (Figure 1-7). These results suggest the presence of specific affinity between glucose residues on the liposome surface and Con A molecules on the cuvette.

From the initial slope of the increase in fluorescence intensity in Figure 1-6, one can evaluate the initial rate $(dCs/dt)_0$ of the binding of the liposome to the surface of the Con A-carrying cuvette. When the increment of fluorescence was plotted as a function of $(\text{time})^{0.5}$, there was an approximately linear relationship for several tens of seconds after the onset of the binding experiment (data not shown). Since the very initial stage of the binding processes was examined in this work, the deviation from the straight line observed several tens of seconds later (due to the presence of liposomes already bound to the cuvette) does not matter. Consequently, it is concluded that the binding of the liposome to the cuvette is diffusion-

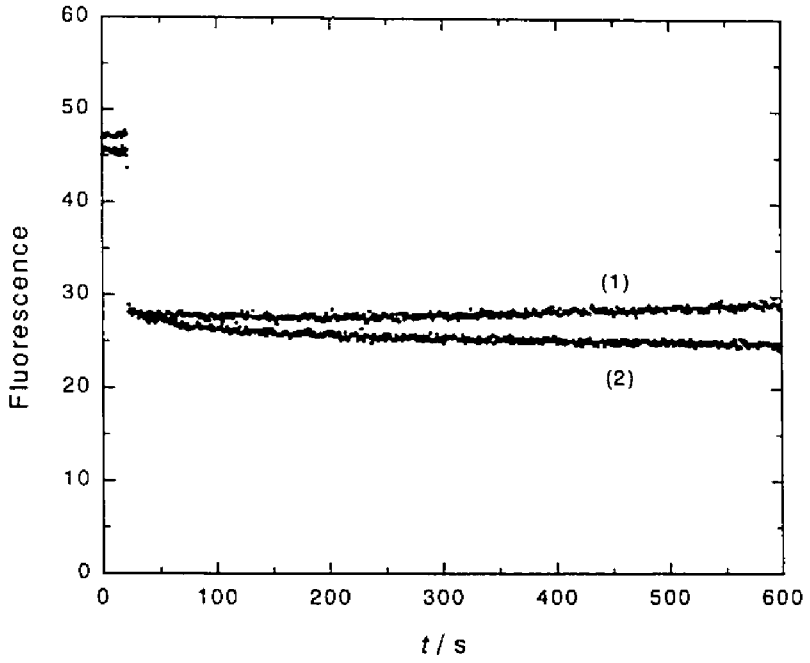

Figure 1-7. Desorption of DODA-PMEGal liposomes attached to the Con A-carrying cuvette. The cuvette had been incubated with a DODA-PMEGlc (DP = 83)/DDPC (polymerized) liposome suspension (800 μg/mL) for 1 h beforehand. In a HEPES (10 mM, pH 8.2) buffer. (1) Incubated with a buffer. (2) Incubated with a buffer containing α-Me-Man (100 mM).

controlled.[13] Assuming that the binding occurs by simple diffusion, one can calculate the theoretical binding rate $(dCs/dt)_{theor}$ as Equation 2.[14] The ratio of theoretical and experimental binding rates is given by R (Equation 3).

$$(dCs/dt)_{theor} = C_0(D/\pi t)^{0.5} \quad (2)$$

$$R = (dCs/dt)_0/(dCs/dt)_{theor} \quad (3)$$

where D is the diffusion coefficient of the liposome (radius, a) ($D = kT/6\pi\eta a$), and C_0 is the initial concentration of liposomes. The R value reflects the effectiveness of the Brownian collision of the liposome to realize a stable attachment to the surface of the cuvette.

When the amount of the sugar-lipid in the liposome was 20 wt.%, the R value was 0.65, which means that the rate of binding is 65 % of that expected upon a perfectly adsorbing surface. On the contrary, in the binding of anti-HSA immunoglobulin G to the PMMA surface

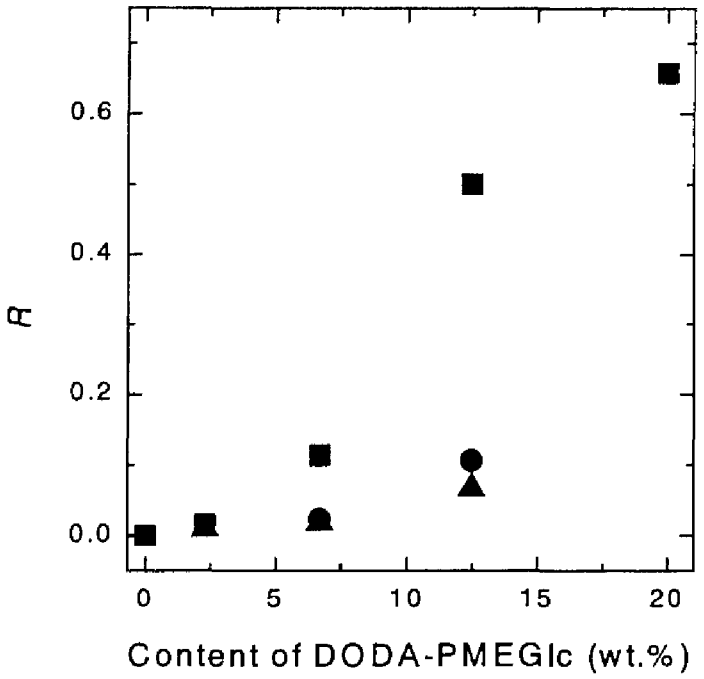

Figure 1-8. Effect of mixing ratio of DDPC and DODA-PMEGlc on the *R* value: (■), DP = 83; (●), 13; (▲), 4. In a HEPES (10 mM, pH 8.2) buffer.

modified with HSA, the *R* value was 0.1 at the most.[4] Liposomes are usually largely hydrated, and the approach of other colloidal surfaces to the liposomes is strongly decelerated due to a need for energy to remove water layers on the liposomes (repulsive hydration).[15] Therefore, it is not easy to accept that the DODA-PMEGlc liposome can be attached to the Con A carrying-surface so rapidly.

By a reduction of the amount of sugar residue or a shortening of the sugar chains in the liposome, the *R* value decreased largely (Figure 1-8). The reduction of *R* value by shortening the sugar chains strongly suggests that a zipping might occur between the Con A molecules on the surface of the cuvette and the long sugar-carrying polymer chain on the liposome surface: Once the sugar-chain attaches to the cuvette, there might be a specific association between a sugar group and Con A, which would significantly increase the probability that the neighboring sugar moiety in the polymer chain approaches the Con A molecule in the vicinity of the Con A already occupied. Such a zipping might reduce the effect of repulsive hydration[15] at the collision of the liposome to the cuvette surface and, consequently, increase the apparent effectiveness of the Brownian collision. There are many kinds of peptidoglycans which stretch

long chains out into a solution on cell surfaces.[16] The association of cells might be largely promoted by the zipping effect between the peptidoglycans on surfaces of the cells.

Previously Wattenbarger *et al.* examined specific adhesion of glycophorin liposomes to a lectin (wheat germ agglutinin) surface in shear flow by the microscopic method.[17] The probability of the liposome sticking to the lectin surface was almost unity at low shear rate and at high concentration regions of glycophorin on the liposome surface and decreased with an increase in shear rate or a decrease in surface concentration of glycophorin. Glycophorin has a long sugar-carrying polypeptide chain (about 70 amino acid residues) stretching out to the outer solution,[18] and the tendency reported (a large sticking probability) are not inconsistent with the author's results.

To examine the effect of surface concentration of Con A on the *R* value, the cuvette with a mixture of gelatin (inert protein) and Con A was incubated at various concentration ratios. The percents of occupation by Con A on the surface were separately estimated from the increase in intensity of fluorescence after a mixture (50 μg/mL) of gelatin and F-Con A (or F-gelatin and Con A) was injected into the cuvette by using the MIRF method (Figure 1-9a). These values were adopted as the percents of occupation by Con A (without fluorescein) under

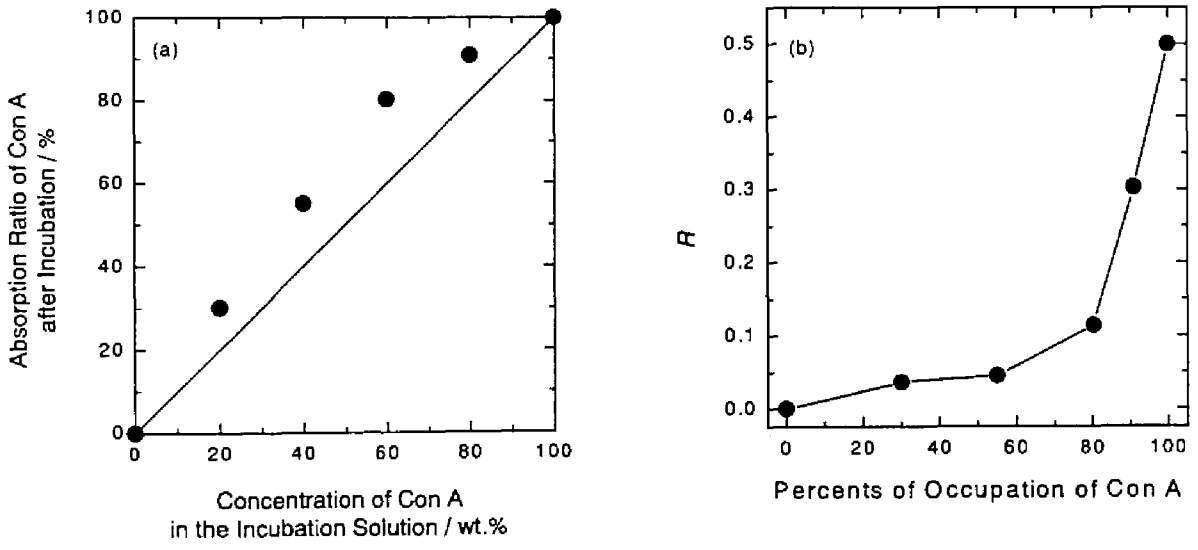

Figure 1-9. (a) Relationship between weight percent of Con A in the incubation solution and weight percent of Con A adsorbed on the PMMA cuvette. (b) Effect of the percents of occupation of Con A on the R value. DP of DODA-PMEGlc, 83. In a HEPES (10 mM, pH 8.2) buffer.

the same injection conditions, because the properties of F-Con A and F-gelatin might not be largely different from those of Con A and gelatin. Previously Hasegawa *et al.* reported that the nonspecific binding behavior of proteins to the PMMA surface is most strongly influenced by the hydrophobicity of the proteins examined, and not by the electrostatic interaction.[3]

By the increase in the percents of occupation by Con A on the cuvette, the R value did not significantly increase at first (< 60 %), and, then, increased steeply (Figure 1-9b), which suggests the presence of a threshold value in the recognition of a sugar moiety by lectin at the cuvette–liposome interface. This is different from the tendency observed in the free Con A/liposome system (Figure 1-5). To realize the stable attachment of the gigantic liposome to the cuvette surface, conjugations between many lectin molecules and sugar residues might be necessary, thus producing a threshold phenomenon.

1-4. Conclusions

The liposomes carrying sugar residues were effectively recognized by concanavalin A molecules attached to the polymer surface. The rate of binding of the liposome to the surface depended on the length of sugar chains and the surface concentrations of both sugar residues on the liposome and Con A on the cuvette.

References

(1) Kitano, H.; Kato, N.; Tanaka, N.; Ise, N. *Biochim. Biophys. Acta* **1988**, *942*, 131.

(2) Kitano, H.; Kato, N.; Ise, N. *J. Am. Chem. Soc.* **1989**, *111*, 6809.

(3) Hasegawa, M.; Kitano, H. *Langmuir*, **1992**, *8*, 1582.

(4) Tanimoto, S.; Kitano, H. *Langmuir* **1993**, *9*, 1315.

(5) Tanimoto, S.; Kitano, H. *Colloids and Surfaces B: Biointerfaces* **1995**, *4*, 259.

(6) Bader, H.; van Wagenen, R.; Andrade, J. D.; Ringsdorf, H. *J. Colloid Interface Sci.* **1984**, *101*, 246.

(7) Kobayashi, K.; Kakishita, N.; Okada, M.; Akaike, T.; Kitazawa, S. *Makromol. Chem., Rapid Commun.* **1993**, *14*, 293.

(8) (a) Kitano, H.; Akatsuka, Y.; Ise, N. *Macromolecules* **1991**, *24*, 42. (b) Winnik, F. M.; Davidson, A. R.; Hamer, G. K.; Kitano, H. *Macromolecules* **1992**, *25*, 1876.

(9) Born, M.; Wolf, E. *Principles of Optics, 5th ed.;* Pergamon: New York, 1975.

(10) Rockhold, S. A.; Quinn, R. D.; van Wagenen, R. A.; Andrade, J. D.; Reichert, M. *J. Electroanal. Chem.* **1983**, *150*, 261.

(11) Farina, R. D.; Wilkins, R. G. *Biochim. Biophys. Acta* **1980**, *631*, 428.

(12) Curatolo, W.; Yau, A. O.; Small, D. M.; Sears, B. *Biochemistry* **1978**, *17*, 5740.

(13) Weaver, D. R.; Pitt, W. G. *Biomaterials* **1992**, *13*, 577.

(14) MacRitchie, F. *Adv. Protein Chem.* **1978**, *32*, 283.

(15) Cowley, A. C.; Fuller, N. L.; Rand, R. P.; Parsegian, V. A. *Biochemistry* **1978**, *17*, 3163.

(16) Gennis, R. B. *Biomembranes; Molecular Structure and Function;* Springer-Verlag: Berlin, 1989.

(17) Wattenbarger, M. R.; Graves, D. J.; Lauffenburger, D. A. *Biophys. J.* **1990**, *57*, 765.

(18) Voet, D.; Voet, J. G. *Biochemistry;* John Wiley & Sons: New York, 1990.

Chapter 2

Synthesis of Galactose-Carrying Amphiphiles by a Lipophilic Radical Initiator: Association Processes between Liposomes Triggered by Enzymatic Reaction

2-1. Introduction

Mutual recognition of cells *in vivo* is an essential factor for the organization of tissues and organs and immunological protection system.[1] In recent years, some potential techniques have been developed using the specific binding of ligand to receptor at the lipid–lipid interface (so-called "cross-linked" liposomes).[2-5] Previously, Novogrodsky reported[6] that lymphocyte cytotoxicity could be induced by treatment with neuraminidase and galactose oxidase or with the periodate of either the effector cells or the target cells, which initiated cross-linkage between the effector and target cells via a Schiff base. In this Chapter, as a model system of this phenomenon, the author has examined the recognition of amino group-carrying liposomes by galactose-carrying liposomes that had been treated with galactose oxidase beforehand.

By the lipophilic radical initiator (DODA-501, Figure 2-1a) and a galactose-carrying vinyl monomer (2-(methacryloyloxy)ethyl-*β-D*-galactopyranoside, MEGal (Figure 2-1b)), galactose-carrying amphiphiles with various degrees of polymerization (Figure 2-1c) were prepared. A lipid carrying only one galactose residue (Figure 2-1d) was also prepared by the lactone method for comparison.[7] By incorporating the galactose-carrying amphiphile in liposomes, the author could study association processes of liposomes mediated by the Schiff bases, which were triggered by the enzymatic reaction.

2-2. Experimental Section

2-2-1. Materials

A lipophilic radical initiator (DODA-501)[8] was synthesized from *N,N*-dioctadecylamine (DODA, Fluka, Switzerland) and 4,4'-azobis(cyanovaleric acid) (V-501, Wako Pure Chemicals, Osaka, Japan) as described in Chapter 1. A galactose-carrying monomer, 2-(methacryloyloxy)ethyl-*β-D*-galactopyranoside (MEGal), was prepared by trans-glycosylation between *o*-nitrophenyl-*β-D*-galactopyranoside and 2-hydroxyethyl methacrylate (HEMA) catalyzed by *β*-galactosidase (from *Escherichia coli*, 340 units/mg, Sigma, St. Louis, MO) in a phosphate buffer (1/15 M, pH 6.4)[9] in the presence of hydroquinone: Anal. Calcd for

$C_{12}H_{20}O_8 \cdot 1/2H_2O$: C, 47.84; H, 7.02; O, 45.14. Found: C, 47.65; H, 6.88; O, 45.47. ^{1}H-NMR (D_2O): δ 6.15 (s, 1H, CH_2=C<, *Z* form H), 5.65 (s, 1H, CH_2=C<, *E* form H), 4.37 (m, 2H, $COOCH_2CH_2$–), 3.68 (m, 2H, $COOCH_2CH_2$–), 1.85 (s, 3H, CH_3), 4.80–3.40 (m, 11H, others), 4.77 (water of crystallization).

N-Diglycyl-*N,N*-dioctadecylamide (GGA) was prepared by the reaction of *N*-benzyloxycarbonyl (Z) diglycine *p*-nitrophenyl ester with dioctadecylamine in THF and subsequent deprotection of the Z group by the HBr/CH_3COOH method.[10] *N*-Glycyl-*N,N*-

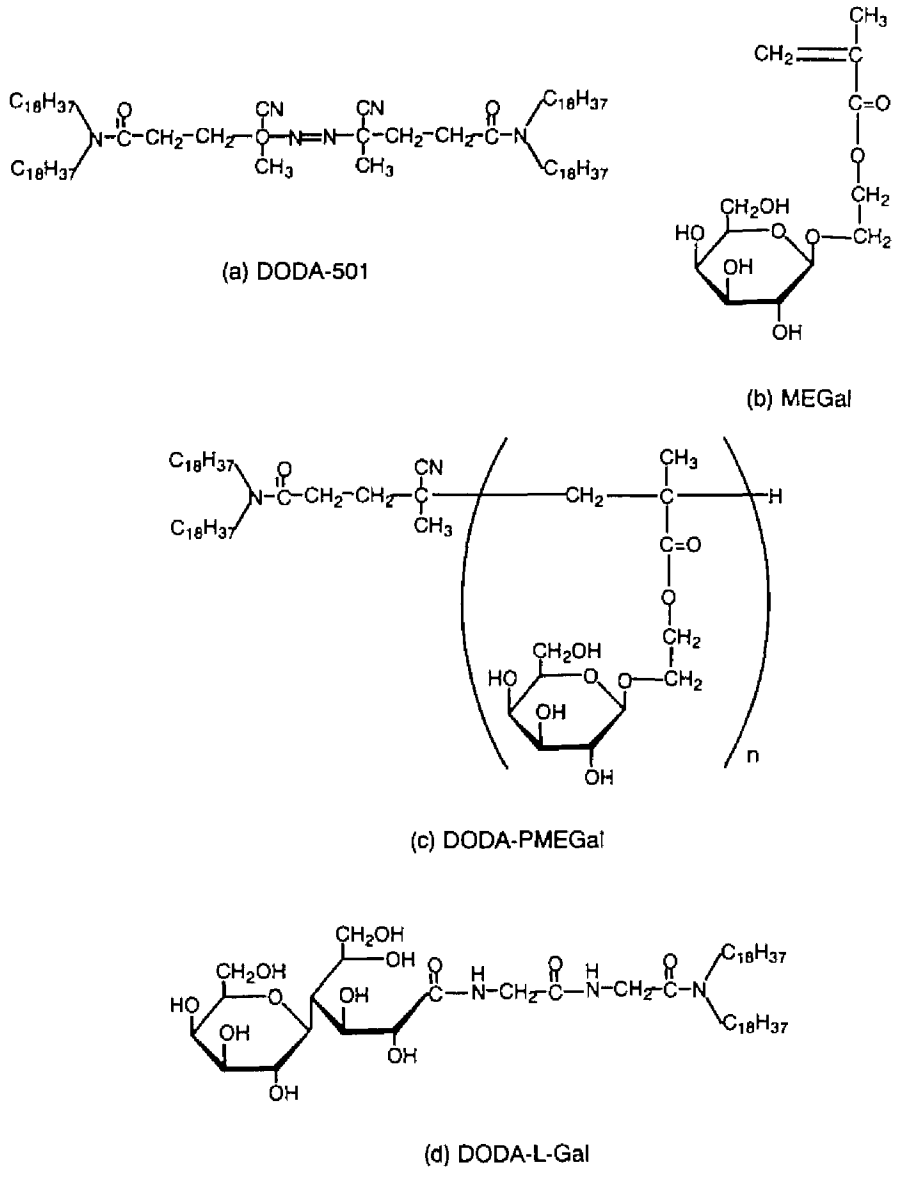

Figure 2-1. Chemical structures of (a) DODA-501, (b) MEGal, (c) DODA-PMEGal, (d) DODA-L-Gal.

dioctadecylamide (GA) was also prepared from *N*-benzyloxycarbonyl (Z) glycine *p*-nitrophenyl ester in a similar way. A polymerizable lipid, bis(*trans,trans*-2,4-octadecadienoyl)phosphatidylcholine (DDPC), was kindly donated by the Japan Fat and Oil Co. (Tokyo, Japan). *L*-α-Dipalmitoylphosphatidylcholine (DPPC), *L*-α-dimyristoylphosphatidylcholine (DMPC), and galactose oxidase (from *Dactylium dendroides*) were from Sigma. 1-Ethyl-3-[3-(dimethylamino)propyl]carbodiimide hydrochloride (WSC) and ammonium chloride were from Wako Pure Chemicals. Other reagents were commercially available. Deionized water was distilled before use.

2-2-2. Preparation of Galactose-Carrying Amphiphile by Polymerization

The MEGal monomer (200 mg) and DODA-501 (176 mg) were dissolved in THF (20 mL), and after N_2 was bubbled for several minutes, the solution mixture was incubated in a tightly sealed test tube at 70 °C for 24 h. After evaporation of the solvent *in vacuo*, the viscous oil was washed with *n*-hexane to remove unreacted initiator by centrifugation at 10 000 rpm and 20 °C for 15 min. After decantation, the precipitate was dried *in vacuo* and dispersed in water (6 mL). Polymers without lipophilic end groups were removed by centrifugation at 10 000 rpm and 4 °C for 15 min. The lipid precipitate was collected and dried *in vacuo* to give white powder (8 mg, DODA-PMEGal, DP=3.1). Further, the products with a higher degree of polymerization in the supernatant solution were purified by passage through a GPC column (Sephacryl S-200, i.d. 2 x 18 cm, mobile phase; water) and lyophilized (69 mg, DODA-PMEGal, DP=8.4). IR: O-H stretching of galactose, 3350–3500 cm^{-1}; C≡N stretching, 2050 cm^{-1}; C=O stretching of the ester bond, 1720 cm^{-1}; C=O stretching of tertiary amide, 1630 cm^{-1}; CH_2 ν_{as}, 2950 cm^{-1}; CH_2 ν_s, 2870 cm^{-1}. The number-average degree of polymerization (DP) of the amphiphile was determined by elemental analysis. DODA-PMEGal (DP=3.1) Anal. Calcd for $C_{42}H_{82}N_2O(C_{12}H_{20}O_8)_{3.1}$: C, 61.78; H, 9.56; N, 1.82. Found: C, 61.71; H, 9.46; N, 1.81. DODA-PMEGal (DP=8.4) Anal. Calcd for $C_{42}H_{82}N_2O(C_{12}H_{20}O_8)_{8.4}$: C, 55.43; H, 8.36; N, 0.91. Found: C, 55.44; H, 8.42; N, 0.91. DODA-PMEGal (DP=15) was also prepared in a similar way (129 mg). DODA-PMEGal (DP=15) Anal. Calcd for $C_{42}H_{82}N_2O(C_{12}H_{20}O_8)_{15}$: C, 53.16; H, 7.68; N, 0.56. Found: C, 53.13; H, 7.74; N, 0.56.

2-2-3. Preparation of Galactose Lipid by the Lactone Method

Details of the preparation were described elsewhere.[11] Briefly, lactose monohydrate was oxidized by iodine in the presence of KOH at 40 °C. The precipitated solid was purified by recrystallization from MeOH–H_2O (12:5). The crystal was dissolved in H_2O, and the solution

was passed through an ion-exchange column (Amberlite IR-120 B, H^+ form) several times. The aqueous solution of the product was mixed with EtOH, and the solvent was evaporated at 70 °C to form a lactose-lactone. *N*-Diglycyl-*N,N*-dioctadecylamide (GGA) was coupled with the lactone in DMF–$CHCl_3$ (3:1) at 60 °C for 6 h. The galactose-carrying lipid was purified by precipitation in *n*-hexane–EtOH (2:1). The precipitate was further dissolved in $CHCl_3$ and passed through a glass filter. The filtrate was finally evaporated to give a slightly yellow powder (DODA-L-Gal).

2-2-4. Preparation of Liposomes

Galactose-Carrying Liposome: DDPC was dissolved in chloroform in a small, round-bottomed flask. After evaporation of the solvent, the thin lipid membrane was dispersed in an *N*-(2-hydroxyethyl)piperazine-*N'*-2-ethanesulfonic acid (HEPES) buffer (pH 6.0, 10 mM) in which DODA-PMEGal had been dispersed beforehand. The dispersion was sonicated by an ultrasonifier (Astrason W-385, Heat System-Ultrasonics, Inc., New York) for 3 min while N_2 gas was passed through the suspension. To remove large aggregates, the liposome suspension obtained was passed through a membrane filter (SLGV025LS, Millipore, pore size 0.22 μm). The liposome passed through the filter was irradiated in a quartz cell by a UV lamp (HB-251A, Ushio, Tokyo, Japan) at room temperature for 4 h to enhance the physical stability of the liposome by polymerization. The progress of polymerization was followed by the decrease in absorbance at 258 nm by using a UV-visible spectrophotometer (Ubest-35, Japan Spectroscopic Co., Tokyo, Japan). To block a very small amount of carboxyl groups, corresponding to methacrylic acid residues that had been generated by cleavage of the ester bond in the galactose-carrying amphiphile, the polymerized liposome suspension was incubated with WSC and ammonium chloride in HEPES buffer (pH 6.0, 10 mM) at room temperature for 12 h. The liposome suspension was separated from unreacted reagents by the GPC column (Sephadex G-10, i.d. 2 x 15 cm, eluting solution; HEPES buffer (pH 6.0, 10 mM)). The turbid fraction was collected, and the ζ potential of the liposome was confirmed to be approximately 0 mV by using a laser zee meter (Model 501, Pen Kem, Inc., Bedford Hills, NY).

Amino Group-Carrying Liposome: A phospholipid (DMPC or DPPC) and the amino group-carrying lipid (GGA or GA) were dissolved in chloroform in a small, round-bottomed flask. After evaporation of the solvent, the thin lipid membrane was dispersed in HEPES buffer (pH 6.0, 10 mM) by using a vortex mixer. The dispersion was further sonicated by the

ultrasonifier for 3 min, while N_2 gas was passed through the suspension. The liposome suspension was finally passed through the membrane filter.

2-2-5. Characterization of Liposomes

Formation of liposomal structure was confirmed by the fluorescence dye incorporation technique using Eosin Y as a probe[8,10] (excitation at 305 nm, emission at 571 nm, FP-777, Japan Spectroscopic Co.).

2-2-6. Dynamic Light Scattering Method

Hydrodynamic diameter of the liposomes was estimated by the dynamic light scattering (DLS) technique (DLS-7000, Otsuka Electronics, Hirakata, Japan. Light source; He-Ne laser 632.8 nm).

2-2-7. Turbidity Measurement

The aggregation of liposomes mediated by Schiff bases was followed by the increase in turbidity at 350 nm by using the UV-visible spectrophotometer. The observation cell was thermostatted at 37 °C by a Peltier device (EHC-363, Japan Spectroscopic Co.). The uncertainties of the rate of turbidity change were within 10 %. The data in the figures represent the mean values of three measurements.

3-2-8. Enzyme Activity Measurement

The oxidation reaction of galactose residues catalyzed by galactose oxidase was followed by using a spectrophotometric method:[12,13] Hydrogen peroxide formed by the oxidation of galactose was reduced by reaction with 4-aminoantipyrine and phenol catalyzed by peroxidase, and the increase in optical density due to the production of quinoneimine dye was measured at 500 nm for 5 min by the spectrophotometer thermostatted at 25 °C. The initial increase in optical density per minute was calculated from the initial linear portion of the curve. One unit of galactose oxidase causes the formation of one micromole of hydrogen peroxide per minute at 25 °C. The stock solution of galactose oxidase was diluted to the appropriate concentrations, and the catalytic activity of the enzyme was checked just before use.

2-2-9. Distribution of Galactose-Carrying Amphiphiles in Liposome

Galactose-carrying DMPC liposomes were incubated with galactose oxidase, and the amount of quinoneimine dye produced was measured simultaneously by using the spectrophotometric method described earlier. After the mixture was sonicated to completely disrupt the liposome structure by the ultrasonifier for 10 min at 60 °C, the production of quinoneimine dye due to oxidation of galactose residues on the reorganized liposomes was measured.

2-2-10. Determinations of Aldehyde Groups and Amino Groups on the Liposome Surfaces

The determination of aldehyde groups was carried out with 3-methyl-2-benzothiazolinone hydrazone:[14] 1 mL of 0.4 wt.% aqueous solution of 3-methyl-2-benzothiazolinone hydrazone hydrochloride was added to 1 mL of sample solution. After 20 min, 1 mL of aqueous solution containing 1 wt.% ferric chloride hexahydrate and 1.6 wt.% sulfamic acid was added to the mixture. Ten minutes later, 2 mL of water was added to the mixture. Subsequently the absorbance at 610 nm of the final mixture was read.

The determination of amino groups was carried out with 2,4,6-trinitrobenzenesulfonic acid:[15] 0.5 mL of 0.1 M $Na_2B_4O_7$ in 0.1 N NaOH was added to 0.5 mL of sample solution at 30 °C. Five minutes later, 20 μL of 1.1 M 2,4,6-trinitrobenzenesulfonic acid solution was added to the mixture. After 5 min, 2 mL of the solution (the mixture of 0.3 mL of 0.1 M Na_2SO_3 and 19.7 mL of 0.1 M KH_2PO_4) was added to the mixture to stop the reaction. Subsequently, the absorbance at 420 nm of the final mixture was read.

2-3. Results and Discussion

2-3-1. Association of Amino Group-Carrying Liposome with Aldehyde Group-Carrying Liposome

By using a dynamic light scattering technique, the average diameters of the galactose-carrying liposomes and the amino group-carrying liposomes were estimated to be 900 and 1400 Å, respectively. After the incubation of galactose-carrying liposome with a solution of galactose oxidase, the production of H_2O_2 was confirmed by the spectrophotometric method. When the concentrations of galactose-carrying DMPC liposome (DODA-PMEGal (DP=8.4), 4.5 mol %) and galactose oxidase were 46 μg of lipid/mL and 0.09 unit/mL, respectively, galactose residues on the outer liposome surfaces were completely oxidized by the enzyme in 30 min, which showed that the enzyme could effectively oxidize galactose residues on the liposome surface.[16] Further investigations on the catalytic behavior of enzymes at membrane interfaces are reported in Chapter 3.

By injecting the solution of galactose oxidase into the mixture of the galactose-carrying liposome suspension and the amino group-carrying liposome suspension, the turbidity increased gradually and then increased steeply (Figure 2-2a), whereas after the amino group-carrying liposome suspension was mixed with the suspension of the galactose-carrying

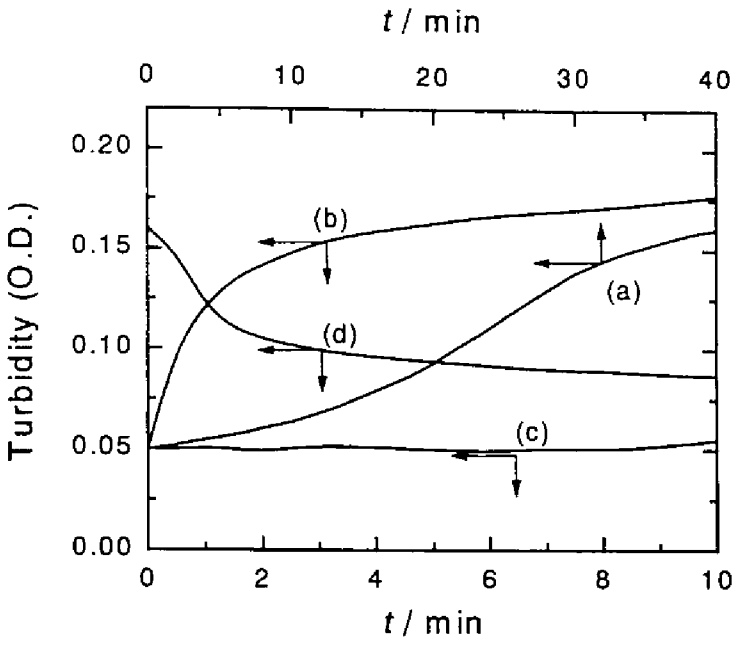

Figure 2-2. Typical profiles of turbidity change. (a) Galactose oxidase solution was injected into the mixture of galactose-carrying liposome suspension and amino group-carrying liposome suspension incubated at 37 °C. (b) Amino group-carrying liposome suspension was injected into galactose-carrying liposome suspension that had been incubated with galactose oxidase solution for 30 min at 37 °C beforehand. (c) Amino group-carrying liposome suspension was injected into galactose-carrying liposome suspension that had been incubated with a buffer for 30 min at 37 °C beforehand. (d) 1/10 N NaOH solution (0.5 mL) was injected into the mixture (3 mL) after experiment b was complete. The final pH of experiment d was 10.5. In all experiments, the contents of galactose-carrying lipid (DP = 8.4) and amino group-carrying lipid (GGA) were 4.5 and 10 mol %, respectively. The concentrations of both liposomes were 100 μg of lipid/mL, and the concentration of enzyme was 0.1 unit/mL (HEPES (10 mM, pH 6.0) buffer; wavelength = 350 nm).

liposomes that had been incubated with a galactose oxidase solution for 30 min at 37 °C, the turbidity increased quickly (Figure 2-2b). On the contrary, when the suspension of the galactose-carrying liposomes incubated only with a buffer solution in place of the enzyme solution was used, there was no increase in the turbidity (Figure 2-2c), which shows that the enzymatic reaction triggers the turbidity change. The apparent liposome diameter after the turbidity had increased and leveled off was estimated to be around 8300 Å by using the dynamic light scattering technique.

To verify that the liposomes were aggregated and not fused, the author examined the leakage of fluorescence dye after mixing the amino group-carrying liposomes (Eosin Y had been incorporated) with the galactose-carrying liposomes that had been incubated with the

galactose oxidase solution for 30 min at 37 °C beforehand. The increase in observed fluorescence intensity was only comparable to that in the control experiment in which the galactose-carrying liposome *without* oxidation by galactose oxidase was used. This result suggests that both liposomes were *not* fusing.

Furthermore, when a 0.1 N NaOH solution was injected into the mixture after the experiment (b) was complete, the turbidity gradually decreased (Figure 2-2d) probably due to the disruption of aggregates. These results show that the increase in turbidity is due to the specific recognition of aldehyde groups on the liposome surfaces by the amino group-carrying liposomes, which results in the aggregation of both liposomes mediated by the Schiff bases. The Schiff base is well-known to be easily cleaved by acids and bases.[17] To confirm whether a number of other things could have happened to affect the turbidity measurement under the strong alkaline conditions (after the injection of 0.1 N NaOH), the amounts of aldehyde groups and amino groups in the mixed liposome suspension after the injection of 0.1 N NaOH were compared with those before aggregation. The amounts of aldehyde groups and amino groups were approximately equivalent in each case. Furthermore, the average diameter of liposome mixtures after the injection of 0.1 N NaOH was estimated to be 1150 Å by the dynamic light scattering method (the average diameters of the galactose-carrying liposomes and the amino group-carrying liposomes were 900 and 1400 Å, respectively). These results support the turbidity decreasing gradually because of the disruption of aggregates. To simplify the reaction system hereafter, the enzymatic treatment of galactose-carrying liposomes was carried out for 30 min prior to mixing with the amino group-carrying liposomes.

2-3-2. Effect of DP on the Association Processes

The rate of turbidity change was largely affected by the degree of polymerization of DODA-PMEGal in the liposomes (Figure 2-3). As for liposomes carrying DODA-L-Gal, which has only one galactose residue, there was no increase in turbidity. When the reactivity of the enzyme with galactose-carrying amphiphiles on the liposome surface was examined, the increment of optical density in 30 min due to the production of quinoneimine dye for the DODA-L-Gal liposome was only 14 % of that for the DODA-PMEGal (DP=8.4) liposome. Furthermore, when the amino group-carrying liposome suspension was injected into the suspension of the DODA-L-Gal-containing liposomes that had been incubated with the solution of galactose oxidase for 24 h at 37 °C beforehand, the increase in turbidity was not observed at all. These results show that the reactivity of the enzyme with DODA-L-Gal on the

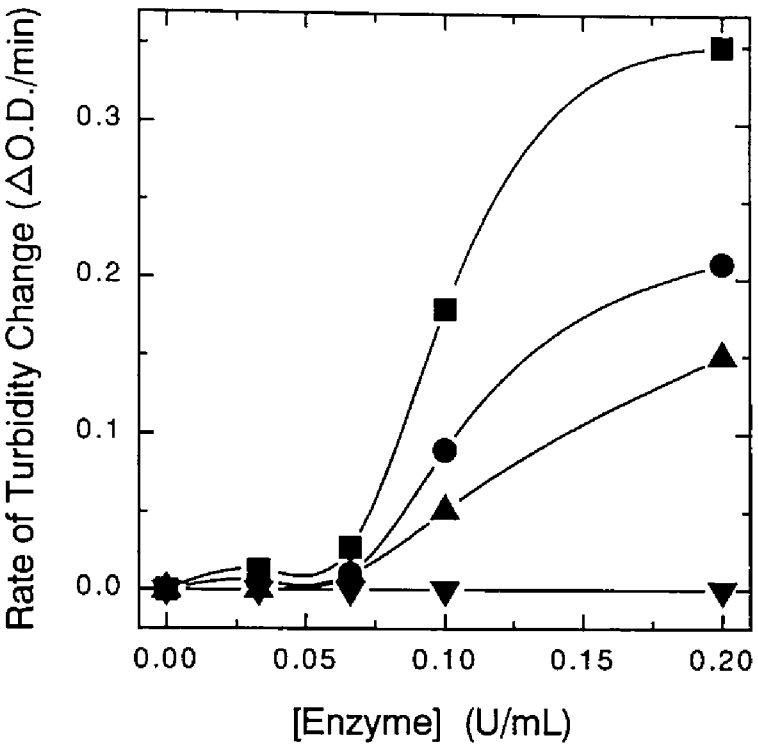

Figure 2-3. Effect of concentration of enzyme on the rate of turbidity change after injection of the amino group-carrying liposome suspension into the galactose-carrying liposome suspension that had been incubated with galactose oxidase for 30 min at 37 °C beforehand: (■) DODA-PMEGal (DP = 15); (●) DODA-PMEGal (DP = 8.4); (▲) DODA-PMEGal (DP = 3.1); (▼) DODA-L-Gal. The contents of galactose-carrying lipid and GGA were 4.5 and 10 mol %, respectively. The concentrations of both liposomes were 100 μg of lipid/mL (HEPES(10 mM, pH 6.0) buffer; wavelength = 350 nm).

liposome surface was very low.

By increasing the degree of polymerization, the rate of turbidity change became larger probably because of the decrease in the steric hindrance. Previously the lectin-induced aggregation of sugar-carrying liposomes was examined.[11,18] The lectin was captured in sugar-carrying long polymer chains on the liposome surface, and it was not so easy for the lectin to bind to sugar residues on the other liposome surface simultaneously, which reduced the rate of turbidity change at high degree of polymerization. In the liposome–liposome system examined here, such a complete capture of the amino group-carrying liposome by the liposome carrying long polymer (PMEGal) chains might not occur because the liposomes are gigantic. Consequently, the increase of the rate of turbidity change with the degree of polymerization of

DODA-PMEGal observed here is understandable.

2-3-3. Effect of Surface Concentration of Aldehyde Group on the Association Processes

The distribution of the galactose-carrying amphiphiles in the liposome was determined by the method described in the Experimental Section. The amount of quinoneimine dye produced after sonication was 8.6 % of that before sonication, which shows that the galactose-carrying amphiphiles were preferentially (85.3 %) distributed in the outer layer of the liposome. Consequently, the number of galactose residues on the outer layer of the liposome was estimated to be about 4300 times as many as that of enzyme molecules when the concentrations of galactose-carrying liposome (DODA-PMEGal (DP=15), 4.5 mol %) and enzyme were 100 μg of lipid/mL and 0.1 unit/mL, respectively.

By varying the concentration of galactose oxidase to be incubated with galactose-carrying liposomes, it was attempted to examine the effect of the concentration of aldehyde groups on the liposome surface on the rate of turbidity change (Figure 2-3). Since the production of aldehyde groups is directly proportional to the concentration of enzyme, the increase in the rate of turbidity change with concentration of enzyme could be expected. The rate of turbidity change, however, did not increase significantly at low concentrations of the enzyme but increased steeply at higher concentrations, which suggests the presence of a threshold value in the recognition of aldehyde groups by amino group-carrying liposomes. This result is in accordance with the steep increase in the turbidity 15 min after the onset of the reaction observed in Figure 2-2a. To realize the stable binding between two kinds of liposomes, the multiple formation of Schiff bases between many aldehyde groups and amino groups might be necessary. This would bring about a threshold phenomenon.

To examine the effect of surface concentration of galactose residues on the rate of turbidity change, liposomes with various molar ratios of DODA-PMEGal (DP=15) and DDPC were prepared. Figure 2-4 shows that the rate of turbidity change increases with the content of DODA-PMEGal (DP=15), in contrast to the results of Figure 2-3. This is probably because the catalytic behavior of the enzyme at interfaces is more complicated compared to that with the free substrate in solution. Further findings about this will be described in Chapter 3.

The role of lipid composition on membrane–membrane dissociation reactions was also investigated: The suspension of the galactose-carrying liposome with various molar ratios of DODA-PMEGal (DP=8.4) and DDPC was incubated with galactose oxidase for 60 min at 37 °C. After the liposome suspension was mixed with the amino group-carrying liposome

suspension, the turbidity increased and leveled off. Subsequently, 0.05 N NaOH was injected into the turbid mixture. The rates of decrease in turbidity had *no* obvious differences for different concentration ratios of DODA-PMEGal to GGA in the studied range (DODA-PMEGal, 1.7-6.6 mol %; GGA, 10 mol %) (data not shown). The number of galactose residues on the liposome surface even at the lowest molar ratio (DODA-PMEGal (DP=8.4), 1.7 mol %) was about 1.4 times as many as that of the amino groups on the liposome surface. Since the growth of the multiple formation of Schiff bases would be restricted due to the steric hindrance, the number of Schiff bases formed until the turbidity leveled off might be approximately similar in each case. Therefore, the surface concentration of aldehyde groups on the liposome might affect the initial association processes between liposomes, but probably not the dissociation processes at lipid–lipid interfaces.

2-3-4. Effects of Membrane Flexibility and Deformability on the Association Processes

The rate of turbidity change due to the association of aldehyde group-carrying liposome with

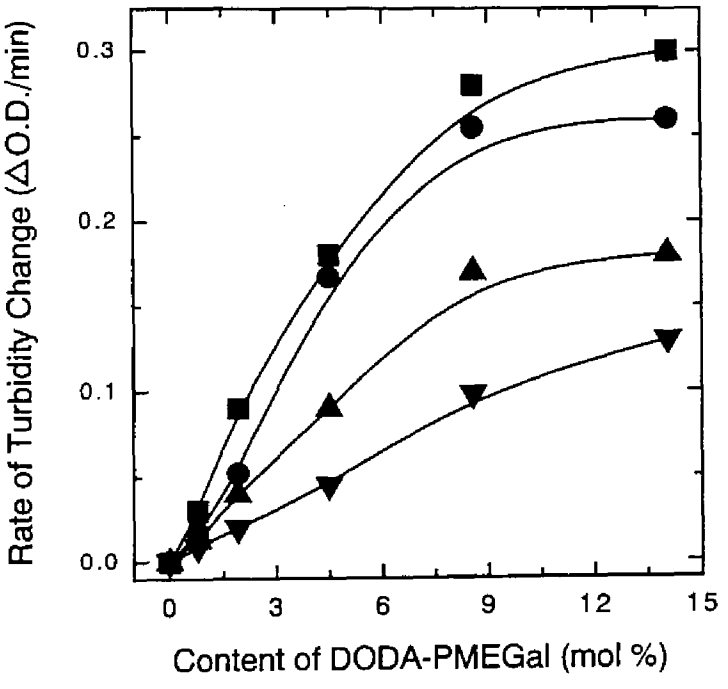

Figure 2-4. Effect of mixing ration of DDPC and DODA-PMEGal (DP = 15) in the liposome on the rate of turbidity change after injection of the amino group-carrying liposome suspension into the galactose-carrying liposome suspension that had been incubated with galactose oxidase for 30 min at 37 °C beforehand: (■) DMPC/GGA liposome; (●) DMPC/GA liposome; (▲) DPPC/GGA liposome; (▼) DPPC/GA liposome. The content of amino group-carrying lipid was 10 mol %. The concentrations of both liposomes were 100 μg of lipid/mL. The concentration of enzyme was 0.1 unit/mL (HEPES(10 mM, pH 6.0) buffer; wavelength = 350 nm).

the amino group-carrying liposome composed of DMPC and GGA was larger than that with the liposome composed of DPPC and GGA. A similar result was obtained when GA was used instead of GGA (Figure 2-4). Since the experiment was carried out at 37 °C, DMPC (T_m = 24 °C) and DPPC (T_m = 42 °C) were in the liquid crystal phase and the gel phase, respectively, where T_m is the temperature of the midpoint of transition. The membrane flexibility and deformability of liposome prepared with DMPC would be, therefore, higher than those of DPPC-liposomes, which makes it easier for amino groups to form the Schiff bases with aldehyde groups.

Previously Kitano *et al.* examined the effect of temperature on the inhibition of trypsin by soybean trypsin inhibitor at the lipid–lipid interface.[4] The K_i value was strongly dependent on the gel–liquid crystal phase transition temperature of the liposome, which supports the importance of deformability of liposomes in the recognition at the lipid–lipid interface.

As shown in Figure 2-4, the rate of turbidity change for the GGA liposome was slightly larger than that for the GA system (the length between a primary amino group and a tertiary amide group of GGA was longer than that of GA by one glycine residue (about 4 Å)). These results show the importance of steric hindrance for the recognition of amino groups by the aldehyde groups.

2-3-5. Effect of Surface Concentration of Amino Group on the Association Processes

To examine the effect of pH in the solution on the rate of turbidity change, a suspension of the amino group-carrying liposome with various pH values was injected into the galactose-carrying liposome suspension that had been incubated with the galactose oxidase solution for 30 min at pH 6 beforehand (Figure 2-5). The rate of turbidity change decreased largely with the increase in pH of the solution after mixing, and at pH > 8.5 no change in turbidity (no aggregation of liposomes) could be observed, which shows the large pH sensitivity of association processes between the liposomes.

By using amino group-carrying liposomes with various ratios of GGA and DMPC, the effect of the surface concentration of amino groups on the rate of turbidity change could be examined. As shown in Figure 2-6, the rate of turbidity change increases with the surface concentration below about 9 mol % of GGA in the liposome and then decreased significantly. The rate of condensation reaction to produce the Schiff base is known to be the largest in the pH range 3 – 5.[19] As a possibility, the pH in the vicinity of the liposome surface with a high content of GGA might become higher than that in bulk solution, which makes it more difficult

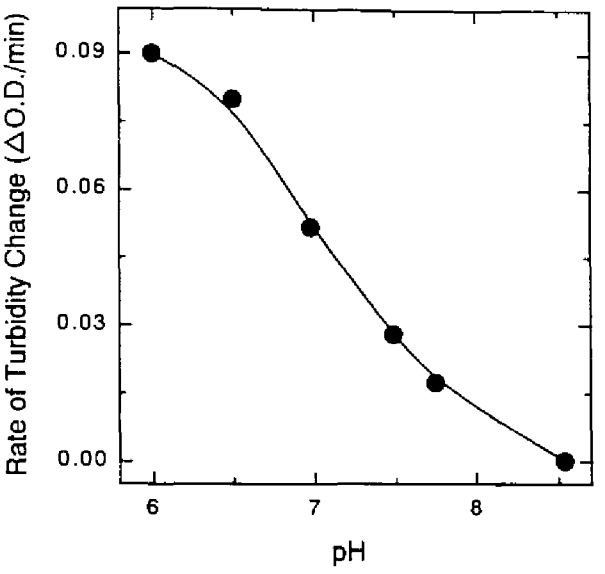

Figure 2-5. Effect of pH in the solution on the rate of turbidity change after injection of the amino group-carrying liposome suspension with various pH values into the galactose-carrying liposome suspension that had been incubated with galactose oxidase for 30 min at 37 °C beforehand. The contents of DODA-PMEGal (DP = 8.4) and GGA were 4.5 and 10 mol %, respectively. The concentrations of both liposomes were 100 μg of lipid/mL. The concentration of enzyme was 0.1 unit/mL. The galactose-carrying liposome was incubated with the enzyme inHEPES (10 mM, pH 6.0) buffer (wavelength = 350 nm).

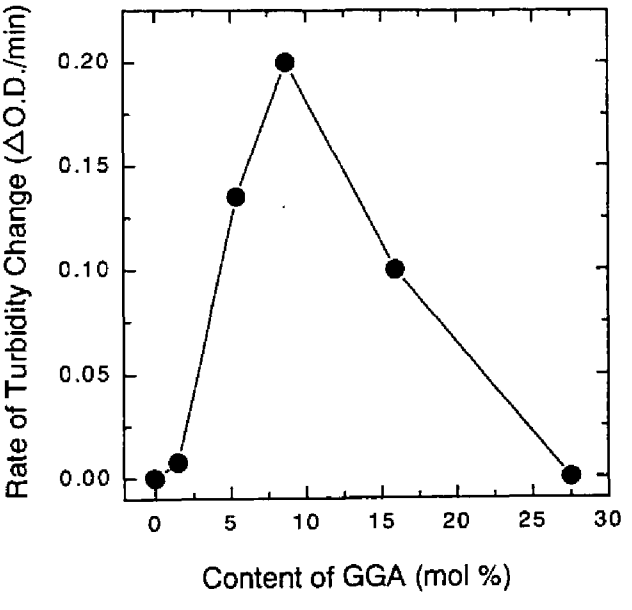

Figure 2-6. Effect of the mixing ratio of DMPC and GGA in the liposome on the rate of turbidity change after injection of the amino group-carrying liposome suspension that had been incubated with galactose oxidase for 30 min at 37 °C beforehand. The content of DODA-PMEGal (DP = 15) was 4.5 mol %. The concentrations of both liposomes were 100 μg of lipid/mL. The concentration of enzyme was 0.1 unit/mL (HEPES (10 mM, pH 6.0) buffer; wavelength = 350 nm).

to form Schiff bases between two kinds of liposomes. Therefore, the surface concentration of amino groups strongly affects the rate of turbidity change. This result is consistent with the pH sensitivity of association processes described earlier.

2-4. Conclusions

Primary hydroxyl groups of galactose residues bound to the polymer chains existing on the liposome surface could be oxidized by galactose oxidase and converted into aldehyde groups. The Schiff bases formed between aldehyde groups and amino groups on the other liposome surfaces resulted in aggregation of the liposomes. The rate of turbidity change depended on the densities of galactose and amino groups on the liposome surfaces, the distance from the liposome surface to the galactose residue and amino end groups, and the membrane flexibility and deformability. Those results also suggest the importance of morphology of the cell surface in cell–cell recognition phenomena such as lymphocyte cytotoxicity.

References

(1) Stevenson, B. R.; Gallin, W. J.; Paul, D. L. *Cell-Cell Interactions;* Oxford University Press: New York, 1992.

(2) Müller, W.; Ringsdorf, H.; Rump, E.; Wildburg, G.; Zhang, X.; Angermaier, L.; Knoll, W.; Liley, M.; Spinke, J. *Science* **1993**, *262*, 1706.

(3) Chiruvolu, S.; Walker, S.; Israelachvili, J.; Schmitt, F-J.; Leckband, D.; Zasadzinski, J. A. *Science* **1994**, *264*, 1753.

(4) Kitano, H.; Kato, N.; Tanaka, N.; Ise, N. *Biochim. Biophys. Acta* **1988**, *942*, 131.

(5) Kitano, H.; Kato, N.; Ise, N. *J. Am. Chem. Soc.* **1989**, *111*, 6809.

(6) Novogrodsky, A. *J. Immunol.* **1975**, *114*, 1089.

(7) Kobayashi, K.; Sumitomo, H.; Ina, Y. *Polym. J.* **1985**, *17*, 567.

(8) Kitano, H.; Akatsuka, Y.; Ise, N. *Macromolecules* **1991**, *24*, 42.

(9) Matsumura, S.; Kubokawa, H.; Toshima, K. *Makromol. Chem., Rapid Commun.* **1993**, *14*, 55.

(10) Kitano, H.; Wolf, H.; Ise, N. *Macromolecules* **1990**, *23*, 1958.

(11) Kitano, H.; Sohda, K.; Kosaka A. *Bioconjugate Chem.* **1995**, *6*, 131.

(12) Cooper, J. A. D.; Smith, W.; Bacila, M.; Medina, H. *J. Biol. Chem.* **1959**, *234*, 445.

(13) Avigad, G.; Amaral, D.; Asensio, C.; Horecker, B. L. *J. Biol. Chem.* **1962**, *237*, 2736.

(14) Pesez, M.; Bartos, J. *Calorimetric and Fluorimeter Analysis of Organic Compounds and Drugs;* Marcel Dekker: New York, 1974; p 264.

(15) Fields, R. *Biochem. J.* **1971**, *124,* 581.

(16) Sharon, N. *Complex Carbohydrates; Their Chemistry, Biosynthesis, and Functions;* Addison-Wesley: Reading, MA, 1975.

(17) March, J. *Advanced Organic Chemistry; Reactions, Mechanisms, and Structure, 2nd ed.;* McGraw-Hill: New York, 1977; p 806.

(18) Kitano, H.; Ohno, K. *Langmuir* **1994**, *10*, 4131.

(19) Pine, S. H. *Organic Chemistry; 5th ed.,* McGraw-Hill: New York, 1987; p 248.

Chapter 3

Catalytic Properties of Galactose Oxidase to Galactose-Carrying Amphiphiles in Liposomes

3-1. Introduction

Galactose oxidase oxidizes exposed primary hydroxyl groups in nonreducing, terminal galactose and *N*-acetylgalactosamine residues.[1] The galactose oxidase/NaB[^{3}H]$_4$ method is well known and widely used as a technique to label cell-surface glycoconjugates.[2-4] It has been found that only a portion of glycolipids is available to galactose oxidase, and different glycolipids vary in their susceptibilities to the enzyme.[5-8] Lampio *et al.* and Masserini *et al.* previously reported the interaction of galactose oxidase with the major red-cell glycolipid (globoside) and G_{M1} ganglioside, respectively, in liposome suspensions.[7,8]

As described in Chapter 2, by incorporating the galactose-carrying amphiphiles in liposome, the author could examine the recognition of amino group-carrying liposomes by galactose-carrying liposomes that had been treated with galactose oxidase beforehand, as a model system of induction of lymphocyte cytotoxicity.[9] In that experiment, the author found a very interesting property of galactose oxidase that its affinity for the galactose residues in the polymer chains on the liposome surface was much higher than that for free galactose.

To verify what happens in the catalytic reaction of enzyme to the carbohydrate chains on the membrane surfaces, galactose-carrying homopolymers and copolymers and galactose-carrying amphiphiles were prepared by using the galactose-carrying vinyl monomer (MEGal) in this study. The author has examined kinetic analyses on the catalytic behavior of galactose oxidase at various reaction fields including liposome surfaces. It will be described below why galactose oxidase exhibits enhanced affinity to the galactose residues on the membrane surfaces.

3-2. Experimental Section

3-2-1. Materials

A lipophilic radical initiator (DODA-501)[10] was synthesized form *N,N*-dioctadecylamine (DODA, Fluka, Switzerland) and 4,4'-azobis(cyanovaleric acid) (V-501, Wako Pure Chemicals, Osaka, Japan) as described in Chapter 1. A galactose-carrying vinyl monomer, 2-

(methacryloyloxy)ethyl-β-D-galactopyranoside (MEGal),[11] was prepared as described in Chapter 2. 1,3-Di-*O*-hexadecylglycerol was synthesized by the reaction of epichlorohydrin and 1-haxadecanol in the presence of sodium hydride at 80 °C overnight.[12] A polymerizable lipid, bis(*trans,trans*-2,4-octadecadienoyl)phosphatidylcholine (DDPC), was kindly donated by the Japan Fat and Oil Co., Tokyo, Japan. Galactose oxidase (from *Dactylium dendroides*, 240 unit/mg) was from Sigma. Other reagents were commercially available. Deionized water was distilled before use.

3-2-2. Preparation of Galactose-Carrying Homopolymer

A homogeneous polymerization of MEGal was carried out using 4,4'-azobis(cyanovaleric acid) (V-501) and cysteamine hydrochloride as initiator and chain transfer reagent, respectively, in methanol–water (1:3) at 70 °C for 24 h. After evaporation of the solvent, the oily product was washed several times with acetone and dried *in vacuo*. The slightly yellow powder obtained was dissolved in water again and repeatedly ultrafiltrated with water (Amicon Model 8010; membrane, YM-1; exclusion limit, 1000) to remove other small impurities. The solution retained above the membrane was lyophilized. Further, the filtrate which contained the products with a lower degree of polymerization was concentrated, purified by passage through a GPC column (Sephadex G-10, i.d. 1.5 x 25 cm; mobile phase, water), and lyophilized. The syntheses of polymer and/or oligomer with different degrees of polymerization (DPs) were carried out under conditions with fixed concentrations of initiator and monomer and varying amount of chain transfer agent. The DP values of MEGal homopolymers were determined by the conductometric titration of the amino group at the end of the polymers with a N/100 NaOH aqueous solution.

3-2-3. Preparation of Poly(acrylamide-*co*-2-(methacryloyloxy)ethyl-β-D-galactopyranoside)

A copolymerization of MEGal (151 mg, 0.514 mmol) and acrylamide (AAm, 37 mg, 0.514 mmol) was carried out using V-501 (2.9 mg, 0.01 mmol) and cysteamine hydrochloride (5.8 mg, 0.051 mmol) as initiator and chain transfer reagent, respectively, in methanol–water (1:3) at 70 °C. The polymers with different DP values were synthesized as described in the preparation of homopolymer, namely, under conditions with fixed concentrations of initiator and monomer and varying amounts of chain transfer agent. The product was purified in the same way as described above for the homopolymers. The molecular weight of the copolymer was determined conductometrically. The monomer ratio (MEGal:AAm) in the copolymers was

evaluated by elemental analysis and ^{1}H-NMR (in D_2O): After the molecular weight of a copolymer sample was estimated to be 1200 by conductometric titration, the monomer ratio (MEGal:AAm) in the copolymer was determined to be 1:7.6 by the ratio of integral absorption of ^{1}H-NMR (calculated from the signals of 1.1–1.3 and 1.4–1.9 ppm corresponding to methyl protons of MEGal unit and methylene protons of AAm, respectively). Furthermore, the validity of supposed chemical structure was clarified by elemental analysis. Anal. Calcd. for $C_2H_8NClS(C_{12}H_{20}O_8)_{1.3}(C_3H_5\text{-}ON)_{9.7} \cdot 4H_2O$: C, 44.67; H, 7.29; N, 12.00. Found: C, 44.09; H, 7.27; N, 12.20.

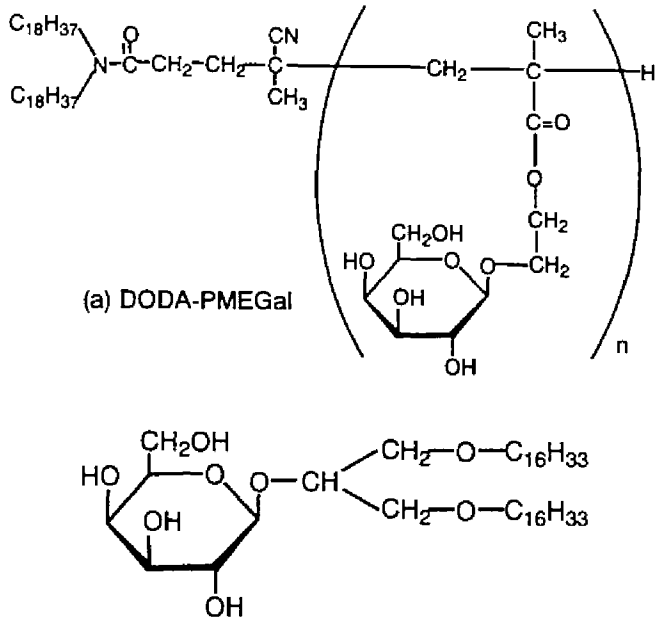

Figure 3-1. Chemical structures of (a) DODA-PMEGal and (b) DHDG-Gal.

3-2-4. Preparation of Galactose-Carrying Amphiphiles by Polymerization

Details of the preparation were described in Chapter 2.[9,13,14] Briefly, MEGal and DODA-501 were dissolved in THF, and after N_2 gas was bubbled for several minutes, the solution mixture was incubated in a tightly sealed test tube at 70 °C for 24 h. After evaporation of the solvent *in vacuo*, the viscous oil was washed with *n*-hexane several times to remove unreacted initiator by centrifugation at 15 000 rpm and 20 °C for 15 min. After decantation, the precipitate was dried *in vacuo* and dispersed in water. The suspension was purified by passage through a GPC column (Sephacryl S-200, i.d. 2 x 18 cm; mobile phase, water) and lyophilized. The DP value

of the amphiphile (Figure 3-1a) was determined by elemental analysis. DODA-PMEGal (DP=8.5) Anal. Calcd. for $C_{42}H_{82}N_2O(C_{12}H_{20}O_8)_{8.5}$: C, 55.51; H, 8.15; N, 0.90. Found: C, 55.43; H, 8.42; N, 0.91.

3-2-5. Preparation of Galactose Lipid by Using Trichloroacetimidate of Carbohydrate

The preparation procedure followed the method of Minamikawa *et al.*:[15] To molecular sieves 4 Å (200 mg, dried *in vacuo* prior to use), 1,3-di-*O*-hexadecylglycerol (300 mg, 0.55 mmol) and 2,3,4,6-tetra-*O*-*D*-acetylgalactopyranosyl-1-α-trichloroacetimidate (273 mg, 0.55 mmol) in dry dichloromethane (10 mL) were added. The solution was cooled at 0 °C, and trimethylsilyl trifluoromethanesulfonate (123 mg, 0.55 mmol) was added dropwise to the solution. After the solution was stirred at 0 °C for 6 h, anhydrous pyridine (40 mL) was added dropwise at 0 °C and the solution was diluted with ethyl acetate (20 mL) at room temperature. After filtration, the filtrate was washed with a saturated sodium bicarbonate solution (30 mL) and saturated aqueous sodium chloride solution (30 mL) successively. The organic layer was dried over anhydrous sodium sulfate, and the solvent was removed under reduced pressure. The residual oil was purified by silica gel chromatography with a 4:1 toluene/acetone mixture eluent to give 1,3-di-*O*-hexadecyl-2-*O*-(β-*D*-tetraacetylgalactopyranosyl)glycerol (157 mg). A 28 % methanol solution of sodium methoxide (50 mL) was added to 1,3-di-*O*-hexadecyl-2-*O*-(β-*D*-tetraacetylgalactopyranosyl)glycerol (150 mg) in a mixture of dry methanol (2.5 mL) and dry DMF (2 mL). The reaction was complete after 2 h at room temperature. The solution was neutralized with ion-exchange resins (Dowex 50W-X4, H^+ form), filtered, and evaporated. The residue was chromatohraphed by silica gel chromatography with a 7:1 chloroform/methanol mixture eluent. The compound was further purified by recrystallization from methanol to give 1,3-di-*O*-hexadecyl-2-*O*-(β-*D*-galactopyranosyl)glycerol (DHDG-Gal, Figure 3-1b) as a white powder (54 mg). ^{1}H-NMR ($CDCl_3$): δ 0.88 (t, 6H, CH_3), 1.1–1.4 (m, 52H, CH_2 of alkyl chains), 1.57 (br, 4H, OCH_2CH_2), 2.8–4.1 (m, 19H, protons of galactose moiety, that of glycerol moiety, and OCH_2CH_2), 4.43 (d, J = 7.6 Hz, 1H, anomeric proton of pyranose ring). IR (KBr, cm^{-1}): O-H stretching of galactose moiety, 3350–3500; ν_{as} C–H, 2917; ν_s C–H, 2850; C–O–C stretching of glycerol moiety, 1040–1130. Anal. Calcd. for $C_{41}H_{82}O_8$: C, 70.02; H, 11.78. Found: C, 70.01; H, 11.83.

3-2-6. Preparation of Galactose-Carrying Liposomes

DDPC (24 mg) was dissolved in chloroform (2 mL) in a small, round-bottomed flask. After evaporation of the solvent, the thin lipid membrane was dispersed in an *N*-(2-

hydroxyethyl)piperazine-*N*'-2-ethanesulfonic acid (HEPES) buffer (pH 6.5, 10 mM, 3 mL) in which DODA-PMEGal (6 mg) had been dispersed beforehand. The dispersion was sonicated (Astrason W-385, Heat System-Ultrasonics, Inc., New York) for 3 min while N_2 gas was passed through the suspension. To remove large aggregates, the liposome suspension obtained was passed through a membrane filter (SLGV025LS, Gelman Sciences; pore size, 0.22 μm) and irradiated in a quartz cell by a UV lamp (HB-251A, Ushio, Tokyo, Japan) at room temperature for 4 h to polymerize the dienoyl groups of DDPC. The progress of polymerization was followed by the decrease in absorbance at 258 nm by using a UV-visible spectrophotometer (Ubest-35, Japan Spectroscopic Co., Tokyo, Japan). Unpolymerized galactose-carrying liposome was also prepared without UV irradiation.

3-2-7. Characterization of Liposomes

Formation of liposomal structure was confirmed by the fluorescence dye incorporation technique using Eosin Y as a probe[10,16] (excitation at 305 nm, emission at 571 nm, FP-777, Japan Spectroscopic Co.). Hydrodynamic diameter of the liposomes was estimated as 1200 Å on average by the dynamic light scattering (DLS) technique (DLS-7000, Otsuka Electronics, Hirakata, Japan; light source He-Ne laser, 632.8 nm).

3-2-8. Enzyme Activity Measurements

The oxidation reaction of galactose residues catalyzed by galactose oxidase was followed using a spectrophotometric method:[17,18] Hydrogen peroxide produced by the oxidation of galactose was reduced by the reaction with 4-aminoantipyrine and phenol catalyzed by horseradish peroxidase (HRP), and the increase in optical density at 500 nm due to the production of quinoneimine dye was measured for 5 min by the spectrophotometer thermostatted at 25 °C. The initial increase in optical density per minute was calculated from the initial linear portion of the curve (ε = 12 000). One unit of galactose oxidase causes the formation of 1 μmol of hydrogen peroxide/min at 25 °C. The stock solution of galactose oxidase was diluted to the appropriate concentration, and the catalytic activity of the enzyme was checked just prior to use.

3-2-9. Kinetic Analyses

The initial velocities of oxidation of galactose at various reaction fields were measured by using the spectrophotometric method described above, in which sufficient amount of HRP, aminoantipyrine, and phenol were added in the reaction system, that is, the reaction of galactose oxidase to galactose residues is the rate-determining step. The substrate

concentrations at various reaction fields were standardized on the basis of the number of galactose residues. Previous report (see Chapter 2) showed that the galactose-carrying amphiphiles were preferentially (about 80 %) distributed in the outer layer of liposomes.[9] Therefore, in the case using sugar-carrying liposomes as a substrate, the author determined the substrate concentration based on the number of all galactose-carrying lipids incorporated inside and outside the liposome. The V_{max} and K_m values of the enzyme reaction were determined by the Hanes-Woolf plot (Equation 1).[19]

$$[S]/v = (1/V_{max})[S] + K_m/V_{max} \qquad (1)$$

where [S] is the concentration of substrate (total concentration of galactose residues in the reacting solution), v is the initial reaction velocity, V_{max} is the limiting value of initial reaction velocity, and K_m is the Michaelis constant. Graphing [S]/v vs [S] yields a straight line where the slope is $1/V_{max}$, the y-intercept is K_m/V_{max}, and the x-intercept is $-K_m$. The data in the figures and table represent the mean values of two measurements. The uncertainties of the kinetic parameters were within 10 %.

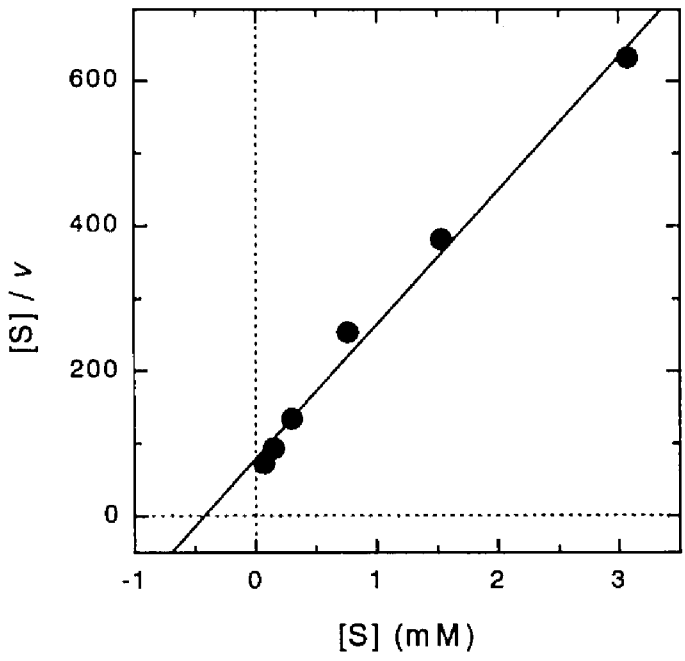

Figure 3-2. Hanes-Woolf plot for the catalytic reaction of galactose oxidase to a galactose-carrying homopolymer (PMEGal, DP = 16). In the HEPES buffer (10 mM, pH 6.5). [Enzyme] = 0.05 units/mL.

Table 3-1. Kinetic Constants of Galactose Oxidase for Various Galactose Residues at Different Reaction Fields[a]

Substrate	DP[b]	K_m (mM)	k_{cat} (mM mL/ min units)	$10^2\ k_{cat}/K_m$ (mL/min units)
Galactose	-	58	1.0	1.7
MEGal	1	4.2	0.018	0.44
Lactose	-	528	0.39	0.081
PNPG	-	22	0.40	1.8
MG	-	52	1.6	3.0
Homopolymer	2.1[c]	2.6	0.23	8.8
	16[c]	0.35	0.091	26
	39[c]	0.13	0.090	69
	53[c]	0.13	0.14	110
Copolymer	11[c,d]	3.0	0.18	6.0
	13[c,e]	0.76	0.24	32
	23[c,f]	0.16	0.14	88
	54[c,g]	0.18	0.042	23
Polymerized liposome	1[h]	N.D.[i]	N.D.[i]	N.D.[i]
	8.5[j]	0.0030	0.012	400
Unpolymerized liposome	8.5[j]	0.0027	0.011	390

[a] In the HEPES buffer (10 mM, pH 6.5) at 25 °C. The ranges of substrate concentration in the experiments using low molecular weight substrates, polymers, and liposomes were 1–100 mM, 0.01–10 mM, and 10^{-4}–0.1 mM, respectively. In the case of lactose, the range was 1 mM to 1 M. Substrate concentrations were standardized on the basis of the number of galactose residues (see Experimental Section). The concentrations of enzyme in the experiment using liposomes and other all substrates were 0.25 and 0.05 units/mL, respectively. [b] Degree of polymerization. [c] Determined by the conductometric method. [d] MEGal:AAm, = 1:7.6. [e] MEGal:AAm = 1.1:1. [f] MEGal:AAm = 1:1.1. [g] MEGal:AAm = 1:5.7. [h] DHDG-Gal was used in place of DODA-PMEGal. [i] Not detected. [j] Determined by the elemental analysis.

3-3. Results and Discussion

3-3-1. Catalytic Behavior of Galactose Oxidase for Galactose-Carrying Polymers

After the incubation of galactose-carrying homopolymer with a solution of galactose oxidase, the production of H_2O_2 was confirmed by the spectrophotometric method. Figure 3-2 shows a typical example of Hanes-Woolf plot for the catalytic reaction of galactose oxidase to a galactose-carrying homopolymer (PMEGal, DP = 16). The affinity (estimated by $1/K_m$ values) of galactose oxidase for PMEGal was larger than those for free galactose and *β-D*-galactopyranosides (MEGal, lactose, PNPG and MG) (Table 3-1). Furthermore, by varying the degree of polymerization of PMEGal, the effect of the length of polymer chains on K_m was examined (Figure 3-3a). The larger the molecular weight of PMEGal was, the larger the

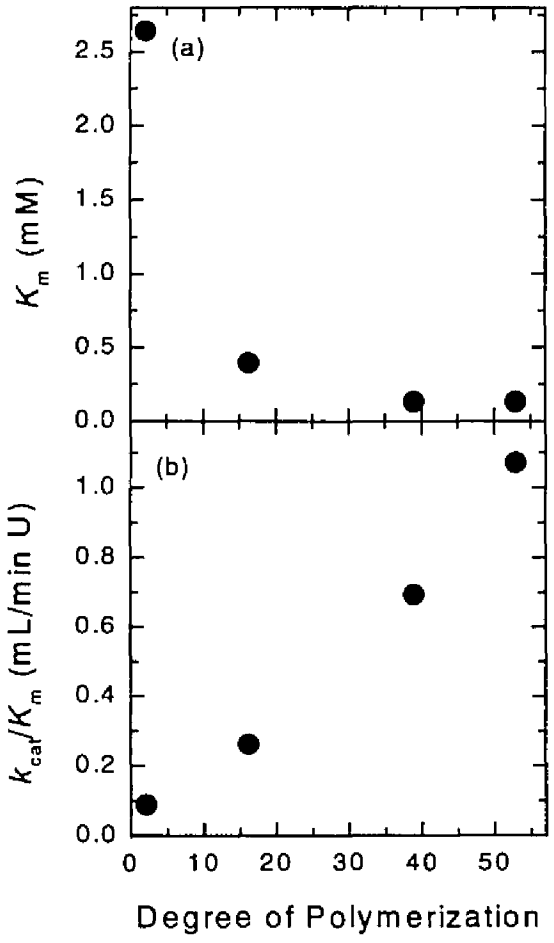

Figure 3-3. Effect of the degree of polymerization of homopolymer (PMEGal) on K_m and k_{cat}/K_m values at 25 °C. In the HEPES (10 mM, pH 6.5) buffer. [Enzyme] = 0.05 units/mL.

affinity of galactose oxidase for PMEGal. These results suggest that galactose oxidase can effectively recognize and oxidize galactose residues which are suspended repeatedly from the polymer chain, probably because the enzyme can easily access the galactose moiety in the vicinity of galactose which has been just oxidized. This phenomenon is consistent with the previous report that the galactose oxidase from *Polyporus circinatus* has a high affinity for galactomannan guaran (polysaccharide constituted from galactose and mannose).[18]

To verify the enhancement of the affinity of galactose oxidase for the substrates sequentially distributed, a similar experiment was carried out by using copolymers of MEGal and acrylamide (inert monomer for galactose oxidase). The affinity of galactose oxidase for the galactose residues in the copolymers with large DP values was comparable to those in the homopolymers with comparable DP values (see Table 3-1), whereas the affinity for the galactose residues in the copolymer with a small DP value seemed to be smaller than that in the homopolymer with a comparable DP value. Since the spatial density of galactose residues existing in the copolymer chain is smaller than that in the homopolymer, the unexpectedly large affinity of the enzyme for the galactose residues in the copolymers with a large DP value shows that the distance between MEGal residues in the copolymers (as for the copolymer with the monomer ratio 1:5.7, for example, 17 Å on average) is still small enough for the enzyme to access the galactose moieties one after another.

Furthermore, the k_{cat}/K_m value, which represents the catalytic efficiency of galactose oxidase for PMEGal, increased with the degree of polymerization of homopolymers (Figure 3-3b), which strongly suggests that the catalytic behavior of galactose oxidase represents an increased efficiency for the PMEGal due to the localization of substrates along the polymer chain.

3-3-2. Catalytic Behavior of Galactose Oxidase for Galactose-Carrying Liposomes

Next, to examine catalytic behavior of galactose oxidase at lipid bilayer–liquid interfaces, we prepared, from the lipophilic radical initiator and MEGal, the galactose-carrying amphiphiles (DODA-PMEGal), which have galactose-carrying polymer chain as a hydrophilic group. A lipid carrying only one galactose residue (DHDG-Gal) was used as a reference.

When the galactose-carrying liposome consisted of DHDG-Gal and polymerized lipid (DDPC) was incubated with the solution of galactose oxidase, no production of H_2O_2 was confirmed by the spectrophotometric method, which contrasts to the results for *β-D*-galactopyranosides with small molecular weights (Table 3-1). Previously, Lampio *et al.*

showed that galactose oxidase cannot oxidize the galactosyl residue of ceramide dihexoside in liposomes, probably because its carbohydrate moiety is too close to the membrane surface.[7] Since the galactose residue of DHDG-Gal is directly attached to the glyceryl group, galactose oxidase would not easily approach the substrate, and therefore, the present result is understandable.

When the similar experiment was carried out on the liposome carrying the DODA-PMEGal, on the other hand, the production of H_2O_2 was definitely confirmed spectrophotometrically, which shows that the galactose-carrying polymer chain functions as a substrate for galactose oxidase not only in bulk solution but also at the lipid bilayer–liquid interface. The K_m value for the galactose-carrying liposome (DODA-PMEGal (DP = 8.5), 0.0030 mM) was much lower than that for the galactose-carrying homopolymer (PMEGal (DP=16), 0.35 mM) (see Table 3-1). Despite the steric disadvantage that the reaction field is above the lipid bilayer surface, the affinity of galactose oxidase for the galactose-carrying polymer chains on the liposome surface is much higher than that for PMEGal in bulk solution.

The galactose-carrying liposomes prepared here probably bring about the phase separation (or in other words, cluster formation) of the galactose-carrying amphiphiles in the liposome by the two-dimensional photo-polymerization of DDPC molecules.[20] To verify clustering of galactose-carrying polymers on the liposome surface, differential scanning calorimetry (DSC) with DODA-PMEGal/DDPC (unpolymerized) mixed liposomes was carried out. This experiment showed a sharp calorific change around 25 °C which is the temperature of the midpoint of gel–liquid crystal transition (T_m) of DDPC, indicating the phase separation due to the respective lipid molecules. If the different lipid molecules are compatible, the DSC curve would exhibit a broad calorific change. Therefore, the DODA-PMEGal/DDPC mixed liposome system is expected to show the phase-separated structure below 25 °C, even in the case when DDPC molecules are not polymerized. More importantly, when the DDPC molecules are polymerized, the Gal-carrying liposomes would show the phase-separated structure. In this phase-separated structure, galactose oxidase, which has attacked the amphiphile, will be surrounded by the galactose residues localizing on the liposome surface and, consequently, the K_m value well be decreased. This result is in agreement with the report by Masserini *et al.*[8] that the K_m value of G_{M1} ganglioside in vesicle was smaller than that of $DesG_{M1}$ (oligosaccharide portion of G_{M1} ganglioside) in bulk solution.

The k_{cat} value, which is defined as the number of substrate molecules converted into

product per enzyme molecule per unit time, of galactose oxidase for the DODA-PMEGal/polymerized DDPC liposomes was lower than those of free galactose and PMEGals, whereas the k_{cat}/K_m value, which represents the catalytic efficiency of an enzyme, of galactose oxidase for the liposomes was larger than those for free galactose and MEGal, and comparable to that for PMEGals (Table 3-1). Since the galactose-carrying polymer chains at liquid–polymerized liposome interface are clustered, the motion of the enzyme molecule attached to the PMEGal domain above the liposome surface might be restricted, and therefore, it is understandable that the turnover number (k_{cat}) of galactose oxidase for DODA-PMEGal was smaller than those for galactose, MEGal and PMEGal. However, the clustering of the

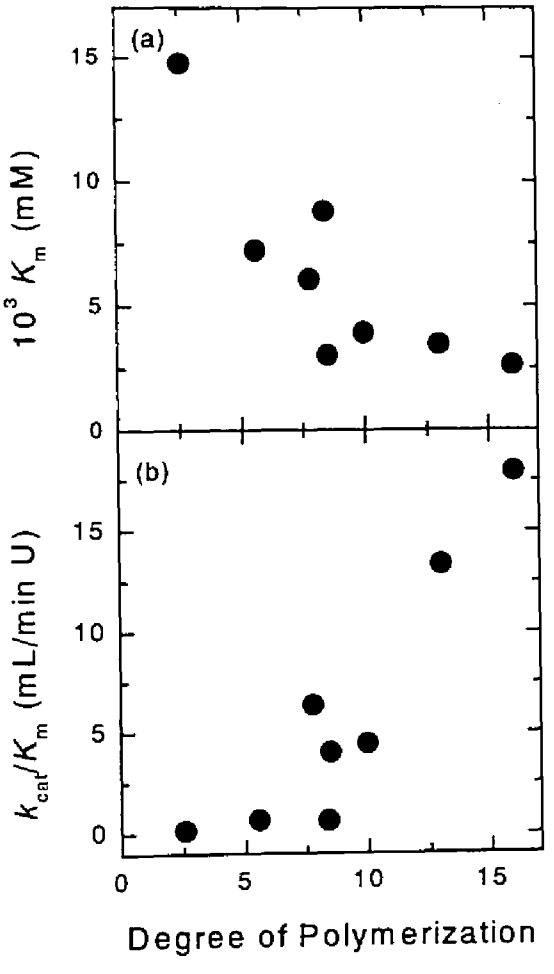

Figure 3-4. Effect of the degree of polymerization of DODA-PMEGal on K_m and k_{cat}/K_m values at 25 °C. [Enzyme] = 0.25 units/mL.

galactose-carrying polymer chains might enhance further the affinity of the enzyme for the substrate, which would consequently make the catalytic efficiency (k_{cat}/K_m) of galactose oxidase for the galactose-carrying liposomes larger than those for small molecular weight *β-D*-galactopyranosides.

Furthermore, the effect of the degree of polymerization of DODA-PMEGal on the catalytic behavior of galactose oxidase was examined. As shown in Figure 3-4a, the K_m value decreases with the degree of polymerization of DODA-PMEGal. Since the distance from the liposome surface to the end galactose residues increases with the DP value, galactose oxidase would be able to more easily approach the substrates above the liposome surface as the DP value becomes larger. It is worth noting that the increase in the degree of polymerization enhanced the affinity of galactose oxidase for galactose residue not only in the bulk solution but also at the lipid bilayer–liquid interfaces. The k_{cat}/K_m showed an increase with the DP value of DODA-PMEGal (Figure 3-4b), due to the decrease in the K_m value with DP.

Next, by varying the weight percents of DODA-PMEGal (DP = 8.5) included in the liposome, one can examine the effect of surface concentration of galactose-carrying amphiphiles on the affinity of galactose oxidase. Figure 3-5a shows that the K_m value was not significantly dependent on the surface concentration of galactose-carrying amphiphiles (DP = 8.5) above 10 wt.% (3.4 mol %). Previously, Masserini *et al.*[8] and Cestaro *et al.*[21] investigated the catalytic properties of galactose oxidase and neuraminidase, respectively, for gangliosides on the liposome surface. They showed that the greatest rates of enzymatic reaction were obtained at an optimal proportion of gangliosides in the liposome. These phenomena were explained by the enhanced hydrogen-bonding interaction between the carbohydrate residues of adjacent ganglioside molecules with an increase in the percentage of the ganglioside. The hydrophilic group of DODA-PMEGal used in this experiment is a polymethacrylate chain and would be more flexible than ganglioside. Therefore, the interaction between carbohydrate residues on the liposome composed of DODA-PMEGal is probably smaller than that between gangliosides, thus, the optimum content of DODA-PMEGal in the liposome for the enzymatic reaction would not be observed in our experiment. The author also thinks that this phenomenon is partly because the local concentration of galactose residue which the galactose oxidase can recognize is similar at any surface concentration due to the phase separation of DODA-PMEGal on the surface of polymerized DDPC liposome.

Furthermore, the k_{cat}/K_m value increased with the content of DODA-PMEGal in the

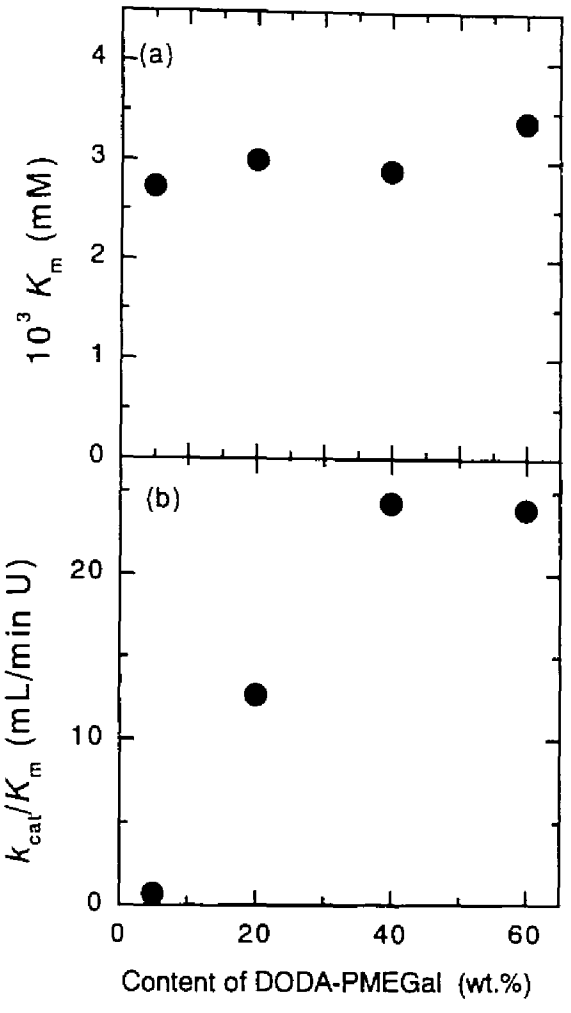

Figure 3-5. Effect of the content of DODA-PMEGal in the liposome on K_m and k_{cat}/K_m values at 25 °C. [Enzyme] = 0.25 units/mL.

galactose-carrying liposome (Figure 3-5b), which means that the enzyme effectively and repeatedly catalyzes oxidation of the substrates which exist on the surface of the same liposome. This is probably because it is not necessary for the enzyme molecule to migrate from the liposome surface about to be catalyzed by it to other liposome surfaces, and the enzyme only needs to oxidize the galactose residues on the same liposome.

Moreover, by using galactose-carrying liposome with unpolymerized DDPC, one can examine the effect of membrane fluidity on the catalytic behavior of galactose oxidase. As shown in Figure 3-6a, the K_m value of galactose oxidase for the unpolymerized galactose-carrying liposome is larger than that for the polymerized galactose-carrying liposome above the T_m of unpolymerized DDPC (25 °C) and comparable below 25 °C. Similar tendency was observed in the Arrhenius plots of k_{cat} (Figure 3-6b).

The membrane fluidity of the unpolymerized galactose-carrying liposome above 25 °C would be higher than that of polymerized one, which makes it difficult for galactose oxidase to face the domain of the galactose-carrying polymer chains on the unpolymerized fluid liposome surface, because the PMEGal chains would not be localized above 25 °C. Previously, Kitano *et al.* examined the effect of temperature on the inhibition of trypsin by soybean trypsin inhibitor

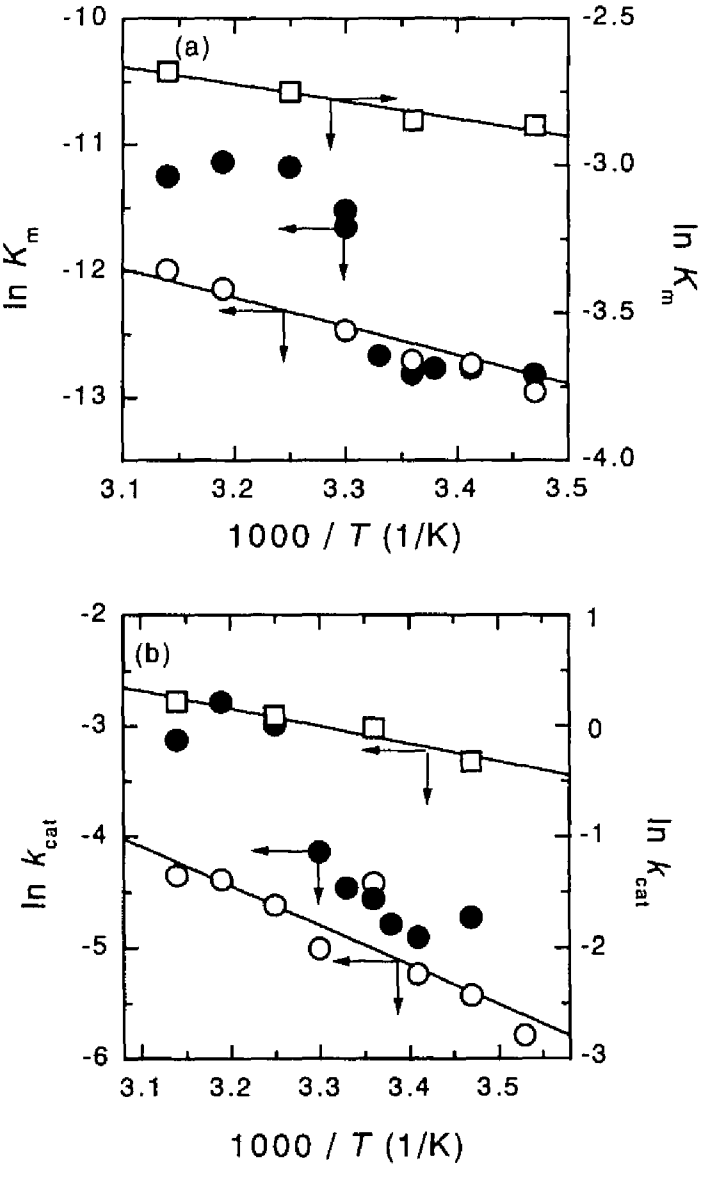

Figure 3-6. van't Hoff and Arrhenius plots of enzymatic reaction for various galactose residues. In the HEPES (10 mM, pH 6.5) buffer. [Enzyme] = 0.25 and 0.05 units/mL for liposomes and free galactose, respectively. Contents of DODA-PMEGal (DP = 8.5) in the liposome, 20 wt.%. (○) polymerized liposome; (●) unpolymerized liposome; (□) free galactose. The units of K_m and k_{cat}/K_m are (molarity) and (millimolar milliliters per minute units), respectively.

at lipid–lipid interfaces.[22] The recognition processes at interfaces were strongly dependent on the gel–liquid crystal phase transition temperature of the liposomes, which supports the importance of fluidity of liposome membranes in the oxidation of MEGal residues by the enzyme at lipid bilayer–liquid interfaces.

3-4. Conclusions

The recognition of galactose residues on the liposome surface by galactose oxidase was more effective compared to those of free galactose and other small *β-D*-galactopyranosides. The affinity of galactose oxidase for sugar residues on the surface of liposomes was dependent on the length of galactose-carrying polymer chain and cluster formation of the amphiphiles on the liposome surface, but not significantly influenced by the surface density of galactolipids on liposomes. The present study indicates that the spatial distribution of substrates significantly affects the catalytic behavior of the enzyme. More importantly, the clustering-effect of sugar residues enhances the affinity of sugar-recognizing proteins not only lectins but also enzymes, which would be valuable information in carbohydrate chain chemistry and polymer science.

References

(1) Suzuki, Y.; Suzuki, K. *J. Lipid Res.* **1972**, *13*, 687.

(2) Eccleston, E. D.; White, T. W.; Howard, J. B.; Hamilton, D. W. *Mol. Peprod. Dev.* **1994**, *37*, 110.

(3) Enrich, C.; Gahmberg, C. G. *Biochem. J.* **1985**, *227*, 565.

(4) Kumarasamy, R.; Blough, H. A. *Arch. Biochem. Biophys.* **1985**, *236*, 593.

(5) Stewart, R. J.; Boggs, J. M. *Biochemistry* **1993**, *32*, 5605.

(6) Lampio, A.; Rauvala, H.; Gahmberg, C. G. *Eur. J. Biochem.* **1986**, *157*, 611.

(7) Lampio, A.; Siissalo, I.; Gehmberg, C. G. *Eur. J. Biochem.* **1988**, *178*, 87.

(8) Masserini, M.; Sonnino, S.; Ghidoni, R.; Chigormo, V. *Biochim. Biophys. Acta* **1982**, *688*, 333.

(9) Ohno, K.; Sohda, K.; Kosaka, A.; Kitano, H. *Bioconjugate Chem.* **1995**, *6*, 361.

(10) Kitano, H.; Akatsuka, Y.; Ise, N. *Macromolecules* **1991**, *24*, 42.

(11) Matsumura, S.; Kubokawa, H.; Toshima, K. *Makromol. Chem., Rapid Commun.* **1993**, *14*, 55.

(12) Kuwamura, T. *Kogyo Kagaku Zasshi* **1961**, *64*, 1958.

(13) Kitano, H.; Ohno, K. *Langmuir* **1994**, *10*, 4131.

(14) Kitano, H.; Sohda, K.; Kosaka, A. *Bioconjugate Chem.* **1995**, *6*, 131.

(15) Minamikawa, H.; Murakami, T.; Hato, M. *Chem. Phys. Lipids* **1994**, *72*, 111.

(16) Kitano, H.; Wolf, H.; Ise, N. *Macromolecules* **1990**, *23*, 1958.

(17) Cooper, J. A. D.; Smith, W.; Bacila, M.; Medina, H. *J. Biol. Chem.* **1959**, *234*, 445.

(18) Avigad, G.; Amaral, D.; Asensio, C.; Horecker, B. L. *J. Biol. Chem.* **1962**, *237*, 2736.

(19) Gerrett, R. H.; Grisham, C. *Biochemistry*; Saunders College Publishing: Orlando, 1995.

(20) Wagner, N.; Dose, K.; Koch, H.; Ringsdorf, H. *FEBS Lett.* **1981**, *132*, 313.

(21) Cestaro, B.; Barenholz, Y.; Gatt, S. *Biochemistry* **1980**, *19*, 615.

(22) Kitano, H.; Kato, N.; Tanaka, N.; Ise, N. *Biochim. Biophys. Acta* **1988**, *942*, 131.

Part II

Synthesis of Well-Defined Glycopolymers by Controlled/"Living" Free Radical Polymerizations

Chapter 4

Synthesis of a Well-Defined Glycopolymer by Nitroxide-Controlled Free Radical Polymerization

4-1. Introduction

The recent accumulation of detailed information on saccharide chemistry has urged the preparation of various types of glycopolymers.[1,2] However, the preparation of well-defined glycopolymers has been dealt with only in a few studies, which include the polymerization of a sugar-residue-carrying monomer with the protected hydroxyl groups by cationic polymerization,[3] ring-opening metathesis polymerization,[4] and ring-opening polymerization of *N*-carboxyanhydrides.[5] As far as the author knows, there has been no previous study in which a well-defined, low-polydispersity glycopolymer has been prepared by a free radical mechanism.

In this Chapter, the author has examined the applicability of nitroxide-mediated free radical polymerization to the synthesis of well-defined glycopolymers. The nitroxide approach has opened up a simple and robust route to the synthesis of narrow-polydispersity polymers[6,7] and found unique and important applications in random,[7i,8,9] block,[7i,10] and graft[11] copolymerization, suspension[6b] and emulsion[12] polymerization, aqueous solution polymerization,[13] and so forth. Effective initiating systems have been developed and applied.[7f-h,7j,14] The mechanism and kinetics of nitroxide-mediated polymerization, mainly of styrene systems, have also been explored in detail.[6h,15,16] The system studied here (the polymerization of a lactose-related oligosaccharide-carrying styrene derivative in *N,N*-dimethylformamide) is distinguished from those previously studied in that the monomer has a bulky sugar residue as a pendent group, the sugar residue has many hydroxyl groups (before protection), the thermal (spontaneous) polymerization of this monomer is unlikely or at least insignificant compared with that of styrene, and the solvent is a highly polar one. In this regard, this system is very interesting to study with respect to the availability of well-defined polymers as well as the kinetics of polymerization. It will be shown below that the nitroxide method is able to provide narrow-polydispersity, high-molecular weight glycopolymers with careful and unique design of experimental conditions.

4-2. Experimental Section

4-2-1. Materials

The sugar-carrying styrene derivative, *N*-(*p*-vinylbenzyl)-[*O*-β-*D*-galactopyranosyl-(1→4)]-*D*-gluconamide (VLA, Figure 4-1a),[17] was provided by NeTech, Japan. Commercially obtained styrene (Wako Pure Chemicals, Osaka, Japan) and benzoyl peroxide (BPO, Nacalai Tesque, Kyoto, Japan) were purified by the standard methods described elsewhere.[18,19] Di-*tert*-butyl nitroxide (DBN) was purchased from Aldrich and used without further purification. Dicumyl peroxide (DCP, Nacalai Tesque) was recrystallized from a chloroform/methanol mixture before use. *N,N*-Dimethylformamide (DMF) was dried over molecular sieves (4 Å) for several days before use. Other reagents were commercially obtained.

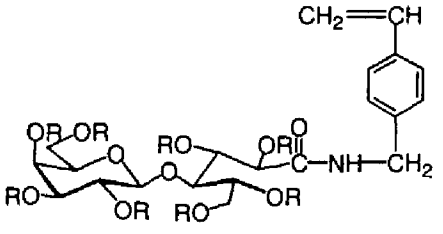

(a) VLA (R = H) (b) Ac-VLA (R = acetyl)

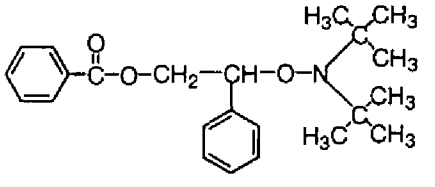

(c) BS-DBN

Figure 4-1. Chemical structures of (a) VLA, (b) Ac-VLA, and (c) BS-DBN.

4-2-2. Preparation of *N*-(*p*-Vinylbenzyl)-2,3,5,6-tetra-*O*-acetyl-4-*O*-(2,3,4,6-tetra-*O*-acetyl-β-*D*-galactopyranosyl)-*D*-gluconamide (Ac-VLA, Figure 4-1b)

To a cold suspension of VLA (10 g) in dry pyridine (100 mL) with 4-(dimethylamino)pyridine (100 mg), acetic anhydride (64 mL) was added at 0 °C. The mixture was gradually warmed to room temperature and magnetically stirred in the dark for 2 days. The obtained clear solution was concentrated *in vacuo*, and the residue was diluted with chloroform (300 mL). The organic solution was washed twice with 1 N H_2SO_4 (2 x 200 mL), twice with saturated $NaHCO_3$ (2 x

200 mL), then twice with saturated brine (2 x 200 mL), and finally with pure water (200 mL). Drying over Na_2SO_4, filtration, and evaporation of the solvent produced a white solid, which was recrystallized from a mixture of ethanol and diethyl ether (15.1 g, 88 %): ^{13}C-NMR ($CDCl_3$, 100 MHz): δ 20.6, 20.7, 20.8, 20.9, and 20.9 (CH_3COO), 43.0 (benzyl methylene), 60.9 (C-6), 61.6 (C'-6), 66.8 (C'-4), 77.2 (C-4), 101.7 (C'-1), 66.8, 69.0, 69.2, 69.8, 71.0, and 71.7 (the remaining pyranose carbons), 114.0 (CH_2=CH–), 126.4 and 127.7 {phenyl (*ipso*)}, 136.0 and 136.9 {phenyl (*meta* and *ortho*)}, 136.9 (CH_2=CH–) 166.8 (CONH), 169.0, 169.3, 169.5, 169.8, 169.9, and 170.2 (CH_3COO). Anal. Calcd for $C_{37}H_{47}NO_{19}\cdot H_2O$: C, 53.68; H, 5.98; N, 1.69. Found: C, 53.98; H, 5.86; N, 1.70.

4-2-3. Preparation of 2-(Benzoyloxy)-1-(phenylethyl)-DBN (BS-DBN, Figure 4-1c)

Freshly distilled styrene (100 mL), BPO (5.2 g), and DBN (4.1 g) were charged in a round-bottomed flask, degassed, and sealed off under vacuum. The mixture was incubated at 90 °C for 3 h. After unreacted styrene was evacuated off, the crude product was purified by flash chromatography on a column of silica gel with a 9:1 hexane/ethyl acetate mixture eluent and then with a 9:1 chloroform/hexane mixture eluent to yield a pale yellow oil as a final product (1.5 g): ^{1}H-NMR ($CDCl_3$, 200 MHz): δ 1.11 (s, 9H, *tert*-butyl group of DBN unit), 1.33 (s, 9H, *tert*-butyl group of DBN unit), 4.55 (q, 1H, C*H*H), 4.87 (q, 1H, CH*H*), 5.07 (q, 1H, C*H*), 7.21–7.53 (m, 8H, Ar*H*), 7.89 (d, 2H, ortho protons of benzoyl group); ^{13}C-NMR ($CDCl_3$, 100 MHz): δ 30.6 ($C(CH_3)_3$), 62.2 and 62.6 ($C(CH_3)_3$), 66.4 (CH_2), 83.8 (*C*H), 127.4, 127.6, 127.9, 128.1, 129.4, 130.0, 132.6, and 140.3 (phenyl), 166.0 (C=O). Anal. Calcd for $C_{23}H_{31}NO_3$: C, 74.75; H, 8.47, N, 3.79. Found: C, 75.00; H, 8.42; N, 3.76.

4-2-4. Gel Permeation Chromatography (GPC)

The GPC measurements using DMF containing 5 vol.% of water as eluent were made on a Tosoh GPC-8010 high-speed liquid chromatograph equipped with Tosoh gel columns G2000H and G4000H. The temperature was maintained at 40 °C. The column system was calibrated with standard poly(ethyleneglycol)s (PEGs). Sample detection and quantification were made with a Tosoh refractive-index detector RI-8010. This system was used for the characterization of poly(VLA) (PVLA).

The GPC measurements using tetrahydrofuran (THF) as eluent were made on a Tosoh GPC-8020 high-speed liquid chromatograph equipped with Tosoh gel columns G2500H, G3000H, and G4000H. The temperature was maintained at 40 °C. The column system was calibrated with standard polystyrenes (PSs). Sample detection and quantification were made

with a Tosoh refractive-index detector RI-8020. This system was used for the characterization of poly(Ac-VLA).

4-2-5. General Procedure for Polymerization of VLA or Ac-VLA

A solution of VLA (25 wt.%) or Ac-VLA (60 wt.%) in DMF containing a prescribed concentration of BS-DBN and DCP was charged in a Pyrex tube, degassed by three freeze-pump-thaw cycles, and sealed off under vacuum. The tube was placed in a temperature-controlled oil bath for a prescribed time, quenched to room temperature, and subjected to a GPC analysis after appropriate dilution with DMF for the VLA system or with THF for the Ac-VLA system. The monomer conversion was estimated by comparing the GPC peak area of the produced polymers with that of a model polymer, poly(VLA) or poly(Ac-VLA), dissolved in DMF or THF, respectively, at a known concentration.

4-3. Results and Discussion

It has been established that the nitroxide-mediated polymerization of styrene is set under control by the dissociation–combination reversible reaction between the alkoxyamine P-X and the polymer and nitroxyl radicals P* and X*:

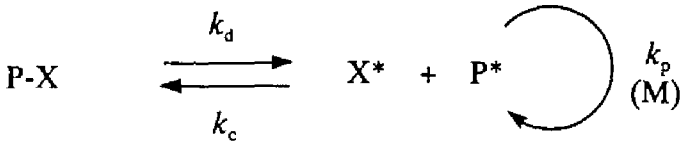

(1)

where k_d and k_c are the dissociation and combination rate constants and, in the presence of the monomer M, P* undergoes propagation with a velocity k_p[M] until it is blocked by X* to form the dormant species P-X. The polymerization rate, $R_p = k_p$[P*][M], in typical styrene/nitroxide systems was found to be essentially independent of alkoxyamine concentration.[7h,15a,b] This means that the stationary concentration of P* is determined, as in the conventional (alkoxyamine-free) system, by the balance of initiation and termination reactions, where initiation may occur either by thermal means (styrene undergoes significant thermal initiation at high temperatures, e.g., > 100 °C) or by the decomposition of an initiator like BPO and DCP. Details of elementary reactions, including values of k_d and k_c, are now available for the styrene/TEMPO (2,2,6,6-tetramethylpiperidinyl-1-oxy) system.[16] The VLA/DBN and Ac-VLA/DBN systems studied here are different in many aspects from the styrene/TEMPO system, as will be described below.

It is also noted that the polymerization of VLA with a TEMPO mediator did not work satisfactorily, presumably due to the partial decomposition of the monomer at the high temperatures (> 120 °C) where the k_d of the VLA/TEMPO system is expected to be sufficiently large. Actually, the system was observed to become brownish after a prolonged polymerization at 125 °C. Reported model experiments[20] and molecular orbital calculations[20,21] suggest that DBN will give a larger k_d than TEMPO when other conditions are the same. This encouraged the author to carry out VLA and Ac-VLA polymerizations at lower temperatures (90 – 105 °C) using DBN as a mediator. At these temperatures, no decomposition of the monomers was detectable in the time scale of the polymerizations.

4-3-2. System with VLA and BS-DBN

Figure 4-2a shows the time–conversion plot for the VLA polymerization in DMF at 105 °C with various concentrations of the alkoxyamine BS-DBN. Clearly, the rate of polymerization depends on [BS-DBN]: the conversion at a fixed polymerization time increases with increasing [BS-DBN]. However, the conversion seems to level off after some time that depends on [BS-DBN]. It is also noted that a polymerization with [BS-DBN] lower than about 1/100 of [VLA] gave no polymer even after 5 h of polymerization (data not shown) and that no thermal polymerization was detectable for the pure VLA (in DMF). The number-average molecular weight M_n and the polydispersity ratio M_w/M_n of the produced polymers are given in Figure 4-2b. The M_n increases nearly linearly with conversion, and it reasonably compares to the theoretical prediction calculated from the conversion/[BS-DBN] ratio (the solid lines in the figure), even though this comparison cannot be a rigorous one because of the use of the PEG-calibrated GPC. The M_w/M_n ratio increases with an increase in conversion when [BS-DBN] is fixed and with a decrease in [BS-DBN] when conversion is fixed.

One of the main reasons for the observed differences of the VLA system from the styrene and *p-tert*-butoxystyrene systems must be the absence (or insignificance) of thermal initiation in the VLA system. The radical concentrations in a nitroxide-mediated system may generally be described by

$$d[P^*]/dt = k_d[P\text{-}X] - k_c[P^*][X^*] + R_i - k_t[P^*]^2 \qquad (2)$$

$$d[X^*]/dt = k_d[P\text{-}X] - k_c[P^*][X^*] \qquad (3)$$

The k_d and k_c terms in eqs 2 and 3 come from the reversible reaction in eq 1, R_i is the initiation rate, and k_t is the rate constant of termination. When $R_i > 0$, [P*] and [X*] eventually reach the stationary values that are analytically obtained by solving the two equations $d[P^*]/dt = d[X^*]/dt = 0$. When $R_i = 0$, eqs 2 and 3 cannot be analytically solved rigorously. A computer simulation has shown that during an initial short time (typically, on the order of tens of milliseconds), [P*] sharply increases and then begins to decrease, passing through a broad maximum, while [X*] increases sharply at first and then more slowly.[15c,22] These initial

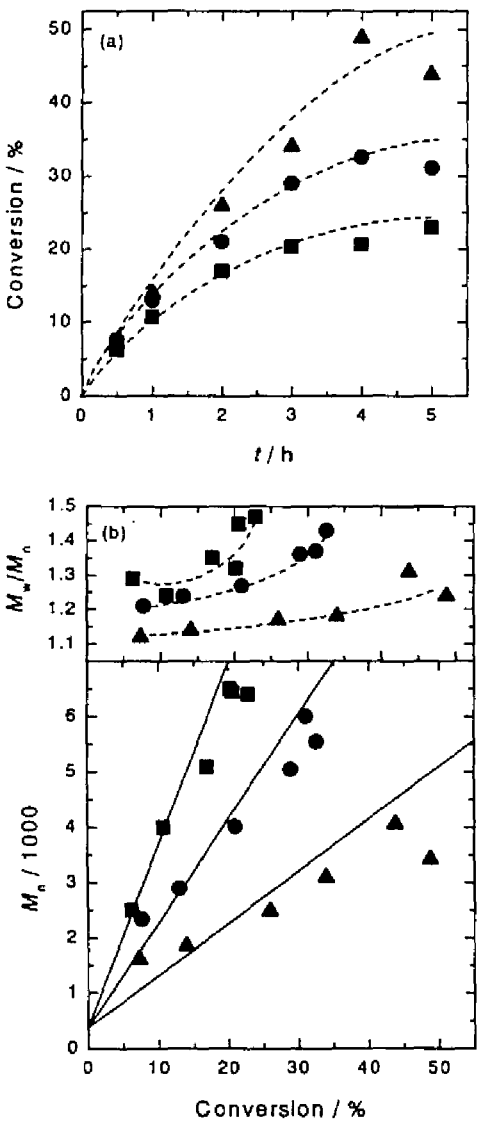

Figure 4-2. (a) Time–conversion plots for the polymerization of VLA and (b) values of M_n and M_w/M_n (estimated by PEG-calibrated GPC) as a function of monomer conversion. Solution polymerization in DMF with different BS-DBN concentrations at 105 °C: [M]/[BS-DBN] = 70/1 (■), 40/1 (●), 20/1 (▲). The full lines in Figure 4-2b represent the theoretical predictions.

behaviors are virtually independent of R_i. When $R_i \neq 0$, [P*] and [X*] gradually approach the mentioned stationary values. When $R_i = 0$, [P*] and [X*] monotonously decrease and increase, respectively, reaching no stationary values. Fischer[23] noted for the first time that [P*] and [X*] in this time region show simple power-law behavior. In fact, eqs 2 and 3 (with $R_i = 0$) can be easily solved under the approximations that $[P\text{-}X] = [P\text{-}X]_0 - [X^*] \simeq [P\text{-}X]_0 >> [X^*] >> [P^*]$ and that $d[X^*]/dt \simeq 0$, which are usually valid for the main part of such a polymerization process of practical interest. With a modification of the Fischer model, in which it was assumed that $k_c = k_t$, we obtain

$$[P^*] = (K[P\text{-}X]_0/3k_t)^{1/3} t^{-1/3} \quad (4)$$

$$[X^*] = (3k_t K^2 [P\text{-}X]_0^2)^{1/3} t^{1/3} \quad (5)$$

where $K = k_d/k_c$. Integration of the relation $-d[M]/dt = k_p[P^*][M]$ with eq 4 leads to

$$\ln([M]_0/[M]) = (3k_p/2)(K[P\text{-}X]_0/3k_t)^{1/3} t^{2/3} \quad (6)$$

Thus the logarithmic conversion index $\ln([M]_0/[M])$ in an initiation-free system is expected to show the characteristic 2/3-order dependence on time and 1/3-order dependence on the mediator concentration $[P\text{-}X]_0$.[23] This relation should be compared to the stationary-state equation valid for systems with nonzero R_i

$$\ln([M]_0/[M]) = (k_p/k_t^{1/2}) R_i^{1/2} t \quad (7)$$

which is first order in t and zeroth order in $[P\text{-}X]_0$.[15a,b,16c]

Figure 4-3 shows the plot of $r^{-1/3}\ln([M]_0/[M])$ vs $t^{2/3}$ for the same data as in Figure 4-2a, where r (= $[P\text{-}X]_0/[M]_0$) is approximately proportional to $[P\text{-}X]_0$ because the volume fraction of P-X is nearly zero in all studied cases (hence $[M]_0$ is nearly constant). For the first 2 h or so ($t^{2/3} < 1.6$), all the data points seem to form a common straight line, as eq 6 predicts. For larger t, downward deviations from the straight line become evident for the runs with r = 1/70 and 1/40, while the 1/20 run is still representable by the straight line. This suggests the presence of side reactions. A possible one may be the decomposition of the active chain end through the β-

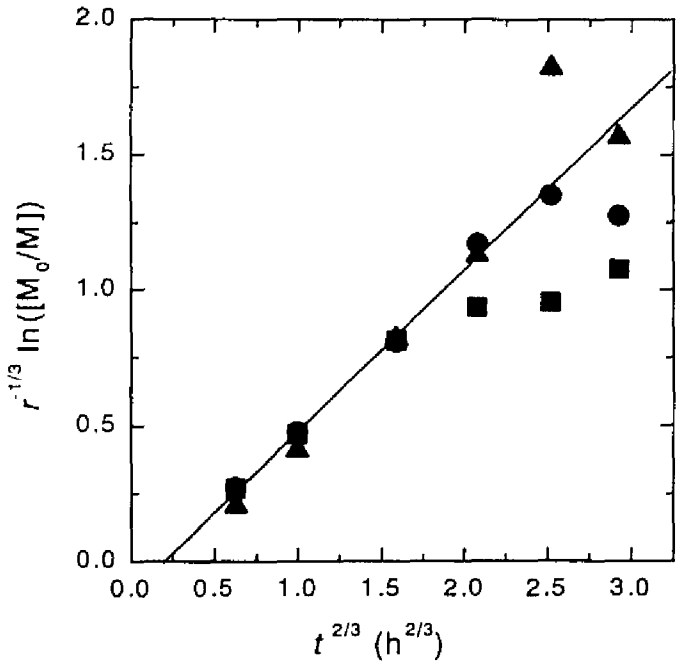

Figure 4-3. Plot of $r^{-1/3}\ln([M]_0/[M])$ vs $t^{2/3}$ for the VLA/BS-DBN system at 105 °C: [M]/[BS-DBN] = 70/1 (■), 40/1 (●), and 20/1 (▲).

proton abstraction by the nitroxyl radical,[15c,24] forming a terminally unsubstituted PVLA and a hydroxyamine. A kinetic study of this process for a polymer–nitroxyl adduct is demonstrated in Appendix (A1). If this is a main side reaction, however, the nonlinear behavior in Figure 4-3 should be independent of r, since the β-proton abstraction is a quasi-first-order reaction that is proportional to the frequency of dissociation (hence of combination) of the alkoxyamine. This conflicts with the experiments. Even though direct evidence is lacking at the moment, it is likely that the retardative (or degradative) transfer to the hydroxyl groups of VLA is responsible for the observed slowing down of the polymerization rate, which becomes more serious with a decrease in $[P\text{-}X]_0$ and hence an increase in chain length. This interpretation is supported by the observation that there seems to be a maximum M_n attainable in this system, which is about 6000, and that the M_w/M_n ratio increases with increasing M_n (Figure 4-2b).

4-3-3. System wth VLA, BS-DBN, and DCP

To increase polymerization rate and chain length, one can add the radical initiator DCP to the VLA/BS-DBN system. In the styrene/nitroxide system, such an initiator was found to work very effectively for the mentioned purpose.[16c,25] Figure 4-4a shows the time–conversion plot,

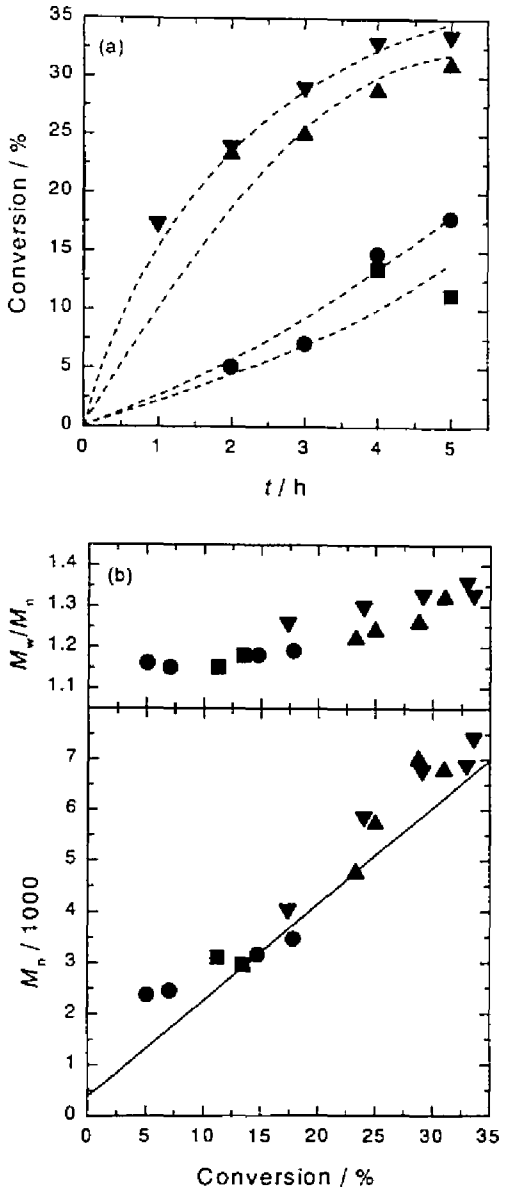

Figure 4-4. (a) Time–conversion plots for the polymerization of VLA and (b) values of M_n and M_w/M_n (estimated by PEG-calibrated GPC) as a function of monomer conversion. Solution polymerization in DMF with different DCP concentrations at 90 °C: [M]/[BS-DBN]/[DCP] = 40/1/6 (▼), 40/1/3 (▲), 40/1/0.3 (●), and 40/1/0 (■). The full line in Figure 4-4b represents the theoretical prediction.

showing the effect of DCP. Clearly, the conversion at a fixed polymerization time increases with increasing [DCP]. The M_n increases approximately linearly with conversion (Figure 4-4b), indicating that the number of polymer chains does not significantly change despite the addition of DCP. However, again, the conversion showed a leveling-off trend (Figure 4-4a), and the M_n did not become much larger than about 7000 with the M_w/M_n value increasing with increasing

M_n (Figure 4-4b). Thus, DCP plays the expected role of enhancing the stationary value of [P*] or R_p without a significant increase of the number of polymer chains, but it fails to increase M_n or conversion. This can be understood again in terms of a retardative (or degradative) transfer.

4-3-4. System with Ac-VLA, BS-DBN, and DCP

Since the transfer to the hydroxyl groups of VLA is likely to be the main cause for the undesirable features of the VLA systems, namely the relatively low M_n and conversion and the broadening of polydispersity with increasing M_n, the author carried out the polymerization of the protected monomer Ac-VLA. Figure 4-5 shows the GPC curves of poly(Ac-VLA) synthesized with BS-DBN in the presence of a small amount of DCP. It can be seen that the molecular weight increases with increasing reaction time, and the M_w/M_n ratio remains remarkably small in all cases. Figure 4-6a shows the time–conversion first-order plot for the polymerization in the presence of a fixed amount of BS-DBN and varying concentration of

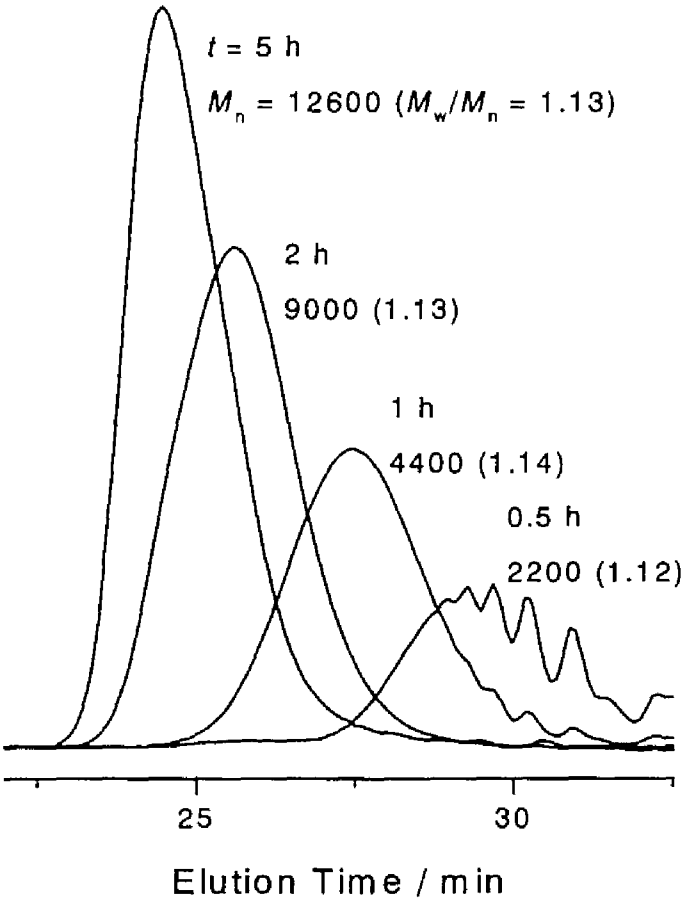

Figure 4-5. GPC curves for the polymerization of Ac-VLA in DMF at 90 °C: [M]/[BS-DBN]/[DCP] = 40/1/2.2.

DCP. The plots are linear, indicating that the radical concentration stays constant during the polymerization. Remarkably, a 90 % conversion has been reached in 5 h with the highest concentration of DCP studied here. There seems to be a short induction period in the Ac-VLA/BS-DBN system (Figure 4-6a), the reason for which is unclear at this moment. Figure 4-6b shows that the M_n of the produced polymer linearly increases with conversion, independent of DCP concentration, and the M_w/M_n ratio stays around 1.1 at all conversions. Particularly noteworthy is the essential role played by the radical initiator.[15b,16c,25] It increases R_p (by more than 15 times when [DCP]/[BS-DBN] = 2.2) without causing appreciable broadening of polydispersity. On the basis of the reported decomposition rate constant of DCP in cumene,[26] the cumulative number of the polymer molecules originating from the decomposition of DCP is estimated to be less than about 5 % of those of the BS-DBN origin even for the run with the highest DCP concentration ([DCP]/[BS-DBN] = 2.2) and the longest polymerization time (5 h). Obviously, the R_p of the DCP-free system is impractically too small (Figure 4-6a).

The M_n values obtained by GPC were significantly smaller than those calculated from the conversion/alkoxyamine ratios. Apparently, the PS-calibrated GPC does not work accurately for this particular system. Thus, we have carried out an ultracentrifuge sedimentation equilibrium (UCSE) analysis with one of the samples. Its M_w was found to be 40000, about 2.7 times as large as the GPC value but reasonably close to the theoretical value. These results show that the protection of the hydroxyl groups of the monomer suppresses side reactions to provide the polymerization system with better "living" characters. Since the deacetylation of poly(Ac-VLA) can be achieved easily and quantitatively by treatment with hydrazine in DMF solution,[27] the proposed polymerization procedure will open up a new and practical route to the preparation of well-defined glycopolymers.

4-4. Conclusions

The free radical polymerization of VLA in DMF in the presence of a BS-DBN adduct proceeded in a "living" fashion under limited conditions, giving relatively narrow polydispersity PVLA. However, the monomer conversion did not become high enough, and polymers with a high enough molecular weight could not be obtained. The polymerization of the monomer with protected hydroxyl groups (Ac-VLA) in the presence of BS-DBN as mediator and DCP as accelerator proceeded in a better-defined "living" fashion, giving higher-molecular weight, narrower polydispersity polymers with a high conversion. Thus this work

has broadened the practical synthetic route to well-defined glycopolymers and the applicability of the nitroxide-mediated "living" radical polymerization. The "living" radical polymerization of Ac-VLA will also find important applications in, e.g., the preparation of amphiphilic block and graft copolymers.

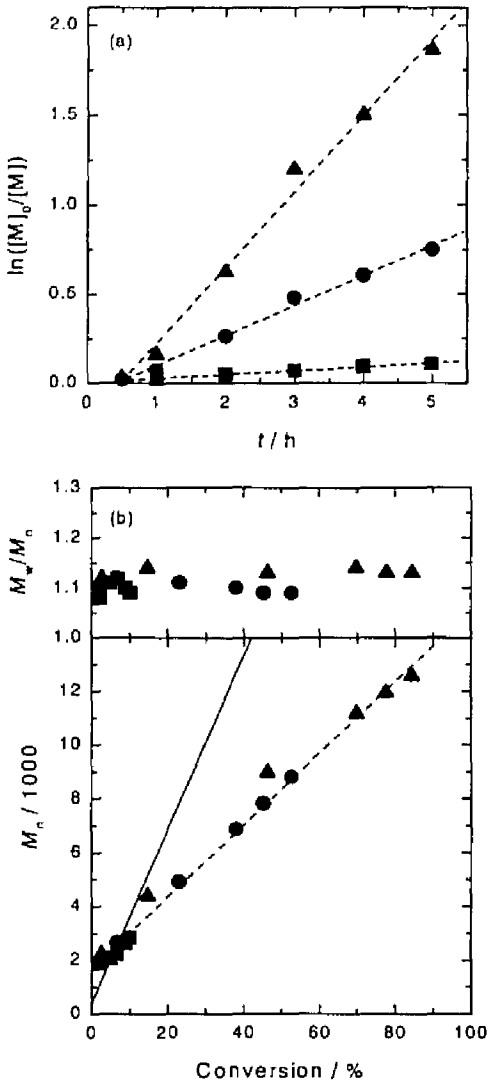

Figure 4-6. (a) Time–conversion plots for the polymerization of Ac-VLA and (b) values of M_n and M_w/M_n (estimated by PS-calibrated GPC) as a function of monomer conversion. Solution polymerization in DMF with different DCP concentrations at 90 °C: [M]/[BS-DBN]/[DCP] = 40/1/2.2 (▲), 40/1/1.1 (●), and 40/1/0 (■). The full line in Figure 4-6b represents the theoretical prediction.

References

(1) Collins, P. M.; Ferrier, R. J. *Monosaccharides: Their Chemistry and Their Roles in Natural Products*; John Wiley & Sons: Chichester, U.K., 1995.

(2) Wulff, G.; Schmid, J.; Venhoff, T. *Macromol. Chem. Phys.* **1996**, *197*, 259 and references therein.

(3) (a) Yamada, K.; Yamaoka, K.; Minoda, M.; Miyamoto, T. *J. Polym. Sci., Part A: Polym. Chem.* **1997**, *35*, 255. (b) Yamada, K.; Minoda, M.; Miyamoto, T. *J. Polym. Sci., Part A: Polym. Chem.* **1997**, *35*, 751.

(4) Fraser, C.; Grubbs, R. H. *Macromolecules* **1995**, *28*, 7248.

(5) (a) Aoi, K.; Suzuki, H.; Okada, M. *Macromolecules* **1992**, *25*, 7073. (b) Aoi, K.; Tsutsumiuchi, K.; Okada, M. *Macromolecules* **1994**, *27*, 875.

(6) For recent reviews, see: (a) Moad, G.; Rizzardo, E.; Solomon, D. H. In *Comprehensive Polymer Science*; Eastmond, G. C., Ledwith, A., Russo, S., Sigwalt, P., Eds.: Pergamon: London, 1989; Vol. 3, p 141. (b) Georges, M. K.; Veregin, R. P. N.; Kazmaier, P. M.; Hamer, G. K. *Trends Polym. Sci.* **1994**, *2*, 66. (c) Matyjaszewski, K.; Gaynor, S.; Greszta, D.; Mardare, D.; Shigemoto, T. *J. Phys. Org. Chem.* **1995**, *8*, 306. (d) Moad, G.; Solomon, D. H. *The Chemistry of Free Radical Polymerization*; Pergamon: Oxford, U.K., 1995; p 335. (e) Davis, T. P.; Haddleton, D. M. In *New Methods of Polymer Synthesis*; Ebdon, J. R., Eastmond, G. C., Eds.; Blackie: Glasgow, U.K., 1995; Vol. 2, p 1. (f) Hawker, C. J. *Trends Polym. Sci.* **1996**, *4*, 183. (g) Sawamoto, M.; Kamigaito, M. In *Polymer Synthesis*; Materials Science and Technology Series; VCH: Deerfield Beach, FL (in press). (h) Fukuda, T.; Goto, A.; Ohno, K.; Tsujii, Y. In *Controlled Radical Polymerization*; Matyjaszewski, K., Ed.; American Chemical Society: Washington, DC, 1998; p 180.

(7) (a) Solomon, D. H.; Rizzardo, E.; Cacioli, P. Eur. Pat. Appl. 135280, 1985; *Chem. Abstr.* **1985**, *102*, 221335q. (b) Rizzardo, E. *Chem. Aust.* **1987**, *54*, 32. (c) Johnson, C. H. J.; Moad, G.; Solomon, D. H.; Spurling, T. H.; Vearing, D. J. *Aust. J. Chem.* **1990**, *43*, 1215. (d) Georges, M. K.; Veregin, R. P. N.; Kazmaier, P. M.; Hamer, G. K. *Macromolecules* **1993**, *26*, 2987. (e) Greszta, D.; Mardare, D.; Matyjaszewski, K. *Macromolecules* **1994**, *27*, 638. (f) Hawker, C. J. *J. Am. Chem. Soc.* **1994**, *116*, 11185. (g) Hawker, C. J.; Hedrick, J. L. *Macromolecules* **1995**, *28*, 2993. (h) Catala, J. M.; Bubel, F.; Hammouch, S. O. *Macromolecules* **1995**, *28*, 8441. (i) Fukuda, T.; Terauchi, T.; Goto, A.; Tsujii, Y.; Miyamoto, T.; Shimizu, Y. *Macromolecules* **1996**, *29*, 3050. (j) Howell, B. A.; Priddy, D.

B.; Li, I. Q.; Smith, P. B.; Kastl, P. E. *Polym. Bull.* **1996**, *37*, 451.

(8) Hawker, C. J.; Elce, E.; Dao, J.; Volksen, W.; Russell, T. P.; Barclay, G. G. *Macromolecules* **1996**, *29*, 2686.

(9) Ide, N.; Fukuda, T. *Macromolecules* **1997**, *30*, 4268.

(10) Ohno, K.; Fukuda, T.; Miyamoto, T.; Shimizu, Y. *Macromol. Chem. Phys.* **1998**, *199*, 291.

(11) Hawker, C. J.; Mecerreyes, D.; Elce, E.; Dao, J.; Hedrick, J. L.; Barakat, I.; Dubois, P.; Jérôme, R.; Volksen, W. *Macromol. Chem. Phys.* **1997**, *198*, 155.

(12) Bon, S. A. F.; Bosveld, M.; Klumperman, B.; German, A. L. *Macromolecules* **1997**, *30*, 324.

(13) Keoshkerian, B.; Georges, M. K.; Boils-Boissier, D. *Macromolecules* **1995**, *28*, 6381.

(14) Hawker, C. J.; Barclay, G. G.; Orellana, A.; Dao, J.; Devonport, W. *Macromolecules* **1996**, *29*, 5245.

(15) (a) Fukuda, T.; Terauchi, T. *Chem. Lett. (Tokyo)* **1996**, 293. (b) Fukuda, T.; Terauchi, T.; Goto, A.; Ohno, K.; Tsujii, Y.; Miyamoto, T.; Kobatake, S.; Yamada, B. *Macromolecules* **1996**, *29*, 6393. (c) Greszta, D.; Matyjaszewski, K. *Macromolecules* **1996**, *29*, 7661. (d) Odell, P. G.; Veregin, R. P. N.; Michalak, L. M.; Georges, M. K. *Macromolecules* **1997**, *30*, 2232.

(16) (a) Goto, A.; Fukuda, T. *Macromolecules* **1997**, *30*, 5183. (b) Goto, A.; Terauchi, T.; Fukuda, T.; Miyamoto, T. *Macromol. Rapid commun.* **1997**, *18*, 673. (c) Goto, A.; Fukuda, T. *Macromolecules* **1997**, *30*, 4272. (d) Fukuda, T.; Goto, A. *Macromol. Rapid Commun.* **1997**, *18*, 682.

(17) Kobayashi, K.; Sumitomo, H.; Ina, Y. *Polym J.* **1985**, *17*, 567.

(18) Fukuda, T.; Ma, Y.-D.; Inagaki, H. *Macromolecules* **1985**, *18*, 17.

(19) Ma, Y.-D.; Fukuda, T.; Inagaki, H. *Polym. J. (Tokyo)* **1983**, *15*, 673.

(20) Moad, G.; Rizzardo, E. *Macromolecules* **1995**, *28*, 8722.

(21) Kazmaier, P. M.; Moffat, K. A.; Georges, M. K.; Veregin R. P. N.; Hamer, G. K. *Macromolecules* **1995**, *28*, 1841.

(22) (a) Tsujii, Y.; et al. To be published. (b) Tsujii, Y.; Fukuda, T.; Miyamoto, T. *Polym. Prepr. (Am. Chem. Soc., Div. Polym. Chem.)* **1997**, *38(1)*, 657.

(23) Fisher, H. *Macromolecules* **1997**, *30*, 5666.

(24) (a) Li, I.; Howell, B. A.; Matyjaszewski, K.; Shigemoto, T.; Smith, P. B.; Priddy, D. B.

Macromolecules **1995**, *28*, 6692. (b) Ohno, K.; Tsujii, Y.; Fukuda, T. *Macromolecules* **1997**, *30*, 2503.

(25) Greszta, D.; Matyjaszewski, K. *J. Polym. Sci., Part A: Polym. Chem.* **1997**, *35*, 1857.

(26) Bailey, H. C.; Godin, G. W. *Trans. Faraday Soc.* **1956**, *52*, 68.

(27) Kunz, H. *Angew. Chem., Int. Ed. Engl.* **1987**, *26*, 294.

Chapter 5

Nitroxide-Controlled Free Radical Polymerization of a Sugar-Carrying Acryloyl Monomer

5-1. Introduction

As described in Chapter 4, the author succeeded in the "living" radical polymerization of styryl monomer with pendent saccharide residue by the nitroxide-controlled free radical polymerization technique.[1] His interest now focuses on developing a synthetic route to well-defined *polyacrylate*-type of glycopolymers, because acrylate derivatives with pendent saccharide residues are easily made available and commonly used in the glycotechnology as monomers polymerizable by the free radical mechanism.[2]

Recent successful applications of nitroxide-mediated polymerization to acrylates include the polymerization of *n*-butyl acrylate (at about 145 °C) mediated by a TEMPO (2,2,6,6-tetramethylpiperidinyl-1-oxy) derivative,[3] that of the same monomer (at 100–120 °C) using the novel nitroxyl which has a diethyl phosphate group at the β-position to the *N* atom,[4] and that of *tert*-butyl acrylate (at 120 °C) initiated with a molecular adduct of DBN (di-*tert*-butyl nitroxide).[5] In view of the potential activity of DBN at relatively low temperatures and its easy availability, the author has attempted the DBN-mediated polymerization of the sugar-carrying acrylate. By the use of a conventional initiator (dicumyl peroxide) as an accelerator, he has succeeded in the synthesis of well-defined acrylate glycopolymers as well as amphiphilic diblock copolymers comprising the glycopolymer subchain, as will be detailed below.

5-2. Experimental Section

5-2-1. Materials

Commercially obtained styrene (Wako Pure Chemicals, Osaka, Japan) and benzoyl peroxide (BPO, Nacalai Tesque, Kyoto, Japan) were purified by the standard methods described elsewhere.[6] An alkoxyamine adduct, 2-(benzoyloxy)-1-(phenylethyl)-di-*tert*-butyl nitroxide (BS-DBN, Figure 1a) was prepared as described in Chapter 4[1] excepting that the reaction temperature was 50 °C. Dicumyl peroxide (DCP, Nacalai Tesque) was recrystallized from a chloroform/methanol mixture before use. *p*-Xylene was dried over molecular sieves (4 Å) for

several days prior to use. All other reagents were purchased from commercial sources and used as received.

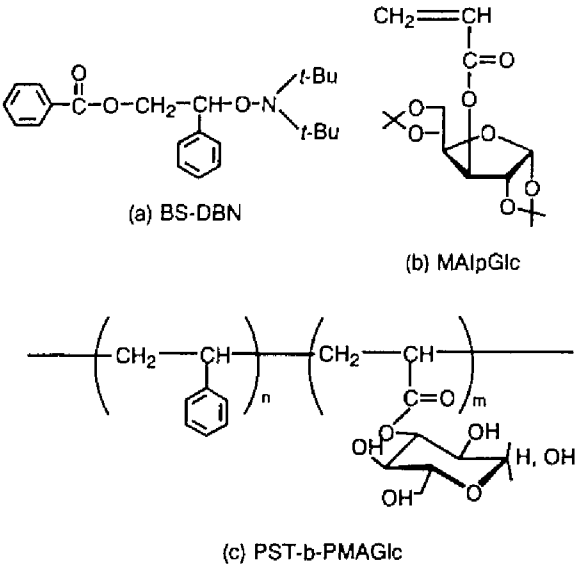

Figure 5-1. Chemical structures of (a) BS-DBN, (b) AIpGlc, and (c) PS-*b*-PAGlc.

5-2-2. Synthesis of 3-*O*-Acryloyl-1,2:5,6-di-*O*-isopropylidene-α-*D*-glucofuranoside (AIpGlc, Figure 1b)

This synthesis was made by a slight modification of the method proposed by Ouchi et al.[7] To a cold solution of 1,2:5,6-di-*O*-isopropylidene-*D*-glucofuranose (26 g, 0.1 mmol) in dry acetone (100 mL) with triethylamine (40 mL, 0.3 mmol), acryloyl chloride (25 mL, 0.3 mmol) was added dropwise at 0 °C. The mixture was magnetically stirred for 1 h at 0 °C and then for another 2 h at room temperature. The system was diluted with a cold water (250 mL) and extracted three times with chloroform (200 mL). The combined extracts were dried over anhydrous sodium sulfate. After the solvent was evacuated off, the crude product was purified by flash silica gel chromatography with a 2:3 hexane/ethyl acetate mixture as an eluent to yield a pale yellow syrup. Crystallization of the syrup was induced in cold *n*-hexane to give a slightly yellow powder (24 g, 77 %): ^{1}H-NMR ($CDCl_3$, 400 MHz): δ 1.25–1.55 (m, 12H, 4 C*H*$_3$ of isopropylidene units), 4.05, 4.25, 4.51, 5.29, and 5.87 (7H, sugar moiety), 5.85–6.50 (3H, three vinyl protons). Anal. Calcd for $C_{15}H_{22}O_7$: C, 57.31; H, 7.07. Found: C, 57.53; H, 7.17.

5-2-3. Nitroxide-Controlled Polymerization of AIpGlc

A solution of AIpGlc (60 wt.%) in *p*-xylene containing a prescribed concentration of BS-DBN and DCP was charged in a Pyrex tube, degassed by three freeze-pump-thaw cycles, and sealed

off under vacuum. The tube was placed in an oil bath thermostatted at 100 °C for a prescribed time, and quenched to room temperature. A part of the sample solution was subjected to a gel permeation chromatography (GPC) analysis after appropriate dilution with tetrahydrofuran (THF). The monomer conversion was estimated by comparing the GPC peak area of the produced polymer with that of a model poly(AIpGlc) (PAIpGlc) dissolved in THF at a known concentration.

The remaining sample solution was diluted with chloroform and poured into methanol. The precipitate was purified by reprecipitation with a chloroform (solvent)/cold methanol (nonsolvent) system and dried *in vacuo* to yield a polymer as a white powder.

5-2-4. Deprotection of PAIpGlc

The transformation of PAIpGlc into the hydroxyl polymer poly(3-*O*-acryloyl-α,β-*D*-glucopyranoside) (PAGlc) was achieved by the conventional method[8]: the protected polymer (170 mg) was dissolved in 80 % formic acid (20 mL) and stirred for 48 h at room temperature, to which 8 mL of water was added and stirred for another 3 h. The solution was dialyzed against distilled water for 2 days, concentrated *in vacuo*, and finally lyophilized to give PAGlc as a white powder with a quantitative yield.

5-2-5. Synthesis of PS-*b*-PAIpGlc and PS-*b*-PAGlc (Figure 5-1c) Diblock Copolymers

Polystyrene precursors (PS-DBN) were prepared by the bulk polymerization of styrene in the presence of BS-DBN and DCP. In a typical run, freshly distilled styrene (3.27 g), BS-DBN (29 mg, 20 mM), and DCP (97 mg, 92 mM) were charged in a Pyrex tube, degassed by three freeze-pump-thaw cycles, and sealed off under vacuum. The mixture was heated at 100 °C for 1.5 h, and after dilution with chloroform (5 mL) the solution was poured into methanol (50 mL). The precipitate was purified by reprecipitation with a chloroform (solvent)/methanol (nonsolvent) system and dried *in vacuo* to give a polymer (P-1 in Table 5-1) as a white powder (770 mg): M_n = 9300 and M_w/M_n = 1.15. The characteristics of the PS-DBN adducts synthesized in this work were summarized in Table 5-1.

Diblock copolymers were synthesized as follows: typically, a solution of AIpGlc (605 mg, 1.9 mmol, 60 wt.%) in *p*-xylene containing PS-DBN (P-1, 96 mg, 0.01 mmol) and DCP (4.7 mg, 0.017 mmol) was charged in a Pyrex tube, degassed by three freeze-pump-thaw cycles, and sealed off under vacuum. The mixture was incubated at 100 °C for 2 h, diluted with chloroform (3 mL), and poured into methanol (50 mL). The precipitated polymer was purified by reprecipitation with a chloroform/methanol system and dried *in vacuo* to give a PS-*b*-

PAIpGlc diblock copolymer as a white powder (220 mg): M_n = 15700, M_w/M_n = 1.64. The PS-*b*-PAIpGlc diblock copolymers prepared in this way were further treated with 80 % formic acid to deblock the isopropylidene groups and purified as described for PAGlc.

Table 5-1. Synthesis of PS-DBN Precursor Polymers [a]

Polymer	Amount of styrene (g)	Amount of BS-DBN (mg)	Amount of DCP (mg)	M_n [b]	M_w/M_n [b]	Conversion (%)
P-1	3.27	29	97	9300	1.15	24
P-2	1.62	29	48	4500	1.10	23
P-3	1.04	37	31	2300	1.07	22

[a] All reactions were carried out for 1.5 h at 100 °C.
[b] Estimated by PS-calibrated gel permeation chromatography.

5-2-6. Measurements

Proton-nuclear magnetic resonance (^{1}H-NMR) spectra were obtained on a JEOL JNM/AL400 400-MHz spectrometer. The GPC analysis was made on a Tosoh GPC-8020 high-speed liquid chromatography equipped with Tosoh gel columns G2500H, G3000H, and G4000H. THF was used as eluent, and temperature was maintained at 40 °C. The column system was calibrated with standard polystyrenes (PSs). Sample detection and quantification were made with a Tosoh refractive-index detector RI-8020. Transmission electron microscopic (TEM) observations of the diblock copolymer surface morphologies were performed on a JEOL transmission electron microscope JEM-1010 operated at 100 kV. A drop of a 0.3 wt.% *N,N*-dimethylformamide (DMF) solution of a diblock copolymer was placed directly on a carbon-coated grid and allowed to air-dry. The cast film was then stained with a saturated aqueous solution of uranyl acetate.

5-3. Results and Discussion

5-3-1. AIpGlc Polymerization by Using BS-DBN Adduct

The polymerization of AIpGlc with BS-DBN and DCP at 120 °C was first conducted but unsatisfactory results were obtained, presumably due to the partial decomposition of the sugar residues at this temperature. Actually, the system was observed to become brownish after a prolonged polymerization at 120 °C. Following the suggestions of the previous reports,[1,9] in which well-controlled polymerizations of styrenic monomers were achieved by a DBN mediator at lower temperatures (≤ 100 °C), the author then attempted the polymerization at 100

°C. At this temperature, no decomposition of the sugar residues was detected. The polymerization proceeded smoothly by the addition of an appropriated amount of DCP.

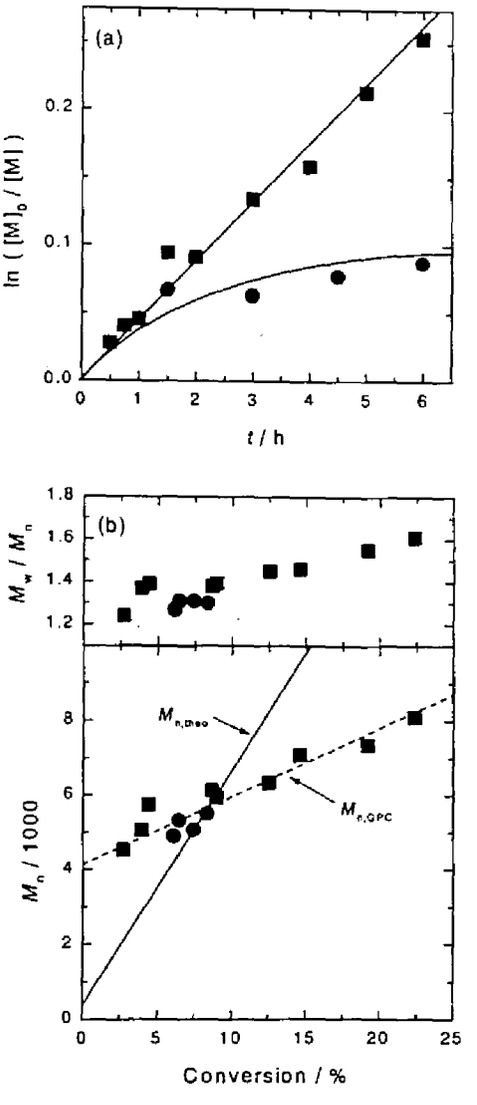

Figure 5-2. (a) Plot of $\ln([M]_0/[M])$ vs t and (b) values of M_n and M_w/M_n as a function of monomer conversion; solution polymerization of AIpGlc (60 wt.%) in *p*-xylene at 100 °C: $[AIpGlc]_0/[BS\text{-}DBN]_0/[DCP]_0$ = 200/1/2.4 (■) and 200/1/0 (●). The full line in Figure 5-2b represents the theoretical prediction.

Figure 5-2a shows the plot of $\ln([M]_0/[M])$ versus polymerization time t, where [M] represents the monomer concentration and the subscript zero denotes the initial state (t = 0). The polymerization rate of the DCP-free system is impractically slow, but it can be clearly increased by the addition of DCP. A closer inspection of the figure reveals that the first-order

plot for the DCP-containing system is linear, indicating that the radical concentration stays constant. On the other hand, the plot for the DCP-free system is non-linear and levels off after a short time. Figure 5-2b shows that the M_n of the produced polymer linearly increases with conversion. Thus, DCP plays the expected role of increasing the polymerization rate and keeping it constant without a significant increase of the number of the chains. Figure 5-2b also shows that the M_w/M_n ratio is fairly small from an early stage of polymerization. This means that the rate constant of activation (homolysis) of the polymer–DBN adduct is sufficiently large. The gradual increase of the M_w/M_n ratio with time is due to side reaction(s). These results are similar to those for the *tert*-butyl acrylate/DBN system, in which the decomposition of the active polymer chain end occurs through the β-proton abstraction by the nitroxyls and the subsequent hydrogen transfer reaction (cf. Appendix, A1).[5,10] The present system possibly undergoes similar side reactions. Incidentally, it is also noted that the polymerization of the unprotected monomer AGlc would be unsuccessful due to the possible chain-transfer reaction of the growing radical to the hydroxyl protons numerously present in the system (cf. Chapter 4).[1]

As shown in Figure 5-2b, the M_n values obtained by GPC, however, were significantly smaller than the theoretical values, $M_{n,theo}$, calculated from the monomer conversion/alkoxyamine molar ratio. This is ascribed predominantly to the inaccuracy of the PS-calibrated GPC employed here. Because of the use of the radical initiator DCP, the total number of polymer chains is larger than the number of the alkoxyamine initiator, but the deviation of M_n from $M_{n,theo}$ for this cause is estimated to be minor even in the later stage of polymerization. We have carried out 400 MHz ^{1}H-NMR measurements for two PAIpGlc samples (S-1 and S-2). A typical ^{1}H-NMR spectrum is given in Figure 5-3a. The number-average molecular weight was estimated on the basis of the ratio of the integral areas of peaks S and B, which are assignable to the anomeric protons of the sugar moieties and the two *ortho* protons of the phenyl ring of the BPO moiety at the chain end, respectively. Table 5-2 compares the NMR and GPC number-average molecular weights. The NMR values ($M_{n,NMR}$) are in good agreement with the theoretical values ($M_{n,theo}$), confirming that the AIpGlc polymerization proceeds in a controlled way, providing low-polydispersity polymers with a predictable molecular weight.

Table 5-3 summarizes the characteristics of all the PAIpGlc polymers prepared in this work.

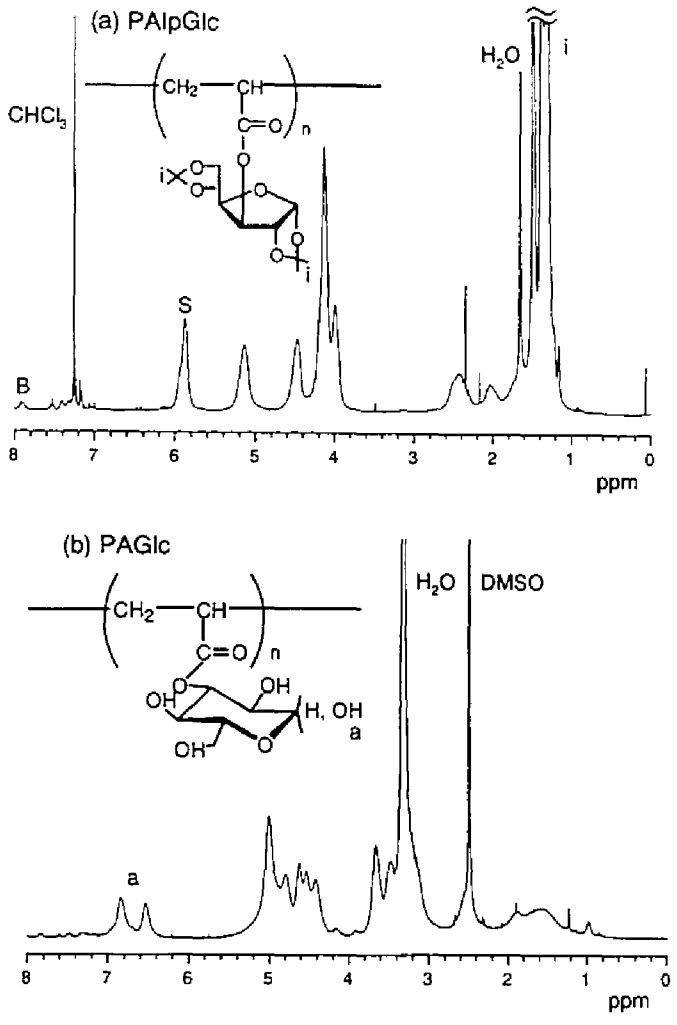

Figure 5-3. Typical ^{1}H-NMR spectra taken (a) before and (b) after the acidolysis of PAIpGlc. The solvents were (a) $CDCl_3$ and (b) DMSO-d_6.

Table 5-2. Comparison of Number-Average Molecular Weight Values

Sample	$M_{n,GPC}$[a]	$M_{n,NMR}$[b]	$M_{n,theo}$[c]
S-1	4100	6100	7400
S-2	6200	10000	12000

[a] Estimated by PS-calibrated gel permeation chromatography.
[b] Determined by ^{1}H-NMR.
[c] Calculated from the ratio of $([M]_0 - [M])/[BS\text{-}DBN]_0$.

Table 5-3. Results of AIpGlc Solution Polymerization in *p*-Xylene at 100 °C [a]

Run	$[M]_0/[B]_0/[D]_0$ [b]	Polymerization time (h)	Conversion (%)	M_n [c]	$M_{n,theo}$ [d]	M_w/M_n [c]
R-1	100/1/4.6	2	26	5300	8500	1.80
R-2	100/1/4.6	5	55	8000	17600	1.99
R-3	100/1/2.3	2	12	3100	4000	1.39
R-4	100/1/2.3	7	29	5300	9300	1.58
R-5	100/1/1.2	2	7.2	2600	2600	1.27
R-6	100/1/1.2	7	13	3300	4400	1.31
R-7	100/1/0	2	5.5	2400	2100	1.27
R-8	100/1/0	7	7.0	2600	2600	1.21
R-9	200/1/4.8	2	18	7500	1160	1.67
R-10	200/1/4.8	5	44	9700	28000	2.18
R-11	200/1/2.4	2	8.7	6100	5800	1.38
R-12	200/1/2.4	5	19	7300	12400	1.55
R-13	200/1/0	3	6.1	4900	4200	1.27
R-14	200/1/0	6	8.4	5500	5700	1.30

[a] The concentration of AIpGlc monomer was 60 wt.% in all reaction conditions.
[b] $[M]_0$, $[B]_0$, and $[D]_0$ represent initial concentrations of AIpGlc, BS-DBN, and DCP, respectively.
[c] Estimated by PS-calibrated gel permeation chromatography. The GPC M_n values can be inaccurate, as demonstrated in Table 5-2.
[d] Calculated from the ratio of $([M]_0 - [M])/[B]_0$.

5-3-2. Deprotection of Isopropylidene Groups of AIpGlc

The PAIpGlc sample was treated with formic acid to obtain PAGlc homopolymer. Figure 5-3 shows typical ^{1}H-NMR spectra of the homopolymer taken before (Figure 5-3a) and after (Figure 5-3b) the acidolysis. The signals of the isopropylidene protons (1.2 – 1.4 ppm in Figure 5-3a) have completely disappeared after the acidolysis and instead a broad absorption assignable to the anomeric hydroxyl groups of the sugar moieties (6.4 – 7.0 ppm in Figure 5-3b) has appeared. This confirms that the deprotection of the isopropylidene groups proceeded quantitatively. The PAGlc polymers obtained here were soluble in water, DMF, and dimethyl sulfoxide.

5-3-3. Synthesis of PS-*b*-PAIpGlc Diblock Copolymers

The synthesis of PS-*b*-PAIpGlc diblock copolymers was made by using PS-DBN adducts as "initiator". Table 5-1 summarizes the characteristics of the PS-DBN adducts studied here, which were prepared by the bulk polymerization of styrene in the presence of varying

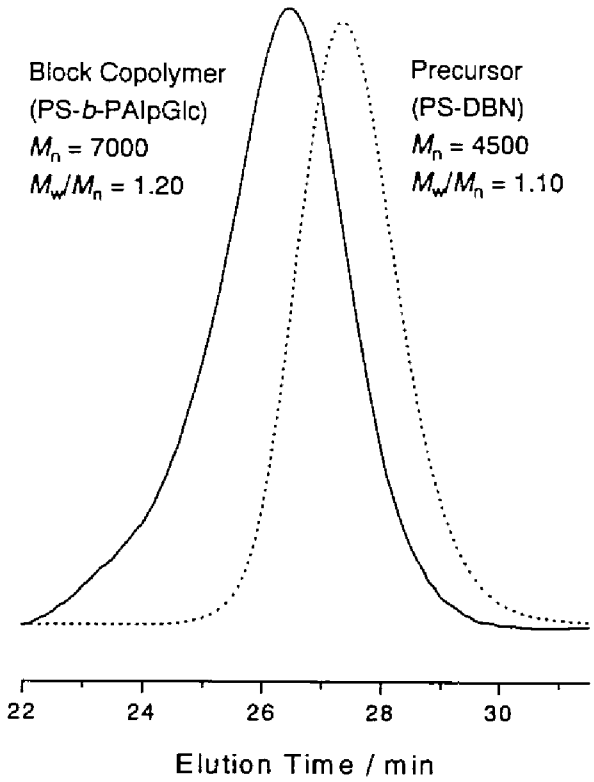

Figure 5-4. GPC curves for the precursor PS and PS-*b*-PAIpGlc block copolymer before purification. The polymerization was carried out for 1h at 100 °C.

Table 5-4. Synthesis of PS-*b*-PAIpGlc Diblock Copolymers [a]

Diblock copolymer	Amount of AIpGlc (g)	Amount of precursor[b] (mg)	Amount of DCP (mg)	T[c] (h)	C[d] (%)	M_n[e]	M_w/M_n[e]	DP[e,f] of PS block	DP[f,g] of PAIpGlc block
B-1	0.61	P-1 96	4.7	2	36	15700	1.64	96	72
B-2	0.91	P-2 72	8.2	3	30	11000	1.68	45	60
B-3	1.05	P-3 33	10	4	52	12200	1.97	22	104

[a] All reactions were carried out at 100 °C. The concentration of AIpGlc monomer was 60 wt.% in all reactions.
[b] See Table 5-1.
[c] Polymerization temperature.
[d] Monomer conversion.
[e] Estimated by PS-calibrated gel permeation chromatography.
[f] Number-average degree of polymerization.
[g] Calculated from the molar ratio of the AIpGlc conversion to the PS-DBN adduct.

concentrations of BS-DBN and a fixed amount of DCP. To minimize unfavorable side reactions,[5] we have limited the polymerization time of all PS-DBN adducts to 1.5 h. Figure 5-4 shows the GPC curves of the PS-DBN precursor polymer (P-2) and the crude polymer obtained by the polymerization of AIpGlc with the PS-DBN initiator. The peak position has shifted to a higher molecular weight region with no appreciable shoulder peak at the elution position of the precursor and the molecular weight distribution remaining fairly narrow. This suggests successful formation of a PS-*b*-PAIpGlc block copolymer. Table 5-4 shows the characteristics of the purified block copolymers. The acidolysis of the PS-*b*-PAIpGlc samples gave amphiphilic block copolymer of the type PS-*b*-PAGlc.

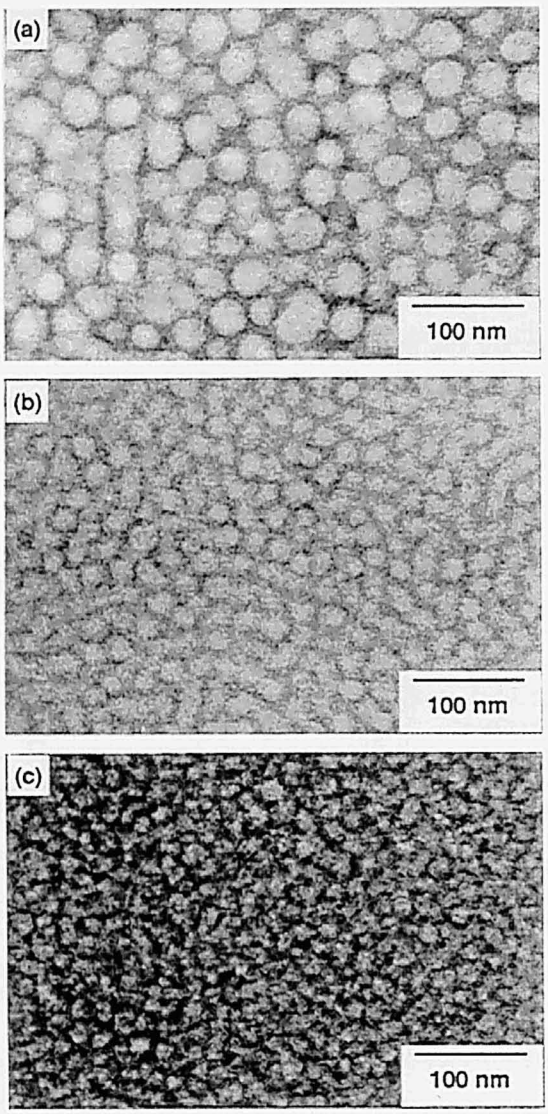

Figure 5-5. TEM micrograph of the surface of solvent-cast PS-*b*-PAGlc block copolymer film; (a) deblocked B-1, (b) deblocked B-2, and (c) deblocked B-3 (cf. Table 5-4). The light and dark regions show the PS and PAGlc domains, respectively.

5-3-4. Surface Morphology of PS-*b*-PAGlc

It is well known that block copolymers often undergo microphase separation and exhibit various microdomain morphologies.[11] The PS-*b*-PAGlc diblock copolymer with an amphiphilic character may come under this case. We have investigated the surface morphologies of the thin film of PS-*b*-PAGlc cast from a DMF solution. The TEM micrographs of the three sample films stained by uranyl acetate are presented in Figure 5-5. Since uranyl acetate selectively stains the hydrophilic polymer (PAGlc), the darker regions in the micrograph correspond to the PAGlc domains. All micrographs clearly show regular, spherical PS domains embedded in a continuous matrix of the PAGlc moieties. The three block copolymer samples shown here have a PS block of roughly the same molecular weight (Table 5-4). In this regard, it is interesting that the size of the spherical PS domain becomes larger with increasing PS content in the diblock copolymers. Note that these observations were made for the surface structures of the solvent-cast films, and they should be very much different from the bulk structures of the block copolymers. Nevertheless, the regular surface morphologies observed here, which must have resulted from the well-defined amphiphilic molecular structure of the polymers, may play an important role to determine the physical properties of the films, e.g., biocompatibility and protein-recognizability.

5-4. Conclusions

The free radical polymerization of AIpGlc in *p*-xylene in the presence of BS-DBN as initiator and DCP as accelerator proceeded in a "living" fashion, giving PAIpGlc with a controlled molecular weight up to M_n = 13000 and a low-polydispersity, $1.2 < M_w/M_n < 1.6$. The polymerization of AIpGlc with PS-DBN as initiator proceeded in a controlled way, providing well-defined diblock copolymers of the type PS-*b*-PAIpGlc. The acidolysis of PAIpGlc and PS-*b*-PAIpGlc provided water-soluble AIpGlc homopolymers and amphiphilic PS-*b*-PAGlc diblock copolymers. Films of PS-*b*-PAGlc diblock copolymers exhibited a microdomain surface morphologies with spherical PS domains embedded in the hydrophilic PAGlc matrix, the size of the PS domains depending on the monomer composition.

Thus, the nitroxide-mediated polymerization offers a practical synthetic route to well-defined sugar-carrying polyacrylates with a reasonably high molecular weight. The development of new nitroxides with less side reactions will lead to even better-defined glycopolymers with a *higher* molecular weight, which will make many contributions to

polymer science and glycoconjugate chemistry.

References

(1) Ohno, K.; Tsujii, Y.; Miyamoto, T.; Fukuda, T.; Goto, M.; Kobayashi, K.; Akaike, T. *Macromolecules* **1998**, *31*, 1064.

(2) (a) Koβmehl, G.; Volkheimer, J. *Liebigs Ann. Chem.* **1989**, 1127. (b) Bird, T. P.; Black, W. A. P.; Colquhoun, J. A.; Dewar, E. T.; Rutherford, D. *Chem. Ind.* **1965**, 1073. (c) Kitazawa, S.; Okuyama, M.; Kinomura, K.; Sakakibara, T. *Chem. Lett.* **1990**, 1733.

(3) Listigovers, N. A.; Georges, M. K.; Odell, P. G.; Keoshkerian, B. *Macromolecules* **1996**, *29*, 8993.

(4) Benoit, D.; Grimaldi, S.; Finet, J. P.; Tordo, P.; Fontanille, M.; Gnanou, Y. In *Controlled Radical Polymerization, ASC Symposium Series 685*; Matyjaszewski, K., Ed.; American Chemical Society, Washington, DC 1998; Chap. 14.

(5) Goto, A.; Fukuda, T. submitted for publication.

(6) (a) Fukuda, T.; Ma, Y.-D.; Inagaki, H. *Macromolecules* **1985**, *18*, 17. (b) Ma, Y.-D.; Fukuda, T.; Inagaki, H. *Polym. J. (Tokyo)* **1983**, *15*, 673.

(7) Ouchi, T.; Jokei, S.; Chikasita, H. *J. Heterocyclic Chem.* **1982**, *19*, 935.

(8) (a) Klein, J.; Herzog, D.; Hajibegli, A. *Makromol. Chem., Rapid Commun.* **1985**, *6*, 675. (b) Wulff, G.; Bellmann, S.; Schimid, J.; Podzimek, S. *Macromol. Chem. Phys.* **1997**, *198*, 763.

(9) Catala, J. M.; Budel, F.; Hammouch, S. O. *Macromolecules* **1995**, *28*, 8441.

(10) Gridnev, A. A. *Macromolecules* **1997**, *30*, 7651.

(11) Malau, G. E. *Block Copolymers*; Plenum Press, New York, 1970.

Chapter 6

Synthesis of a Well-Defined Glycopolymer by Atom Transfer Radical Polymerization

6-1. Introduction

As described in Chapter 4, the author succeeded for the first time in the synthesis of a low-polydispersity glycopolymer by a free radical mechanism, which was based on the use of a styryl derivative as a monomer and a nitroxide as a mediator.[1] Furthermore, the system was successfully applied to the synthesis of a well-defined glycopolymer of poly(acrylate) type (see Chapter 5).[2] Nitroxide-mediated polymerization is among those several controlled/"living" free radical polymerization techniques that have been rapidly developed in recent years. Each of them has merits and demerits with differing applicability to differing monomers. The alkyl halide/transition-metal systems independently reported from Sawamoto's[3a] and Matyjaszewski's[3b] groups appear to have promising applicability to various types of monomers including methacrylates. In an attempt to widen the simple synthetic route to well-defined glycopolymers, the author, in this chapter, has applied the technique based on the use of an alkyl halide/copper-complex system, the so-called "atom transfer radical polymerization (ATRP)"[4], to the synthesis of a glucose-carrying methacrylate polymer. It will be shown below that the ATRP technique is capable of providing low-polydispersity, high-molecular weight glycopolymers as well as an amphiphilic block copolymer with a glycopolymer sequence.

6-2. Experimental Section

6-2-1. Materials

Commercially obtained styrene (Wako Pure Chemicals, Osaka, Japan) was purified by vacuum distillation from CaH_2 before use. Cu(I)Br (99.999 %, Aldrich) was used as received without further purification. 4,4'-Di-*n*-heptyl-2,2'-bipyridine (dHbipy) was prepared by the dilithiation of 4,4'-dimethyl-2,2'-bipyridine followed by coupling with *n*-hexyl bromide, according to Matyjaszewski *et al.*[4b] Ethyl 2-bromoisobutylate (2-(EiB)Br, Figure 6-1a) and 1-phenylethyl bromide (1-(PE)Br) were used as received from Nacalai Tesque, Kyoto, Japan, and Wako Pure Chemicals, respectively. Veratrole (*o*-dimethoxybenzene) was purchased from Nacalai Tesque and dried over molecular sieves (4 Å) for several days before use. All other reagents were

commercially obtained and used without further purification.

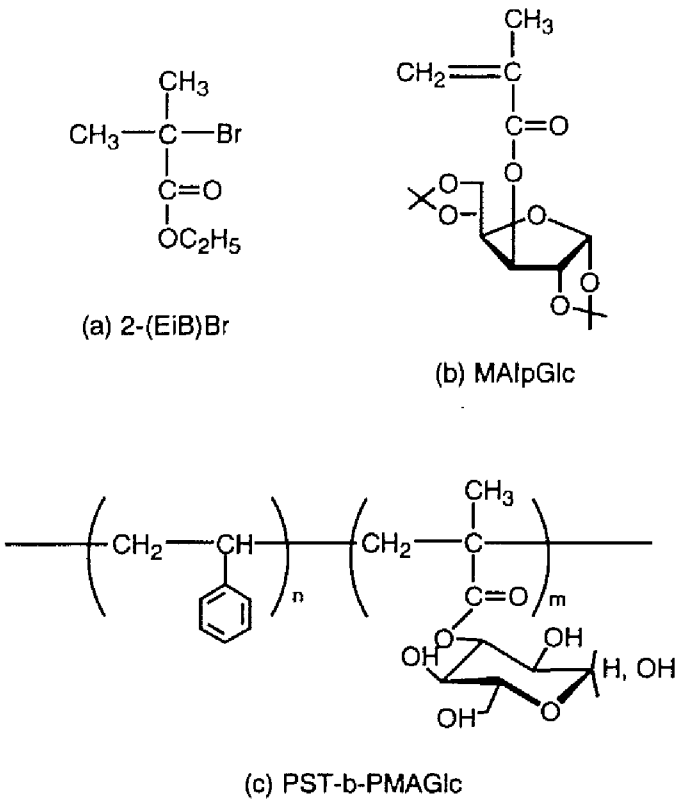

Figure 6-1. Chemical structures of (a) 2-(EiB)Br, (b) MAIpGlc, and (c) PS-*b*-PMAGlc.

6-2-2. Synthesis of 3-*O*-Methacryloyl-1,2:5,6-di-*O*-isopropylidene-*D*-glucofuranose (MAIpGlc, Figure 6-1b)

This synthesis was made by a slight modification of the method proposed by Klein *et al.*[5] To a solution of 1,2:5,6-di-*O*-isopropylidene-*D*-glucofuranose (10 g, 38.4 mmol) in 50 mL of absolute pyridine, 10 mL of methacrylic anhydride (67.1 mmol) was added dropwise at room temperature. The mixture was heated at 65 °C for 4 h and for another 1 h after the addition of 35 mL of water, being stirred magnetically. The system was allowed to get cool to room temperature overnight and then extracted three times with 50 mL of petroleum ether (boiling range, 30 – 70 °C). The combined extracts were washed twice with 100 mL of 5 % aqueous sodium hydroxide solution and three times with 60 mL of water and dried over anhydrous sodium sulfate. After the solvent was evacuated off, the crude product was purified by flash silica gel chromatography with a 7:2:1 ethyl acetate/toluene/methanol mixture eluent to yield the sugar-carrying monomer as a colorless oil (9.4 g, 75 %): ^{1}H-NMR ($CDCl_3$, 200 MHz) δ

1.25–1.55 (m, 12 H, 4 CH_3), 1.95 (s, 3 H, CH_3–C=CH_2), 5.60 (s, 1 H, CH_2=C<, *E* form H), 6.10 (s, 1 H, CH_2=C<, *Z* form H), 4.05, 4.25, 4.51, 5.29, 5.87 (7 H, sugar moiety). Anal. Calcd for $C_{16}H_{24}O_7$: C, 58.51; H, 7.38. Found: C, 58.51; H, 7.50.

6-2-3. Polymerization Kinetics of MAIpGlc

A glass tube was charged with a predetermined amount of a (solid) mixture of Cu(I)Br and dHbipy, to which a (liquid) mixture of MAIpGlc (50 wt.%) and veratrole containing a prescribed concentration of 2-(EiB)Br was quickly added. The mixture was immediately degassed by three freeze–thaw cycles, sealed off under vacuum, and finally placed in an oil bath thermostatted at 80 °C. Soon after the reaction mixture was heated at 80 °C, no trace of Cu(I)Br powder was observed in the system. The color of the homogeneous solution was originally reddish brown and became light brown as the polymerization proceeded. After a prescribed time *t*, the reaction mixture was quenched to room temperature, and analyzed by gel permeation chromatography (GPC) after appropriate dilution with tetrahydrofuran (THF). The monomer conversion was estimated by comparing the GPC peak area of the produced polymer with that of a model PMAIpGlc polymer dissolved in THF at a known concentration.

6-2-4. Synthesis of Poly(3-*O*-methacryloyl-1,2:5,6-di-*O*-isopropylidene-*D*-glucofuranose) (PMAIpGlc)

In a typical run, Cu(I)Br (2.8 mg, 0.019 mmol) and dHbipy (14 mg, 0.038 mmol) were charged in a glass tube, to which MAIpGlc (1.25 g, 3.8 mmol) in veratrole (1.21 g) containing 2-(EiB)Br (7.4 mg, 0.038 mmol) was quickly added. The mixture was immediately degassed by three freeze–thaw cycles, and sealed off under vacuum. The tube was incubated at 80 °C for 90 min, and the content was diluted with chloroform (5 mL) and poured into methanol (120 mL). The precipitate was purified by reprecipitation with a chloroform/methanol system and dried *in vacuo* to give a polymer as a white powder (0.9 g): M_n = 13,500 and M_w/M_n = 1.21 (estimated by GPC, see below), where M_n and M_w are the number- and weight-average molecular weights, respectively.

6-2-5. Preparation of Poly(3-*O*-methacryloyl-α,β-*D*-glucopyranose) (PMAGlc, Figure 6-1c)

The transformation of PMAIpGlc into the water-soluble polymer PMAGlc was achieved by the conventional method:[5,6] the protected polymer PMAIpGlc (500 mg) was dissolved in 80 % formic acid (60 mL) and stirred for 48 h at room temperature. Additional 25 mL of water was added and stirred for another 3 h. The solution was dialyzed against distilled water for 2 days,

concentrated *in vacuo*, and finally lyophilized to give PMAGlc as a white powder with a quantitative yield.

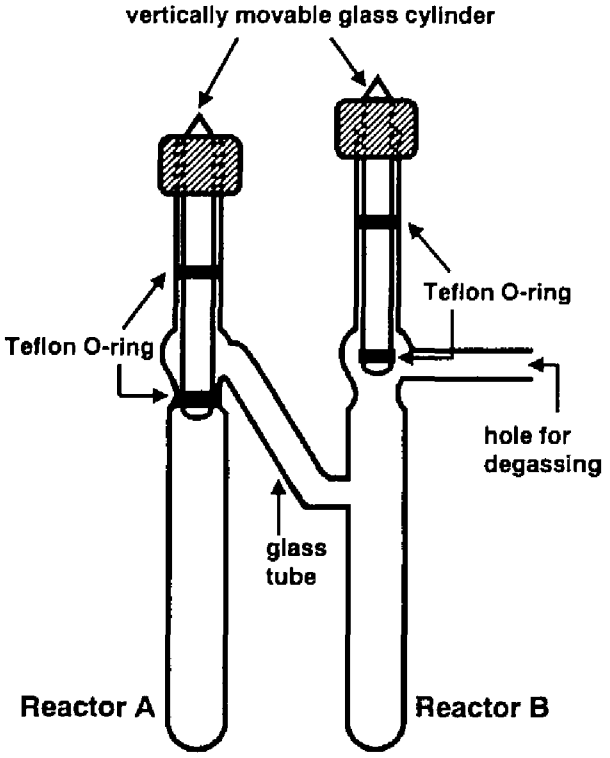

Figure 6-2. The reaction vessel used for the block copolymerization.

6-2-6. Synthesis of PS-*b*-PMAIpGlc Diblock Copolymer

The polymerization was carried out using a H-shaped reaction vessel composed of two glass reactors A and B connected with a glass tube (Figure 6-2). Each of the two reactors could be evacuated and maintained at a reduced pressure down to 10^{-6} Torr by means of greaseless stoppers equipped with double Teflon O-ring. Cu(I)Br (2.75 mg, 0.0192 mmol), dHbipy (13.54 mg, 0.0384 mmol), and then a styrene solution (200 mg, 1.92 mmol) containing 1-(PE)Br (3.55 mg, 0.0192 mmol) were quickly charged in reactor A. The mixture was immediately degassed by three freeze–thaw cycles. The reactor was then sealed under vacuum by the greaseless stopper and placed in an oil bath thermostatted at 110 °C for 5.5 h. After the system was cooled to room temperature, a mixture of Cu(I)Br (1.375 mg, 0.00958 mmol), dHbipy (6.77 mg, 0.0192 mmol), MAIpGlc (630 mg, 1.918 mmol), and veratrole (630 mg) was charged in reactor B, and immediately degassed. Then the path connecting the two reactors was opened and the content of reactor B was poured into reactor A, which contained the precursor product

(PS). Reactor A was sealed again and heated at 80 °C for 24 h. The produced polymer was purified by reprecipitation with a chloroform/methanol system. This polymer was further treated with 80 % formic acid to deblock the isopropylidene groups and purified as described for PMAGlc.

6-2-7. ^{1}H-NMR Measurement

Proton-nuclear magnetic resonance spectra were obtained on a Varian VXR-200 200-MHz spectrometer.

6-2-8. Gel Permeation Chromatography (GPC)

GPC measurements were made on a Tosoh GPC-8020 high-speed liquid chromatograph equipped with Tosoh gel columns G2500H, G3000H, and G4000H. THF was used as eluent, and temperature was maintained at 40 °C. The column system was calibrated with standard polystyrenes (PSs). Sample detection and quantification were made with a Tosoh refractive-index detector RI-8020. This system was used for the characterization of relatively low molecular weight samples with a number-average molecular weight $M_n < 50000$.

For the characterization of higher molecular weight polymers, GPC measurements were made on a Tosoh HLC-802 UR high-speed liquid chromatograph equipped with Tosoh gel columns G6000H6, G5000H6, and G2000H6. Standard PSs were used to calibrate the columns.

6-2-9. Light Scattering Measurement

Light scattering measurements were made in THF solvent at 25 °C on a DLS-7000 photometer (Otsuka Electronics, Japan), which was calibrated with benzene. A He-Ne laser (wave length 633 nm) was used as a light source. The refractive index increment, dn/dc, in THF solution of PMAIpGlc at 25 °C was determined to be 0.0735 mL/g by a DRM1030 differential refractometer (Otsuka Electronics).

6-2-10. Transmission Electron Microscopy (TEM)

TEM observation of the block copolymer surface morphology was performed in the same way as described in Chapter 5.

6-3. Results and Discussion

The key role of ATRP is played by a number of activation–deactivation cycles in which the alkyl halide P-X is reversibly transformed to the polymer radical P*. This process is activated by a metal halide complex, e.g., Cu(I)X/2L (X = Cl or Br, and L = 4,4'-disubstituted-2,2'-

bipyridine, for example)[4]:

$$\text{P-X} + \text{Cu(I)X/2L} \underset{k_{2,\text{deact}}}{\overset{k_{2,\text{act}}}{\rightleftharpoons}} \text{P}^* \xrightarrow{k_p} \text{Monomer} + \text{Cu(II)X}_2\text{/2L} \qquad (1)$$

where k_p is the propagation rate constant, and $k_{2,act}$ and $k_{2,deact}$ are the rate constants of activation and deactivation, respectively. The subscript 2 attached to the rate constants implies that these reactions are second order. The activation process in the homogeneous ATRP of styrene is second order as a whole, i.e., first order with respect to both [P-X] and [Cu(I)X/2L].[7] This process has been kinetically confirmed for the first time by the experiments carried out by this author and co-workers (cf. Appendix, A2). It has also been reported for the homogeneous ATRP of styrene and methyl methacrylate (MMA) that the polymerization rate, $R_p = k_p[P^*][M]$, is first order with respect to both [P-X] and [Cu(I)X/2L], and it also follows first-order kinetics

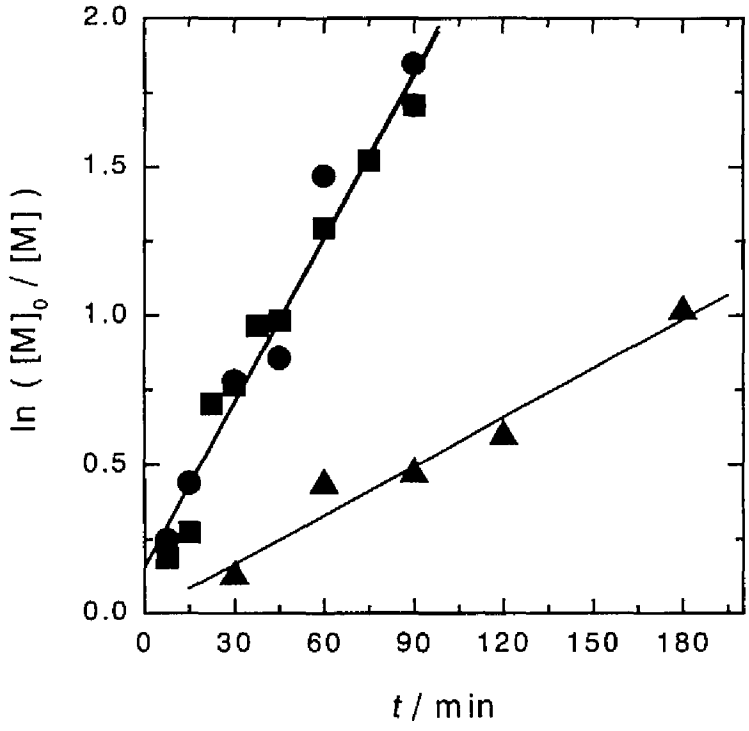

Figure 6-3. Plot of $\ln([M]_0/[M])$ vs t for the solution polymerization of MAIpGlc (50 wt.%) in veratrole at 80 °C: $[MAIpGlc]_0/[2\text{-(EiB)Br}]_0/[Cu(I)Br]_0/[dHbipy]_0$ = 100/1/0.5/1 (■); 200/1/1/2 (●); 200/1/0.5/1 (▲).

with respect to monomer concentration.[4b,h]

6-3-2. ATRP of MAIpGlc, the Glucose-Carrying Monomer

Figure 6-3 shows the plot of $\ln([M]_0/[M])$ vs polymerization time t, where the subscript 0 denotes the initial state (t = 0). In all studied three cases, the plot can be approximated by a straight line, i.e., the system follows first-order kinetics with respect to monomer conversion. However, the dependence of R_p on the concentrations of the initiator 2-(EiB)Br and the activator Cu(I)Br/2dHbipy is not simple. The curves for the two different values of [initiator] with the common [activator] are nearly the same with each other. On the other hand, the curves for the two different values of [activator] with the common value of [initiator] differ in slope by a factor of about 3, while the activator concentrations differ only by factor 2. The reason for the failure of the simple kinetics as observed for the styrene and MMA ATRPs is not clear at

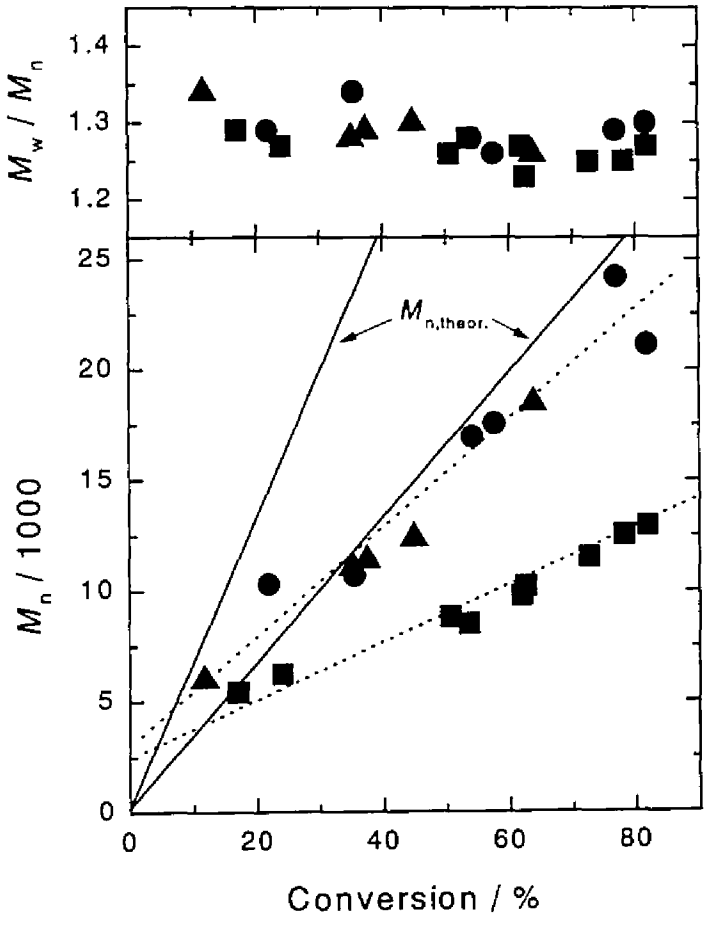

Figure 6-4. Values of M_n and M_w/M_n as a function of monomer conversion for the solution polymerization of MAIpGlc (50 wt.%) in veratrole at 80 °C: $[MAIpGlc]_0/[2\text{-}(EiB)Br]_0/[Cu(I)Br]_0/[dHbipy]_0$ = 100/1/0.5/1 (■); 200/1/1/2 (●); 200/1/0.5/1 (▲). The full lines in the figure represent the theoretical predictions.

this moment. Nevertheless the values of M_n of the produced polymers increased approximately linearly with conversion, and the M_w/M_n ratios were remarkably small (smaller than 1.3 for most samples), as shown in Figure 6-4.

These results have encouraged us to attempt to prepare low-polydispersity MAIpGlc polymer with higher molecular weights. For this purpose, we have carried out two series of polymerization runs with reduced initiator concentrations. In one series (series A), the $[monomer]_0/[activator]_0$ ratio was 200, and in the other (series B), it was 400. Results are summarized in Table 6-1, which, for the sake of comparison, reproduces part of the results

Table 6-1. Results of MAIpGlc Solution Polymerization in Veratrole at 80 °C [a]

Run	$[MAIpGlc]_0/[2\text{-}(EiB)Br]_0$	Time (h)	Conversion (%)	$M_{n,theor.}$ [b]	$M_{n,GPC}$ [c]	M_w/M_n
A1[d]	100	1.5	82	27100	13000	1.27
A2[d]	200	1.5	84	55400	22000	1.33
A3[d]	400	3.5	88	115500	51900	1.63
A4[d]	600	3.5	83	164300	75000	1.82
A5[d]	800	3	69	181500	106900	1.56
B1[e]	200	3	64	42200	18500	1.26
B2[e]	400	12	83	108600	47000	1.33
B3[e]	600	12	74	145000	67000	1.43
B4[e]	800	20	74	195200	98000	1.50

[a] The monomer concentration is 50 wt.%. $[Cu(I)Br]_0/[dHbipy]_0 = 1/2$.
[b] Calculated from the conversion/$[initiator]_0$ ratio.
[c] Estimated by gel permeation chromatography.
[d] $[monomer]_0/[Cu(I)Br]_0 = 200$.
[e] $[monomer]_0/[Cu(I)Br]_0 = 400$.

Table 6-2. Comparison of Weight-Average Molecular Weight Values

Sample	$M_{w,GPC}$ [a]	$(M_w/M_n)_{GPC}$ [a]	$M_{w,LS}$ [b]	$M_{w,theor.}$ [c]
P1	20500	1.21	50000	47000
P2	73000	1.45	169000	168000
P3	203000	1.60	458000	386000

[a] Estimated by gel permeation chromatography.
[b] Determined by light scattering.
[c] $M_{w,theor.} = M_{n,theor.} \times (M_w/M_n)_{GPC}$, where $M_{n,theor.}$ is the M_n value calculated from the $([M]_0 - [M])/[initiator]_0$ ratio.

with the higher initiator concentrations (runs A1, A2, and B1). Clearly, a decrease of initiator concentration or increase of $[monomer]_0/[2\text{-(EiB)Br}]$ ratio increases M_n, keeping the M_w/M_n ratio fairly small. When compared at a common level of molecular weight, the polydispersities of series-B polymers are generally lower ($M_w/M_n \leq 1.5$ in all cases) than those of series-A polymers.

The values of M_n estimated by GPC are significantly smaller than the theoretical values calculated as the molar ratio of polymerized monomer to initiator (see Figure 6-4 and Table 6-1). This indicates the inadequacy of the polystyrene-calibrated GPC analysis. To confirm this, we have carried out light scattering measurements for the three PMAIpGlc samples (P1, P2, and P3) prepared by the ATRP method in a relatively large scale for this purpose. An example of the Zimm plot is given in Figure 6-5. As Table 6-2 shows, the light scattering (LS) M_w values are much larger than the GPC values and fairly close to the $M_{w,theor.}$ values calculated as the product of the theoretical M_n and the GPC M_w/M_n value. In the examined range of molecular weight, the ratio $M_{w,LS}/M_{w,GPC}$ is about 2.4 in all cases. If we multiply the $M_{n,GPC}$ values in Table 6-1 and Figure 6-4 by this factor 2.4, we finds that they come close to the theoretical M_n values. All these results show that the ATRP of MAIpGlc proceeds in a controlled fashion with predictable molecular weight, providing low-polydispersity polymers ($M_w/M_n < 1.5$) with a molecular weight up to 200,000.

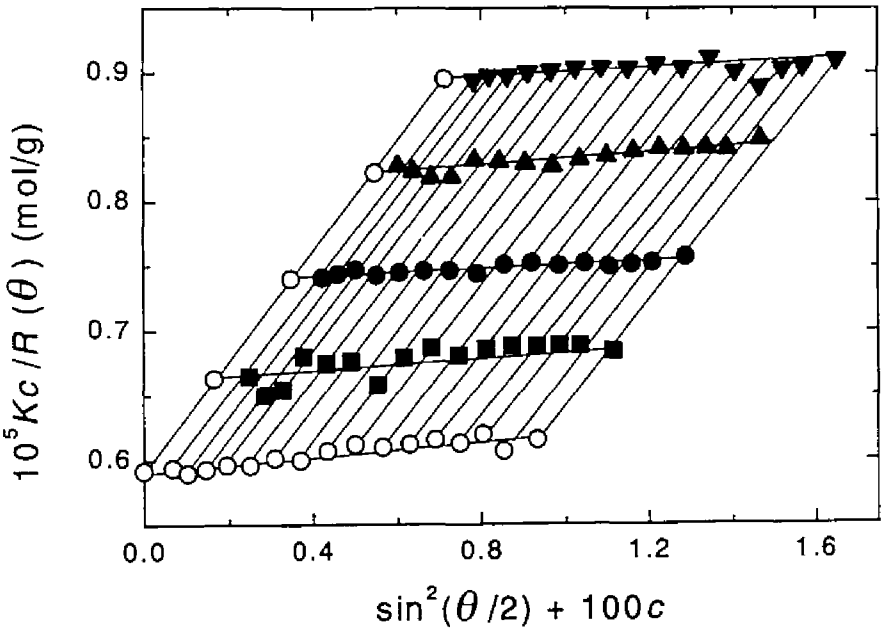

Figure 6-5. Zimm plot for PMAIpGlc polymer P2.

6-3-3. Preparation of PS-*b*-PMAIpGlc Diblock Copolymers

We have attempted to synthesize PS-*b*-PMAIpGlc type block copolymers by the sequential monomer addition technique: as the first step, styrene S was polymerized in bulk with Cu(I)Br/2dHbipy complex and 1-phenylethyl bromide (1-PEBr) as an initiator at 110 °C. After S was nearly completely consumed (more than 90 % conversion, according to a reference run carried out under the same reaction condition), a fresh feed of MAIpGlc with Cu(I)Br/2dHbipy complex dissolved in veratrole was added under vacuum into the system including the precursor PS and then the mixture was heated at 80 °C for 24 h. Figure 6-6 shows the GPC

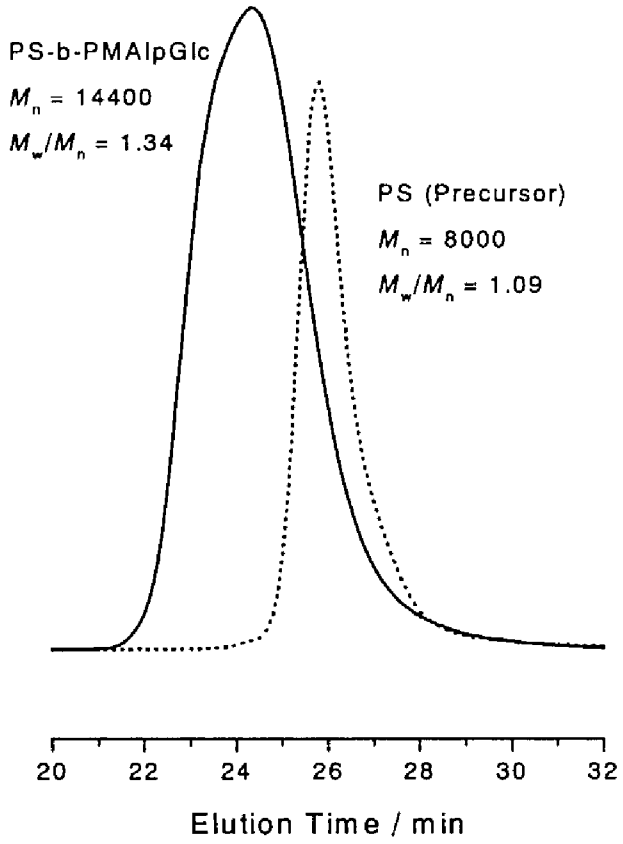

Figure 6-6. GPC curves for the precursor PS and PS-*b*-PMAIpGlc block copolymer before purification: the curve PS was obtained for a reference run carried out under the same reaction condition.

curve of the crude polymer thus obtained (before purification). The peak position shifts to a higher molecular weight region with no detectable shoulder peak at the elution position of the precursor and the molecular weight distribution remaining fairly narrow. This suggests successful formation of a PS-*b*-PMAIpGlc type block copolymer. To be strict, the second

block may not be a pure PMAIpGlc sequence but a statistical copolymer of MAIpGlc with a small fraction of S due to the S monomer remaining unremoved after the first step. However, its fraction is so small that the properties of the block copolymer thus obtained would be approximately the same as those of the equivalent block copolymer with a pure PMAIpGlc sequence. The ^{1}H-NMR measurement of the purified block copolymer showed that the ratio of the number-average degrees of polymerization of PS : PMAIpGlc is 100 : 40 (on the basis of the phenyl ring protons of S block and the sugar residue protons of PMAIpGlc block).

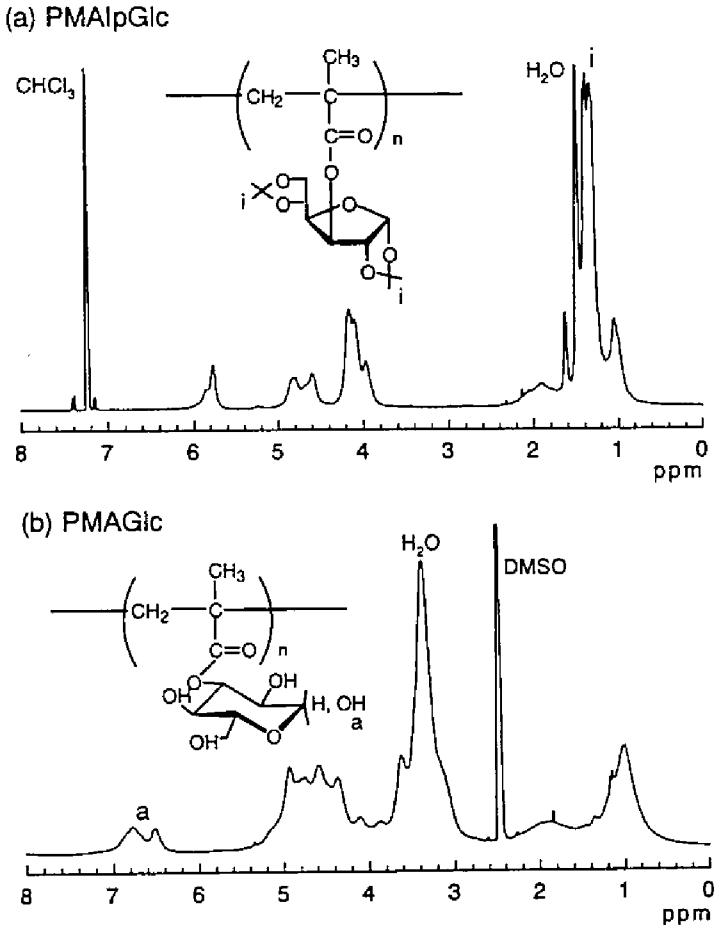

Figure 6-7. Typical ^{1}H-NMR spectra taken (a) before and (b) after the acidolysis of PMAIpGlc. The solvents were (a) $CDCl_3$ and (b) DMSO-d_6.

6-3-4. Deprotection of MAIpGlc Units into MAGlc Units

The PMAIpGlc and PS-*b*-PMAIpGlc samples were treated with formic acid to obtain PMAGlc homopolymers and PS-*b*-PMAGlc block copolymer. Figure 6-7 shows typical ^{1}H-NMR spectra taken before and after the acidolysis. The isopropylidene protons (1.2 – 1.4 ppm in Figure 6-

7a) have completely disappeared after the acidolysis, and instead, a broad signal assignable to the anomeric hydroxyl groups of sugar moieties (6.4 – 7.0 ppm in Figure 6-7b) has appeared. This confirms that the deprotection of isopropylidene groups proceeded quantitatively. The PMAGlc polymers obtained here were soluble in water, DMF, and dimethyl sulfoxide.

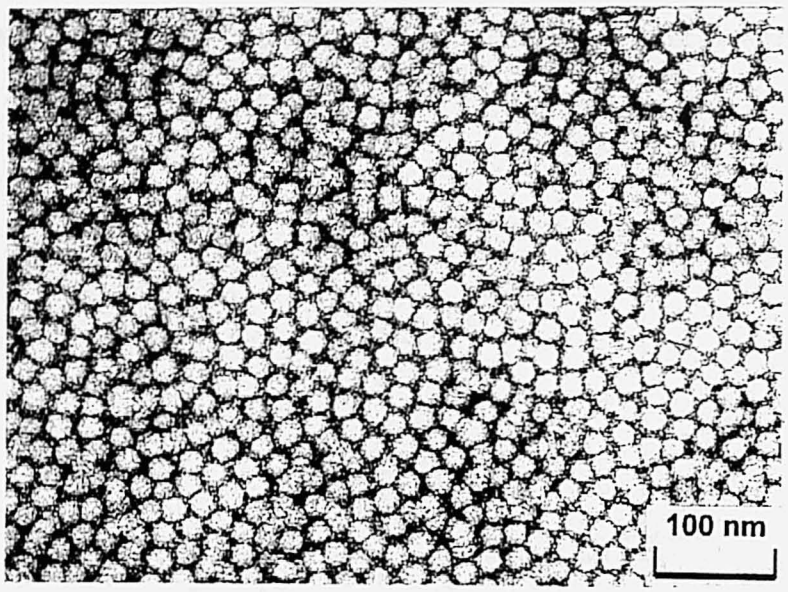

Figure 6-8. TEM micrograph of the surface of a solvent-cast PS-*b*-PMAGlc block copolymer film. The light and dark regions show the PS and PMAGlc domains, respectively.

6-3-5. Surface Morphology of PS-*b*-PMAGlc

Block copolymers often undergo microphase separation and exhibit various microdomain morphologies.[8] The diblock copolymer PS-*b*-PMAGlc obtained here is expected to show microphase separation due to its amphiphilic character. We have investigated the surface morphology of the PS-*b*-PMAGlc film prepared by casting from a DMF solution of the polymer. A TEM micrograph is presented in Figure 6-8. Because uranyl acetate selectively stains hydrophilic regions (PMAGlc domains), the darker regions in the micrograph correspond to PMAGlc domains. The micrograph clearly shows regular, spherical PS domains of about 20 nm in diameter embedded in a continuous matrix of the PMAGlc moieties. It should be noted that this observation was made for the surface of the solvent-cast film, and therefore, the relationship between the microdomain and molecular structure cannot be

rigorously discussed. Nevertheless, the regular surface morphology observed here must have resulted from a well-defined amphiphilic molecular structure.

6-4. Conclusions

The free radical polymerization of MAIpGlc in veratrole in the presence of alkyl halide/copper-complex proceeded in a "living" fashion, giving PMAIpGlc with controlled molecular weight up to M_n = 200 000 and low-polydispersity, $1.2 \leq M_w/M_n \leq 1.5$. The acidolysis of those polymers provided water-soluble PMAGlc polymers. The sequential monomer addition technique, in which the first and the second monomer were S and MAIpGlc, respectively, was successfully adopted to give a diblock copolymer of the type PS-*b*-PMAIpGlc with narrow molecular weight distribution. After the acidolysis of the PMAIpGlc sequence, a film of this block copolymer exhibited a microdomain surface structure with spherical PS domains embedded in the hydrophilic PMAGlc matrix. Thus, this work has broaden the practical synthetic route to well-defined glycopolymers. The ATRP of sugar-carrying monomer will find unique applications in, e.g., the preparation of sugar-carrying amphiphile like glycolipid and graft polymers by constructing various initiating system.

References

(1) Ohno, K.; Tsujii, Y.; Miyamoto, T.; Fukuda, T.; Goto, M.; Kobayashi, K.; Akaike, T. *Macromolecules* **1998**, *31*, 1064.

(2) Ohno, K.; et al. To be published.

(3) (a) Kato, M.; Kamigaito, M.; Sawamoto, M.; Higashimura, T. *Macromolecules* **1995**, *28*, 1721. (b) Wang, J. S.; Matyjaszewski, K. *J. Am. Chem. Soc.* **1995**, *117*, 5614.

(4) (a) Patten, T. E.; Xia, J.; Abernathy, T.; Matyjaszewski, K. *Science* **1996**, *272*, 866. (b) Matyjaszewski, K.; Patten, T. E.; Xia, J. *J. Am. Chem. Soc.* **1997**, *119*, 674. (c) Gaynor, S. G.; Edelman, S.; Matyjaszewski, K. *Macromolecules* **1996**, *29*, 1079. (d) Grimaud, T.; Matyjaszewski, K. *Macromolecules* **1997**, *30*, 2216. (e) Matyjaszewski, K.; Gaynor, S. G.; Kulfan, A.; Podwika, M. *Macromolecules* **1997**, *30*, 5192. (f) Qiu, J.; Matyjaszewski, K. *Macromolecules* **1997**, *30*, 5643. (g) Matyjaszewski, K.; Jo, S. M.; Paik, H.-j.; *Macromolecules* **1997**, *30*, 6398. (h) Wang, J.-L.; Grimaud, T.; Matyjaszewski, K. *Macromolecules* **1997**, *30*, 6507.

(5) Klein, J.; Herzog, D.; Hajibegli, A. *Makromol. Chem., Rapid Commun.* **1985**, *6*, 675.

(6) Wulff, G.; Bellmann, S.; Schmid, J.; Podzimek, S. *Macromol. Chem. Phys.* **1997**, *198*, 763.

(7) Ohno, K.; Goto, A.; Fukuda, T.; Xia, J. Matyjaszewski, K. *Macromolecules* **1998**, *31*, 2699.

(8) Molau, G. E. *Block Copolymers*; Plenum Press: New York, 1970.

Chapter 7

Synthesis of a Well-Defined Novel Glycolipid by Nitroxide-Controlled Free Radical Polymerization

7-1. Introduction

Molecular recognition mediated by sugar residues at interfaces between, e.g., two lipid layers or a lipid layer and a liquid phase *in vivo* is an essential process including virus infection, fertilization, and immunological protection.[1] A wide variety of synthetic glycolipids have attracted much attention in designing model systems for the basic understanding of saccharide recognition events at membrane surfaces.[2] Kitano *et al.* and the author[3] have prepared a new type of sugar-carrying amphiphile, in which glucose- and galactose-carrying vinyl monomers were polymerized with a lipophilic azo-type radical initiator to give a glycolipid with sugar-carrying polymer (or oligomer) chain as a hydrophilic group (see Chapter 1 – 3). A single drawback of the method was the difficulty of obtaining well-defined (low-polydispersity) sugar-carrying polymer chains when the conventional free radical polymerization was employed.

As described in Chapters 4 through 6, the author succeeded in the first synthesis of a low-polydispersity glycopolymers by free radical mechanism, in which "living" polymerizations of styrenic and methacryloyl monomers with pendent saccharide groups were achieved by nitroxide-controlled[4] and atom transfer[5] radical polymerizations, respectively.

These successes have encouraged the author to synthesize well-defined artificial glycolipids by "living" radical polymerization. At first, the work appeared him to be a rather straightforward application of the established techniques. However, the first lipophilic initiator systems designed by him have failed to give satisfactory results with respect to the predictability of the molecular weight and/or low polydispersity of the product. The author finally achieved a truly successful result with a newly designed lipophilic alkoxyamine initiator and a styryl monomer having a pendent saccharide group. The following was the first report of the synthesis of a well-defined artificial glycolipid by free radical mechanism and its formation of a liposomal structure upon mixing with a phospholipid.

7-2. Experimental Section

7-2-1. Materials

N,N-Dioctadecylamine (DODA) was from Fluka. Di-*tert*-butyl nitroxide (DBN) and 4-ethylbenzoyl chloride were from Aldrich. Concanavalin A (Con A, from *Canavalia ensiformis*), agglutinin RCA_{120} (RCA, from *Ricinus communis*), and *L*-α-dimyristoylphosphatidylcholine (DMPC) were from Sigma. *N*-(*p*-Vinylbenzyl)-2,3,5,6-tetra-*O*-acetyl-4-*O*-(2,3,4,6-tetra-*O*-acetyl-β-*D*-galactopyranosyl)-*D*-gluconamide (Ac-VLA, Figure 7-1a) was prepared as described in Chapter 4.[4a] 2-Pyridinecarbaldehyde *n*-propylimine was prepared according to the method proposed by Haddleton *et al.*[6] 1,2-Dichloroethane was dried over molecular sieves (4 Å) for several days before use. Other reagents were commercially obtained.

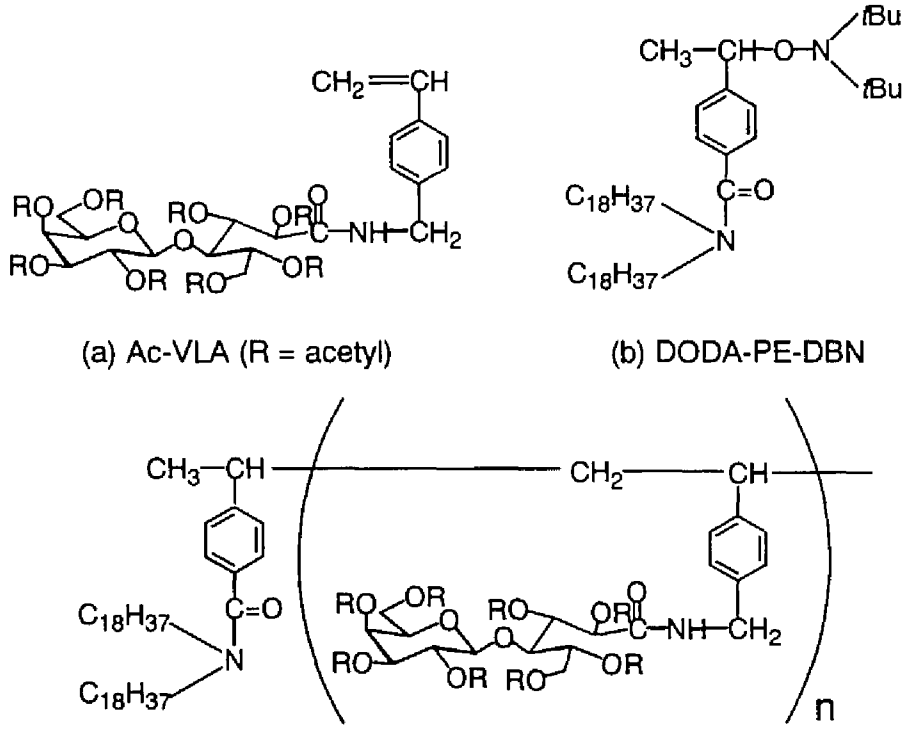

Figure 7-1. Chemical structures of (a) Ac-VLA, (b) DODA-PE-DBN, (c) DODA-PAcVLA, and (d) DODA-PVLA.

7-2-2. Synthesis of 1-(4-*N,N*-Dioctadecylcarbamoylphenyl)ethyl-DBN (DODA-PE-DBN, Figure 7-1b)

DODA-PE-DBN was synthesized via the three step reactions described below. First step: (4-

N,N-dioctadecylcarbamoylphenyl)ethane (DODA-PE) was prepared by the reaction of 4-ethylbenzoyl chloride with DODA in dry chloroform (yield, 86 %). Second step: the bromination of benzyl position of DODA-PE was carried out according to the conventional method[7] using *N*-bromosuccinimide and catalytic amount of benzoyl peroxide in dry carbon tetrachloride to obtain 1-bromo-1-(4-*N,N*-dioctadecylcarbamoylphenyl)ethane (DODA-PE-Br) (yield, 82 %). Third step: Cu(I)Br (1.15 g, 8.02 mmol) was charged in a round-bottomed flask, to which DODA-PE-Br (1.18 g, 1.61 mmol) dissolved in a mixture of dry benzene (5.3 mL) and dry *N,N*-dimethylformamide (9.5 mL) containing 2-pyridinecarbaldehyde *n*-propylimine (3.03 g, 20.4 mmol) and DBN (710 mg, 4.92 mmol) was quickly added. The mixture was immediately degassed by three freeze–pump–thaw cycles, sealed off under vacuum, and then stirred magnetically at room temperature for one week. After the solvent was evacuated off, the crude product was purified by flash chromatography on a silica gel column with a 5:1 hexane/ethyl acetate mixture eluent to yield a pale yellow oil as the final product (yield, 81 %). ^{1}H-NMR ($CDCl_3$, 400 MHz): δ 0.88 (t, 6H, CH_3CH_2), 1.00 (s, 9H, $C(CH_3)_3$ of DBN unit), 1.21–1.29 (br s, 64H, CH_2 of alkyl chains), 1.30 (s, 9H, $C(CH_3)_3$ of DBN unit), 1.47 (d, 3H, CH_3CH), 3.16 and 3.46 (br, 4H, CH_2N), 4.82 (q, 1H, CH_3CH), 7.30 (m, 4H, ArH); ^{13}C-NMR ($CDCl_3$, 100 MHz): δ 14.2 (CH_3CH_2), 22.8 (CH_3CH), 29.4–29.8 (CH_2 of alkyl chains), 30.7 ($C(CH_3)_3$), 32.0 (CH_2N), 61.8 ($C(CH_3)_3$), 82.6 (CH_3CH), 126.0, 126.7, 135.7, and 146.0 (phenyl), 171.4 (NC=O). Anal. Calcd for $C_{53}H_{100}N_2O_2$: C, 79.81; H, 12.66; N, 3.51. Found: C, 79.90; H, 12.52; N, 3.58.

7-2-3. General Procedure for Polymerization of Ac-VLA "Initiated" by DODA-PE-DBN Adduct

A Pyrex tube was charged with a predetermined amount of Ac-VLA (55 wt.%), to which a solution of 1,2-dichloroethane containing a prescribed amount of DODA-PE-DBN and dicumyl peroxide (DCP) was added. The mixture was degassed by three freeze–pump–thaw cycles, and sealed off under vacuum. The tube was placed in an oil bath thermostatted at 90 °C for a prescribed time, quenched to room temperature, and subjected to a gel permeation chromatography (GPC) analysis after appropriate dilution with tetrahydrofuran (THF). The monomer conversion was estimated by comparing the GPC peak area of the produced polymers with that of DODA-PAcVLA (Figure 7-1c) model polymer dissolved in THF at a known concentration. The produced polymer was purified by reprecipitation with a chloroform (solvent)/cold methanol (nonsolvent) system.

7-2-4. Deprotection to Obtain Sugar-Carrying Amphiphile (DODA-PVLA, Figure 7-1d)

To a cold solution of the protected polymer DODA-PAcVLA (350 mg) in DMF (33 mL) was added at 0 °C hydrazine monohydrate (6.6 mL). The mixture was magnetically stirred for 30 min at 0 °C and for another 4.5 h at room temperature, to which 11 mL of acetone was added and stirred for several minutes, and then 33 mL of water was added to dissolve the resulting oily precipitate. The obtained clear solution was dialyzed against distilled water for 5 days, concentrated by evacuation of the solvent, and finally lyophilized to give DODA-PVLA as a white powder with a quantitative yield.

7-2-5. Preparation of Liposome

DMPC (24 mg) was dissolved in chloroform (2 mL) in a small round-bottomed flask. After evaporation of the solvent, the lipid thin membrane was dispersed in a *N*-(2-hydroxyethyl)piperazine-*N*'-2-ethanesulfonic acid (HEPES) buffer (5 mL, pH 7.2, 10 mM) in which DODA-PVLA (6 mg) had been dispersed beforehand. The system was sonicated by ultrasonifier (Astrason W-385, Heat-System-Ultrasonics, Inc., New York) for 5 min at 40 °C. Thus obtained liposome suspension was fractionated by passing through a GPC column (Sephacryl S-200, 2 cm i.d. x 20 cm, eluting solution HEPES buffer (10 mM, pH 7.2)) equipped with a UV-monitor to confirm that DODA-PVLA molecules had completely been incorporated in the liposomes (vide infra).

7-2-6. Measurements

The GPC analysis was made on a Tosoh GPC-8020 high-speed liquid chromatography equipped with Tosoh gel column G2500H, G3000H, and G4000H. THF was used as eluent, and temperature was maintained at 40 °C. Sample detection and quantification were made with a Tosoh differential refractometer RI-8020 calibrated with a known concentration of THF solution of the DODA-PAcVLA. Proton-nuclear magnetic resonance (^{1}H-NMR) spectra were obtained on a JEOL JNM/AL400 400MHz spectrometer. Hydrodynamic diameter of the liposome was estimated by the dynamic light scattering (DLS) technique (DLS-7000, Otsuka Electronics, Japan, light source He-Ne laser, 632.8 nm). The aggregation processes of liposomes mediated by lectins were followed by observing the evolution of turbidity at 350 nm with a stopped-flow spectrophotometer (RA-401, Otsuka Electronics). The optical cell was thermostatted at 25 °C.

7-3. Results and Discussion

7-3-1. Ac-VLA Polymerization by Using DODA-PE-DBN Adduct

Previous reports[8] on nitroxide-controlled free radical polymerization have shown that the use of a limited amount of a conventional radical initiator along with an alkoxyamine brings about

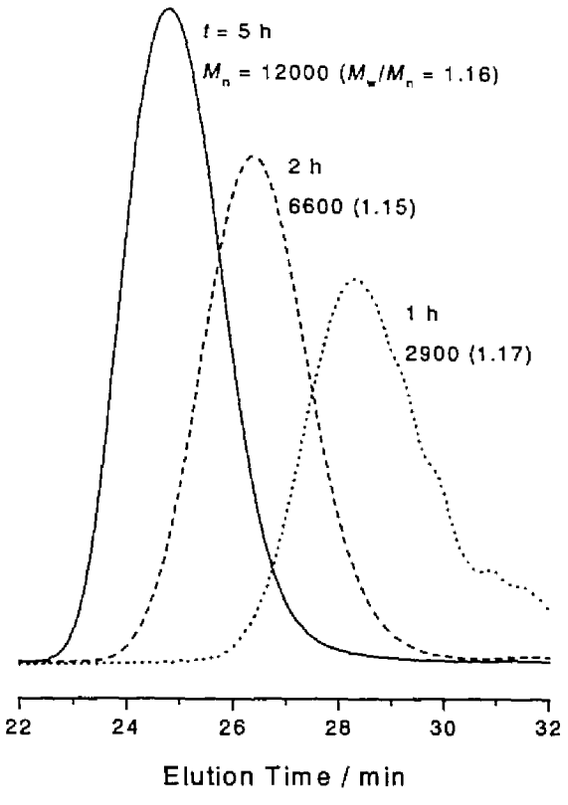

Figure 7-2. GPC curves for the polymerization of Ac-VLA in 1,2-dichloroethane at 90 °C: $[\text{Ac-VLA}]_0/[\text{DODA-PE-DBN}]_0/[\text{DCP}]_0 = 50/1/3$.

an increase in polymerization rate and, consequently, the chain length, for a given polymerization time without causing any appreciable broadening of molecular weight distribution. Thus, Ac-VLA was polymerized with the DODA-PE-DBN adduct in the presence of a small amount of dicumyl peroxide (DCP). As the GPC curves in Figure 7-2 show, the molecular weight increases with increasing reaction time, keeping the M_w/M_n ratio remarkably small, where M_w and M_n are the weight- and number-average molecular weights, respectively. Figure 7-3 shows the time–conversion first-order plot for the polymerization in the presence of a fixed amount of DODA-PE-DBN and varying concentrations of DCP. The plots are linear, indicating that the radical concentration stays approximately constant throughout the polymerization. More interestingly, an over 90 % conversion has been reached in 3 h with the

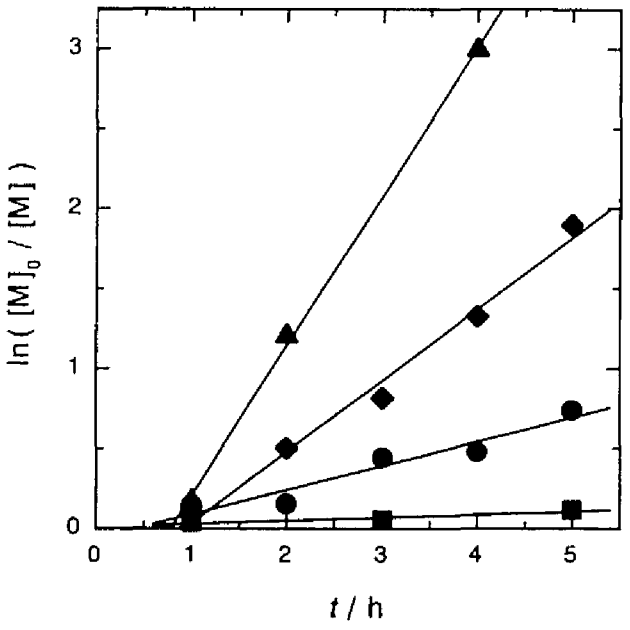

Figure 7-3. Plot of $\ln([M]_0/[M])$ vs t for the solution polymerization of Ac-VLA (55 wt.%) in 1,2-dichloroethane at 90 °C: $[Ac\text{-}VLA]_0/[DODA\text{-}PE\text{-}DBN]_0/[DCP]_0$ = 50/1/0 (■); 50/1/2 (●); 50/1/3 (◆), 50/1/4 (▲).

highest concentration of DCP studied here. There seems to be a short induction period, which was observed also in the 2-(benzoyloxy)-1-(phenylethyl)-DBN (BS-DBN)/Ac-VLA system examined earlier (see Chapter 4).[4a] The reasons for these phenomena are unclear at this moment. Figure 7-4 shows that the M_n of the produced polymer increases linearly with conversion, independently of DCP concentration, and the M_w/M_n ratio stays below 1.2 at all conversions for all concentrations of DCP. This means that the cumulative number of polymer species initiated by the decomposition of DCP is negligibly small compared with the number of adduct molecules. Clearly, the polymerization without DCP is impractically too slow, as Figure 7-3 suggests. Details of the role played by the conventional radical initiator in such a system were discussed by Fukuda's and Matyjaszewski's groups.[8]

The M_n values obtained by GPC are much smaller than the theoretical values, $M_{n,theor.}$, calculated from the monomer conversion/$[DODA\text{-}PE\text{-}DBN]_0$ ratios. This is attributable to the inadequacy of the polystyrene-calibrated GPC analysis. The author has carried out 400 MHz ^{1}H-NMR measurements for the three DODA-PAcVLA samples (P1, P2, and P3). A typical ^{1}H-NMR spectrum is given in Figure 7-5a. The number-average molecular weight was estimated

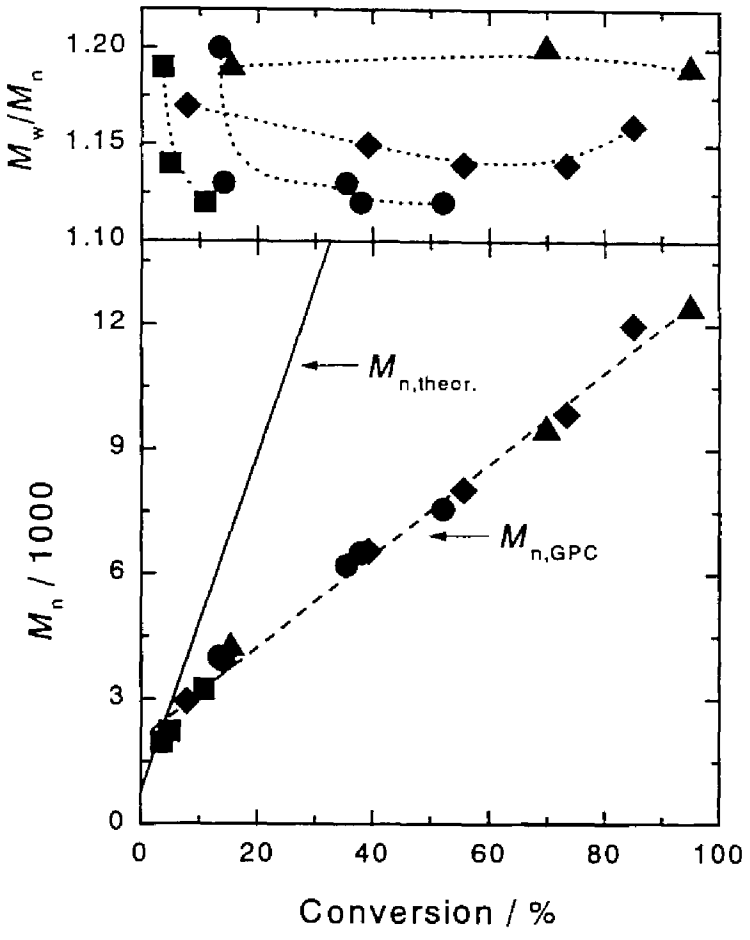

Figure 7-4. Values of M_n and M_w/M_n as a function of monomer conversion for the solution polymerization of Ac-VLA (55 wt.%) in 1,2-dichloroethane at 90 °C: $[Ac\text{-}VLA]_0/[DODA\text{-}PE\text{-}DBN]_0/[DCP]_0$ = 50/1/0 (■); 50/1/2 (●); 50/1/3 (◆), 50/1/4 (▲). The full line in the figure represents the theoretical prediction.

on the basis of the ratio of the integral areas of peaks d and a, which are assignable to the aromatic ring protons of the polymer chain and the terminal methyl protons of the alkyl chain moieties, respectively. As shown in Table 7-1, the $M_{n,NMR}$ values are, on the average, 2.4 times as large as the $M_{n,GPC}$ values and fairly close to the $M_{n,theor.}$ values. This factor 2.4 also explains most part of the discrepancies between $M_{n,GPC}$ and $M_{n,theor.}$ demonstrated in Figure 7-4. These results show that the polymerization with the specific lipophilic alkoxyamine initiator proceeds in a "living" fashion providing low-polydispersity polymers.

7-3-2. Deprotection of Acetyl Groups of DODA-PAcVLA

The DODA-PAcVLA samples were treated with hydrazine to obtain DODA-PVLAs. Figure 7-

5 shows typical ^{1}H-NMR spectra before and after the hydrolysis. The acetyl group protons (around 2 ppm in Figure 7-5a) have completely disappeared after the hydrolysis, and instead broad overlapping signals (3.2–5.4 ppm in Figure 7-5b) assignable to the hydroxyl groups and hydrogens of the sugar moieties have newly appeared. This confirms that the deprotection of acetyl groups proceeded quantitatively. The DODA-PVLAs obtained here formed a stable suspension in water.

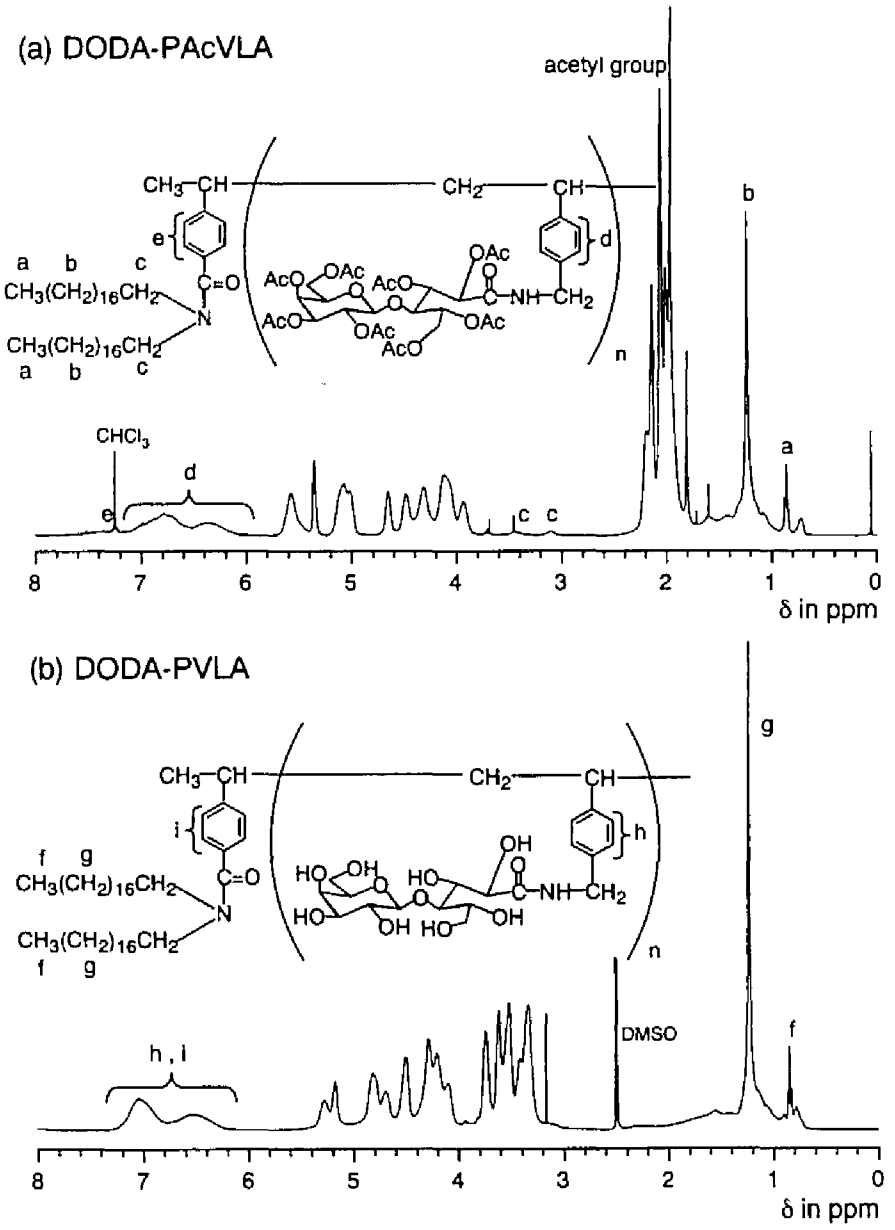

Figure 7-5. Typical ^{1}H-NMR spectra taken (a) before and (b) after the hydrolysis of DODA-AcVLA (P1). The solvents were (a) $CDCl_3$ and (b) DMSO-d_6.

Table 7-1. Comparison of Number-Average Molecular Weight Values

Sample	$M_{n,GPC}$[a]	$M_{n,NMR}$[b]	$M_{n,theor.}$[c]
P1	5200	10200	10500
P2	7000	16500	19300
P3	12400	36000	38000

[a] Estimated by gel permeatin chromatography.
[b] Determined by ^{1}H-NMR.
[c] Calculated from the $([M]_0 - [M])/[DODA\text{-}PE\text{-}DBN]_0$ ratio.

7-3-3. Interactions of Lectins with Sugar-Carrying Polymer Chains on the Liposome Surface

The liposome was purified by passing through the Sephacryl S-200 column to confirm that the DODA-PVLA molecules form a stable liposomal structure by mixing with phospholipid. The GPC curve detected by UV-monitor was clearly mono-modal, suggesting the formation of a stable liposomal structure. By the DLS technique, the average diameter of the sugar-carrying liposome composed of DMPC and DODA-PVLA (P1) was estimated to be 950 Å. Upon mixing with a solution of RCA, which mainly recognizes β-galactose, the sugar-carrying liposome suspension quickly increases its turbidity (Figure 7-6a), whereas, after the liposome suspension is mixed with a solution of Con A, which mainly recognizes α-mannose and α-glucose, the system shows no appreciable increase in turbidity (Figure 7-6b). Next, when the sugar-carrying liposome suspension incubated with an RCA solution for 2 min is mixed with a lactose (4-*O*-β-*D*-galactopyranosyl-*D*-glucose) solution, the turbidity decreases steeply at first and then gradually (Figure 7-6c). Furthermore, upon the addition of maltose (4-*O*-α-*D*-glucopyranosyl-*D*-glucose) instead of lactose, there is no detectable change in turbidity (Figure 7-6d). This unequivocally shows that the increase in turbidity in Figure 7-6a has resulted from the tetrameric RCA molecules' specific recognition of galactose residues on the liposome surfaces to form large aggregates composed of the liposomes and lectins.

7-4. Conclusions

The free radical polymerization of Ac-VLA in the presence of DODA-PE-DBN as a mediator and DCP as an accelerator proceeded in a "living" fashion, giving DODA-PAcVLA with low-polydispersities, $1.1 < M_w/M_n \leq 1.2$. The hydrolysis of the polymers provided a new type of glycolipid with a well-defined glycopolymer subchain as a hydrophilic group (DODA-PVLA).

Mixing DODA-PVLA with a phospholipid gave a stable liposome. The galactose residues on the liposome surfaces were specifically and effectively recognized by the galactose-specific lectin RCA. Thus, this work has broaden the practical synthetic route to well-defined glycolipids. A vesicle composed of DODA-PVLA will be useful for a fundamental understanding of the roles of sugar chains at membrane surfaces and also find important applications in, e.g., drug delivery systems based on a drug-encapsulated liposome with a sugar-specific interaction ability.

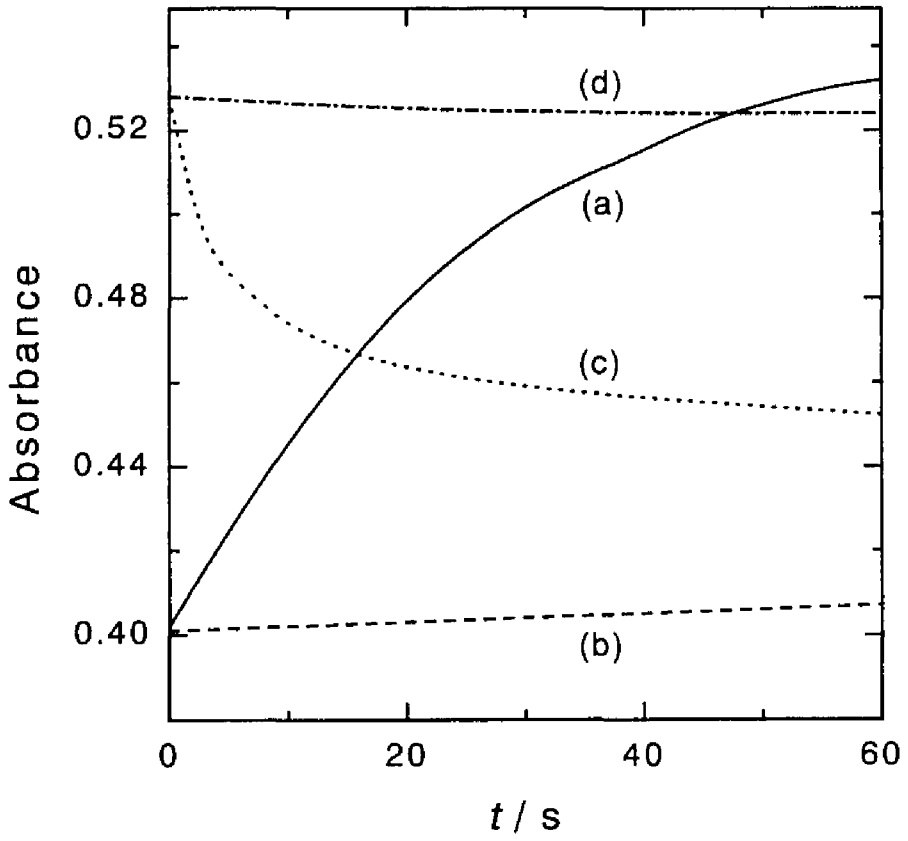

Figure 7-6. Typical profiles of turbidity change: Final concentrations; (a) [liposome] = 500 μg of lipid/mL and [RCA] = 100 μg/mL, (b) [liposome] = 500 μg of lipid/mL and [Con A] = 100 μg/mL, (c) [liposome] = 250 μg of lipid/mL, [RCA] = 50 μg/mL, and [lactose] = 0.5 mM, (d) [liposome] = 250 μg of lipid/mL, [RCA] = 50 μg/mL, and [maltose] = 0.5 mM. In HEPES (10 mM, pH 7.2) buffer; wavelength = 350 nm.

References

(1) (a) Wassarman, P. M. *Science* **1987**, *235*, 553. (b) Sharon, N.; Lis, H. *Sci. Am.* **1993**, *268*, 82. (c) Lowe, J. B. In *Molecular Glycobiology*; Fukuda, M., Hindsgaul, O. Eds.; Oxford University Press: New York, 1994; p IV/163.

(2) In *Methods in Enzymology*; Lee, Y. C., Lee, R. T. Eds.; Academic Press: San Diego, CA, 1994; Vol. 242, p II/127.

(3) (a) Kitano, H.; Ohno, K. *Langmuir* **1994**, *10*, 4131. (b) Kitano, H.; Sohda, K.; Kosaka, A. *Bioconjugate Chem.* **1995**, *6*, 131. (c) Ohno, K.; Sohda, K.; Kosaka, A.; Kitano, H. *Bioconjugate Chem.* **1995**, *6*, 361.

(4) Ohno, K.; Tsujii, Y.; Miyamoto, T.; Fukuda, T.; Goto, M.; Kobayashi, K.; Akaike, T. *Macromolecules* **1998**, *31*, 1064.

(5) Ohno, K.; Tsujii, Y.; Fukuda, T. *J. Polym. Sci., Part A: Polym. Chem.*, in press.

(6) Haddleton, D. M.; Jasieczek, C. B.; Hannon, M. J.; Shooter, A. J. *Macromolecules* **1997**, *30*, 2190.

(7) (a) Pine, S. H. *Organic Chemistry, 5th ed.;* McGraw-Hill: New York, 1987. (b) Campaigne, E.; Tullar, B. F. *Org. Synth.* **1963**, IV, 921.

(8) (a) Goto, A.; Fukuda, T. *Macromolecules* **1997**, *30*, 4272. (b) Greszta, D.; Matyjaszewski, K. *J. Polym. Sci., Part A: Polym. Chem.* **1997**, *35*, 1857.

Appendix

Some Kinetic Aspects of Controlled/"Living" Radical Polymerizations

A1. Thermal Decomposition of Polymer–Nitroxyl Adduct

A1-1. Introduction. The free radical polymerization mediated by stable nitroxyl radicals such as 2,2,6,6-tetramethylpiperidinyl-1-oxy (TEMPO) and its derivatives has aroused much interest as a novel and simple synthetic route to well-defined polymers.[1] The key process of this method is the reversible dissociation–combination reaction of the alkyl–nitroxyl adduct (Scheme A1-1a).[1c,2] However, a side reaction can possibly occur. It is the decomposition of the adduct molecule through the abstraction of the β-proton of the polymer radical by the nitroxyl, producing terminally unsaturated polymer and hydroxyamine (Scheme A1-1b). This reaction was suggested by Li et al.,[3] who observed the decomposition of the model compound S-TEMPO (Figure A1-1a) according to a similar mechanism.[4] Depending on the magnitude of the decomposition rate constant, k_{dec}, this reaction can bring about a severe limitation to the "livingness" of the system, causing a serious broadening of the product polydispersities. Therefore, k_{dec} also is another essential parameter characterizing a given polymer/nitroxyl system. The following demonstrates the determination of k_{dec} of two model compounds, i.e., an oligomeric-PS adduct with TEMPO (PS-TEMPO; Figure A1-1b) and its unimer model (BS-TEMPO; Figure A1-1c). The results indicate that the thermal decomposition of these compounds are less serious than that of the model compound S-TEMPO, as will be described below.

A1-2. Experimental Section. The PS-TEMPO was synthesized as follows: freshly distilled styrene, benzoyl peroxide (BPO, 0.094 mol L^{-1}), and TEMPO (0.112 mol L^{-1}) were charged in a round-bottomed flask, degassed by several freeze-pump-thaw cycles, and sealed off under vacuum. The mixture was heated at 95 °C for 2.5 h to achieve complete decomposition of BPO and then at 125 °C for 2 h. After unreacted monomer was removed by vacuum evaporation, the viscous oily product was diluted with chloroform and subjected to fractionation on a Tosoh semipreparative gel permeation chromatograph (GPC) Model HLC-827 with chloroform as eluent. This gave a PS-TEMPO adduct as a main fraction. The unimer model compound

Scheme A1-1. Main Reactions That a PS-TEMPO Adduct Can Make at High Temperature: (a) Reversible Dissociation; (b) Decomposition (β-Proton Abstraction); (c) Bialkyl Combination (Termination).

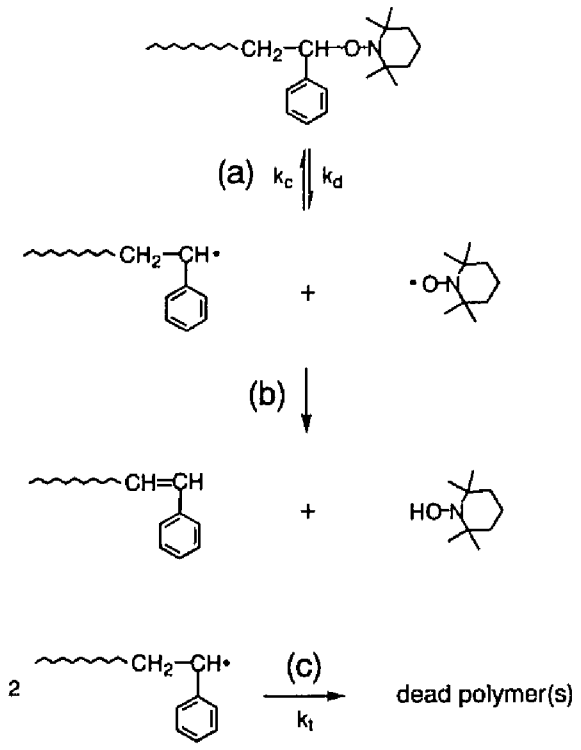

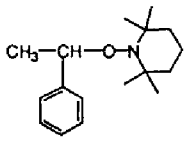

(a) S-TEMPO

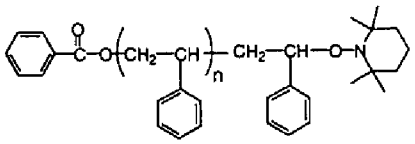

(b) PS-TEMPO

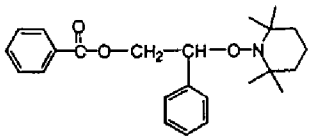

(c) BS-TEMPO

Figure A1-1. Chemical structures of (a) S-TEMPO, (b) PS-TEMPO, and (c) BS-TEMPO

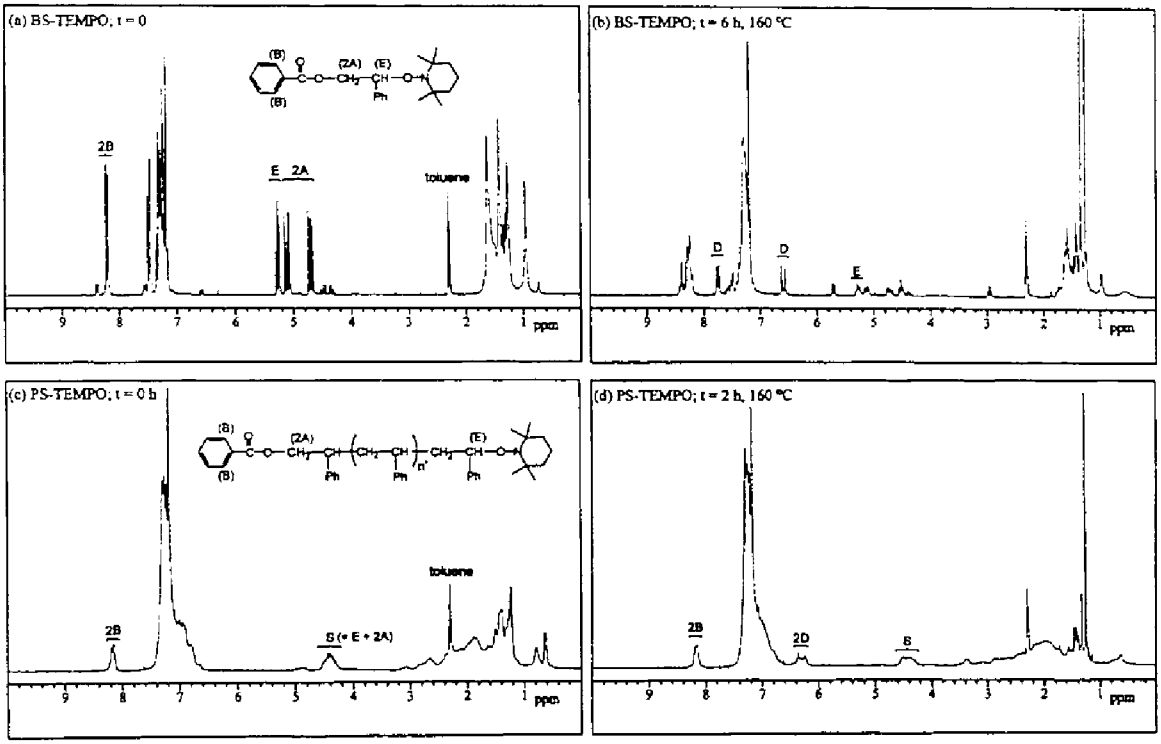

Figure A1-2. ^{1}H-NMR spectra of BS-TEMPO (a and b) and PS-TEMPO (c and d) before (a and c) and after (b and d) the thermal treatment at 160 °C. See the text for assignments.

BS-TEMPO was prepared according to Hawker.[1h]

Parts a and c of Figure A1-2 show the proton nuclear magnetic resonance (^{1}H-NMR) spectra of the two model compounds. Figure A1-2a suggests that the BS-TEMPO adduct is contaminated by some impurities (about 5%), but it should not affect the results. The number-average molecular weight M_n of the PS-TEMPO estimated from the spectrum in Figure A1-2c was 1100 after appropriately correcting for the protonous toluene impurities included in toluene-d_8 used as solvent (see below for the main assignments). The polydispersity index M_w/M_n estimated by GPC was 1.03. Incidentally, the GPC value of M_n is less reliable for such a low-mass sample because of the differences in end groups between this sample and the standard PSs used for calibration.

The process of thermal decomposition was followed by ^{1}H-NMR spectroscopy: each model compound was dissolved in toluene-d_8 ([BS-TEMPO] = 0.080 mol L^{-1}, and [PS-TEMPO] = 0.040 mol L^{-1}), charged in a NMR tube, carefully degassed, and sealed off under vacuum. It was heated at a prescribed temperature T for a prescribed time t, quenched to room temperature, and studied by ^{1}H-NMR.

A1-3. Results and Discussion. Parts b and d Figure A1-2 show the ^{1}H-NMR spectra of BS-TEMPO and PS-TEMPO, respectively, taken after the thermal treatment. In the case of BS-TEMPO (Figure A1-2b), we followed the signals of the α-proton (5.2 – 5.3 ppm) next to the TEMPO moiety for the concentration E of active molecules, and those of the double-bond protons (6.5 – 6.7 and 7.7 – 7.8 ppm) for the concentration D of decomposed molecules. In the case of PS-TEMPO (Figure A1-2d), the α-proton (E) next to the TEMPO moiety and the methylene protons ($2A$) connected to the oxygen of the BPO moiety appear in group at 4.2 – 4.6 ppm ($S = E + 2A$), the double-bond protons ($2D$), at 6.2 – 6.4 ppm, and the two *ortho* protons ($2B$) of the BPO phenyl ring at 8.1 – 8.3 ppm. Because A has to be equal to B, we obtained E as $E = S - 2B$.

Here we make two assumptions, which will be justified later on: (1) the decomposition is a first-order reaction and (2) other side reactions such as bialkyl termination (see Scheme A1-1) are unimportant. Then, since $E + D = E_0$, where E_0 is the concentration of active (adduct) molecules at $t = 0$, we may write

$$\ln[E/(E + D)] = -k_{dec}t \qquad (1)$$

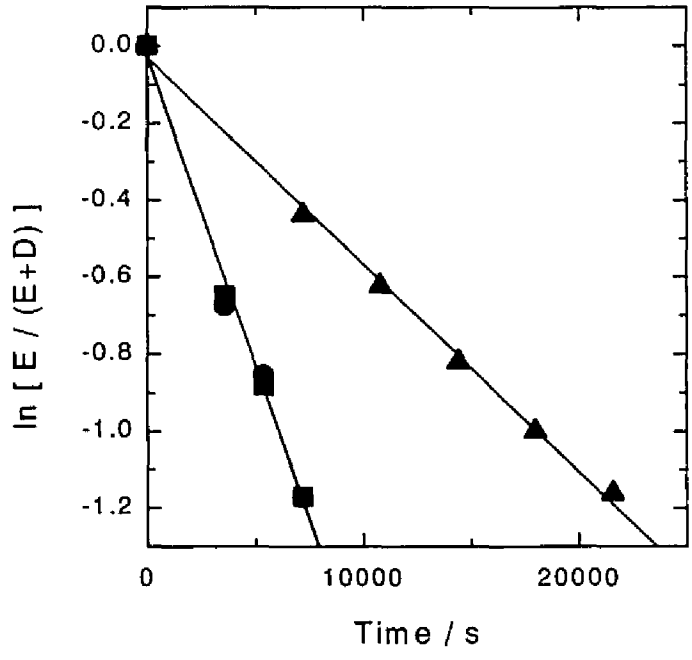

Figure A1-3. Plot of ln $[E/(E+D)]$ vs t for the decomposition experiment at 160 °C: (■) PS-TEMPO; (●) PS-TEMPO containing 1.8 mM of TEMPO; (▲) BS-TEMPO. The lines shown are the best least-squares linear fits.

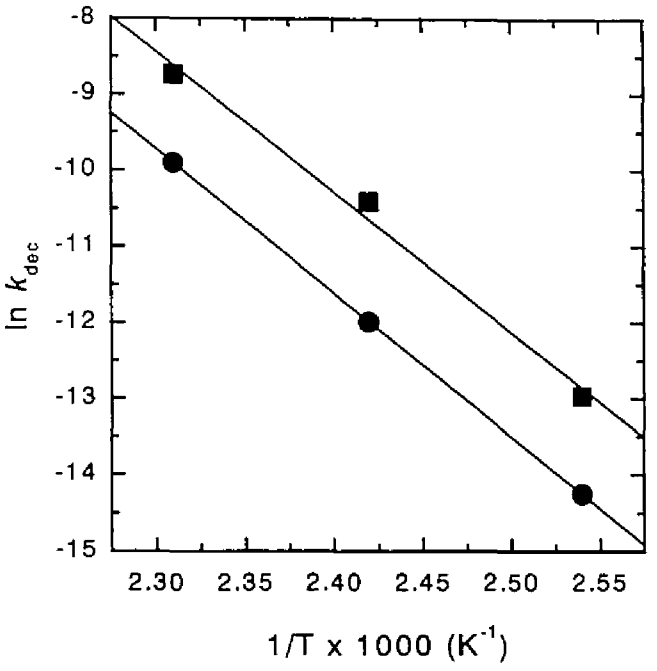

Figure A1-4. Arrhenius plots of k_{dec}: (■) PS-TEMPO; (●) BS-TEMPO.

Figure A1-3 shows the plot of $\ln[E/(E + D)]$ vs t for BS-TEMPO and PS-TEMPO at 160 °C. In each case, the data points fall on a straight line, from which a well-defined value of k_{dec} can be obtained.

Figure A1-4 shows the Arrhenius plots of k_{dec} thus determined at three different temperatures. The straight lines read

$$k_{dec} = A_{dec}\exp(-E_{dec}/RT) \qquad (2)$$

with

$$A_{dec} = 4.7 \times 10^{14}\ s^{-1} \quad E_{dec} = 157\ kJ\ mol^{-1} \qquad \text{(BS-TEMPO)} \qquad (3)$$

and

$$A_{dec} = 5.7 \times 10^{14}\ s^{-1} \quad E_{dec} = 153\ kJ\ mol^{-1} \qquad \text{(PS-TEMPO)} \qquad (4)$$

Regarding this analysis, several points may need discussion. It would be reasonable to consider that the β-proton abstraction occurs competitively with the alkyl–nitroxyl dissociation as well as combination. The chances of abstraction at the two stages would be essentially equal and usually small compared with the frequencies of dissociation and combination. Since, in the absence of other side reactions, a dissociation is necessarily followed by a combination, the proton abstraction or decomposition has to be first order in the adduct concentration, like the dissociation is. The nitroxyl concentration just controls the "transient" lifetime τ_l of the alkyl radicals,[5] but not the frequency of decomposition. In fact, if we add (free) TEMPO molecules to the PS-TEMPO system, we observe no change in k_{dec}, as Figure A1-3 shows. Thus the first assumption given above is justified.

The alkyl–alkyl termination, if any occurs, is believed to have no important influence on these results. According to a computer simulation[6] based on the known kinetic data of the PS-TEMPO system,[5,7] the termination occurs at an appreciable rate only at an early stage of thermal treatment, because free TEMPO molecules, rapidly accumulating in the system due to the termination, make the radical lifetime τ_l shorter and shorter or its concentration lower and lower as time elapses. As a result, the total amount of bimolecularly terminated species is estimated to be much less than 10 % of the originally active molecules in all studied cases. The above-mentioned result that the addition of free TEMPO has no influence on k_{dec} indicates also that the termination is unimportant here.

On the other hand, the rate of alkyl–alkyl termination in the BS-TEMPO system may not be so small. The extra peaks at around 2.9 and 4.5 ppm observable in Figure A1-2b can be assigned to dimerized 2-(benzoyloxy)-1-phenylethyl. The production rate of this compound is similar to that of 2,3-diphenylbutane in the S-TEMPO system started with the same adduct concentration of 0.080 mol/L (cf. Figure 1 in ref 3). In the case presented in Figure A1-2b, about 19 % of the original adduct has gone to the dimer after 6 h of the heat treatment, while 56 % has changed to the unsaturated compound. Nevertheless, it can be confirmed that the presented results of analysis are correct as a remarkably good approximation owing to the mathematical structure of eq 1. The analysis based on this equation is admirably insensitive to impurities present from the onset and/or produced afterward. This is the main reason why we have adopted this analysis. The alkyl–alkyl termination in the PS-TEMPO system should occur at a much lower level, since the initial adduct concentration is half that in the BS-TEMPO and

S-TEMPO systems (hence the chance of bialkyl reaction is 1/4) and since polymer–polymer reactions should be slower than those between low-mass radicals. This has been confirmed by the computer simulation mentioned above.

As already implied, the decomposition reaction is first order in the adduct concentration, and the rate constant k_{dec} may be properly written

$$k_{dec} = p_{dec}\, k_d \qquad (5)$$

where k_d is the rate constant of dissociation and p_{dec} is a probability factor ($p_{dec} << 1$, usually). Combination of the present result for k_{dec} (eqs 2 and 4) with the previous one for the dissociation rate constant,[5] $k_d = 2.0 \times 10^{13} \exp(-124200/RT)$, allows us to write

$$p_{dec} = 29 \exp(-29000/RT) \qquad (7)$$

Namely, the activation energy of the β-proton abstraction is estimated to be 29 kJ mol^{-1}.

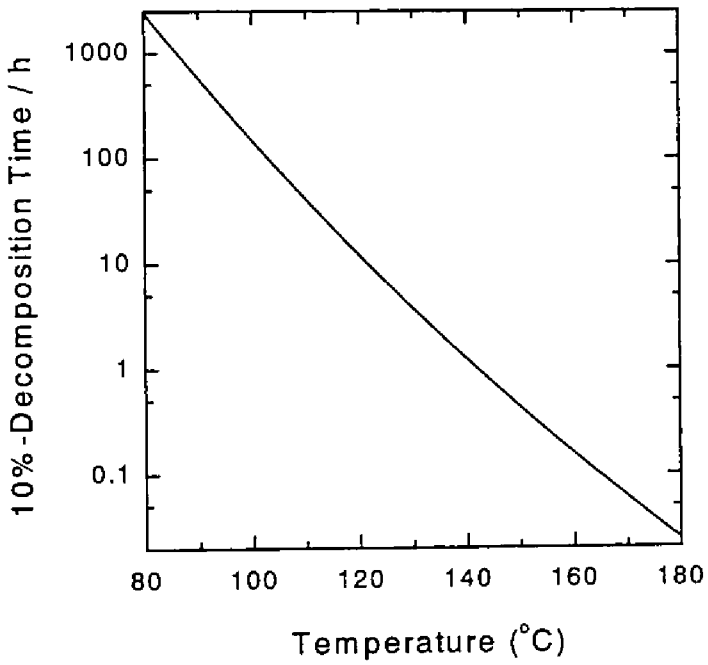

Figure A1-5. 10% Decomposition time of PS-TEMPO as a function of temperature (in toluene).

A1-4. Conclusions. We have determined the decomposition rate constants of the two model compounds BS-TEMPO and PS-TEMPO. The results indicate that in the TEMPO-mediated polymerization of styrene, the decomposition of the active chain-ends would occur less seriously than implied by the experiments with S-TEMPO[3] but still at an important level especially at high temperatures. For reference, Figure A1-5 gives the times required for PS-TEMPO to decompose by 10 % at various temperatures. These results should be important for designing polymerization processes and predicting product characteristics.[6] However, it should be stressed that these results refer to the reactions in the particular solvent. In the presence of the monomer or other solvent, results can be different.

References

(1) (a) Solomon, D. H.; Rizzardo, E.; Cacioli, P. U.S Pat. 4,581,429, March 27, 1985. (b) Rizzardo, E. *Chem. Aust.* **1987**, *54*, 32. (c) Johnson, C. H. J.; Moad, G.; Solomon, D. H.; Spurling, T. H.; Vearing, D. J. *Aust. J. Chem.* **1990**, *43*, 1215. (d) Georges, M. K.; Veregin, R. P. N.; Kazmaier, P. M.; Hamer, G. K. *Macromolecules* **1993**, *26*, 2987. (e) Georges, M. K.; Veregin, R. P. N.; Kazmaier, P. M.; Hamer, G. K. *Trends Polym. Sci.* **1994**, *2*, 66. (f) Greszta, D.; Mardare, D.; Matyjaszewski, K. *Macromolecules* **1994**, *27*, 638. (g) Matyjaszewski, K.; Gaynor, S.; Greszta, D.; Mardare, D.; Shigemoto, T. *J. Phys. Org. Chem.* **1995**, *8*, 306. (h) Hawker, C. J. *J. Am. Chem. Soc.* **1994**, *116*, 11185. (i) Hawker, C. J.; Hedrick, J. L. *Macromolecules* **1995**, *28*, 2993. (j) Catala, J. M.; Bubel, F.; Hammouch, S. O. *Macromolecules* **1995**, *28*, 8441. (k) Fukuda, T.; Terauchi, T.; Goto, A.; Tsujii, Y.; Miyamoto, T.; Shimizu, Y. *Macromolecules* **1996**, *29*, 3050.

(2) Veregin, R. P. N.; Odell, P. G.; Michalak, L. M.; Georges, M. K. *Macromolecules* **1996**, *29*, 2746.

(3) Li, I.; Howell, B. A.; Matyjaszewski, K.; Shigemoto, T.; Smith, P. B.; Priddy, D. B. *Macromolecules* **1995**, *28*, 6692.

(4) Matyjaszewski and coworkers have confirmed this reaction, using a polystyryl adduct with TEMPO: Greszta, D.; Matyjaszewski, K. *Macromolecules* **1996**, *29*, 7661.

(5) Goto, A.; Terauchi, T.; Fukuda, T.; Miyamoto, T. *Polym. Prepr., Jpn.* **1996**, *45*, 1261.

(6) Tsujii, Y.; Fukuda, T.; Miyamoto, T. *Polym. Prepr. (Am. Chem. Soc., Div. Polym. Chem.)* **1997**, *38(1)*, 657.

(7) Fukuda, T.; Terauchi T.; Goto, A.; Ohno, K.; Tsujii, Y.; Miyamoto, T.; Kobatake, S.; Yamada, B. *Macromolecules* **1996**, *29*, 6393.

A2. Activation Process in Atom Transfer Radical Polymerization

A2-1. Introduction. Controlled/"living" radical polymerization techniques have attracted much attention as new and robust synthetic routes to well-defined polymers.[1] Mechanistically, they are commonly based on an alternating activation–deactivation process in which the potentially active (dormant) species P-X is reversibly transformed to the active species (polymer radical) P* or vice versa by thermal, photochemical and/or chemical stimuli:

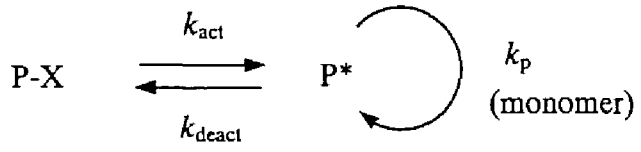

(1)

Here k_p is the rate constant of propagation, and k_{act} and k_{deact} are those of activation and deactivation, respectively, with a reaction order dependent on mechanistic details. When necessary, the reaction order will be specified by a numerical subscript: for example, $k_{1,act}$ denotes that the activation reaction is, or is viewed as, first-order, and $k_{2,deact}$ implies that the overall order of deactivation reaction is second-order or so assumed. Two general methods to determine $k_{1,act}$ have been proposed and applied to nitroxide-mediated and iodide-mediated systems to disclose the mechanistic details of these techniques of "living" radical polymerization.[2,3]

In the atom transfer radical polymerization (ATRP) in which a copper(I) complex, Cu(I)X/2L (X = Cl or Br, and L = 4,4'-disubstituted-2,2'-bipyridine, for example), is used as an activator,[4]

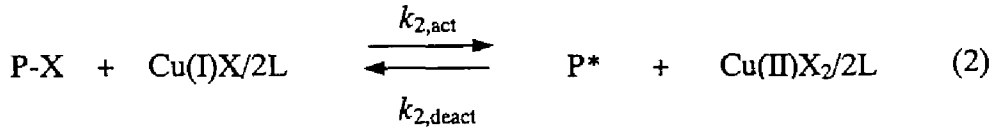

(2)

the $k_{1,act}$ defined as above would take the form

$$k_{1,act} = k_{2,act}\,[\mathrm{Cu(I)X/2L}] \qquad (3)$$

where $k_{2,act}$ is the second-order rate constant. As has been reported,[4] the homogeneous ATRP of styrene can yield polymers with predetermined degrees of polymerization up to DP ≈ 100 and

polydispersity indices, M_w/M_n, as low as 1.04 – 1.05 from an early stage of polymerization. Since an essential requirement for a low polydispersity in such a system is a sufficiently large number of activation–deactivation cycles,[3,5] the reported result indicates that the magnitude of $k_{1,act}$ of the ATRP system is exceptionally large. In what follows, we have confirmed this by directly measuring $k_{1,act}$ by the GPC (gel permeation chromatography) curve-resolution method.[2] At the same time, this work presents experimental evidence for the mechanistic scheme given by eq 2.

A2-2. Experimental Section. A polystyryl bromide (PS-Br) was prepared by the homogeneous ATRP.[4] According to the PS-calibrated GPC (see below), it has a number-average molecular weight M_n of 1400 and a M_w/M_n ratio of 1.06. This PS-Br will be used as a model adduct P_0-X. A chain-extension test has demonstrated that about 6 % of the chains are potentially inactive without a halogen atom at the end (Figure A2-1). Styrene and *tert*-butyl hydroperoxide (BHP) were purified by fractional distillation. Cu(I)Br (99.999 %, Aldrich) was used without further purification.

In a typical run, a Schlenk flask was charged with a predetermined amount of Cu(I)Br/2L (in this work, L = 4,4'-di-*n*-heptyl-2,2'-bipyridine), to which 4 mL of styrene

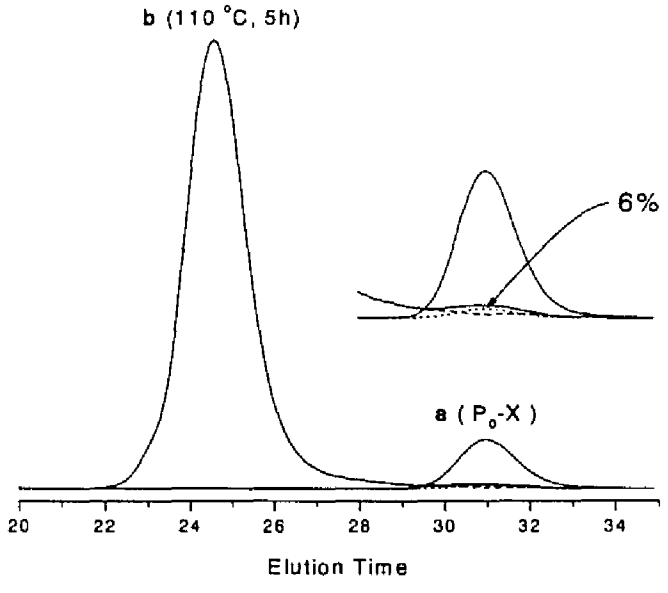

Figure A2-1. GPC elution curves for (a) the PS-Br adduct P_0-X and (b) the product obtained after a long enough (t = 5 h) polymerization of styrene "initiated" with P_0-X ($[PS\text{-}Br]_0$ = 35 mmol L^{-1} and $[Cu(I)Br/2L]_0$ = 80 mmol L^{-1}). The tail part of curve b contains about 6 % of P_0-X remaining unreacted, which means that P_0-X originally contains this much of potentially inactive species.

solution with BHP (20 mmol L^{-1}) and P_0-X (12 mmol L^{-1}) dissolved in advance was quickly added, and the flask with a glass stopper was immediately attached to a vacuum line, followed by three cycles of evacuation and dry-argon introduction. The system was then kept at 110 °C and stirred magnetically. After a prescribed time t, an aliquot (0.1 mL) of the solution was taken out by a syringe and quenched to room temperature, and a known amount of the solution was injected to a GPC apparatus for a quantitative analysis.

The GPC analysis was made on a Tosoh GPC-8020 high-speed liquid chromatograph equipped with Tosoh gel column G2500H, G3000H, and G4000H. Tetrahydrofuran (THF) was used as eluent, and temperature was maintained at 40 °C. Sample detection and quantification were made with a Tosoh differential refractometer RI-8020 calibrated with a known concentration of THF solution of P_0-X adduct.

A2-3. Results and Discussion. The direct method for determining $k_{1,act}$ used here is based on the GPC observation of an early stage of the polymerization "initiated" with a probe adduct P_0-X:[2] when P_0-X is activated via the halogen atom transfer to Cu(I)Br/2L, the resulting P_0* radical will take up monomer unit(s) and then be deactivated by Cu(II)Br_2/2L to give a new adduct P_1-X, where the subscript 1 denotes one redox cycle. Hence P_0-X may be distinguishable from P_1-X (or any other species possibly produced in the system) by GPC, owing to the difference in molecular weight and its distribution. Then $k_{1,act}$ may be determined according to the first-order plot:

$$\ln (S_0 / S) = k_{1,act} t \qquad (4)$$

where S_0 and S are the concentrations or the peak areas of P_0-X at times 0 and t, respectively.

Accurate resolution of the GPC curve into the mentioned two components requires that a sufficiently large number of monomer units be added to the polymer radical during one activation–deactivation (redox) cycle. To meet this requirement, the ratio of [Cu(I)Br/2L] to [P_0-X] was greatly reduced (usually,[4] this ratio is set to unity), and a small amount of the radical initiator BHP, which has a long half-life time at the reaction temperature, was added. Such radical initiators have been found to play the expected role of an accelerator in nitroxide systems.[2,3a,6]

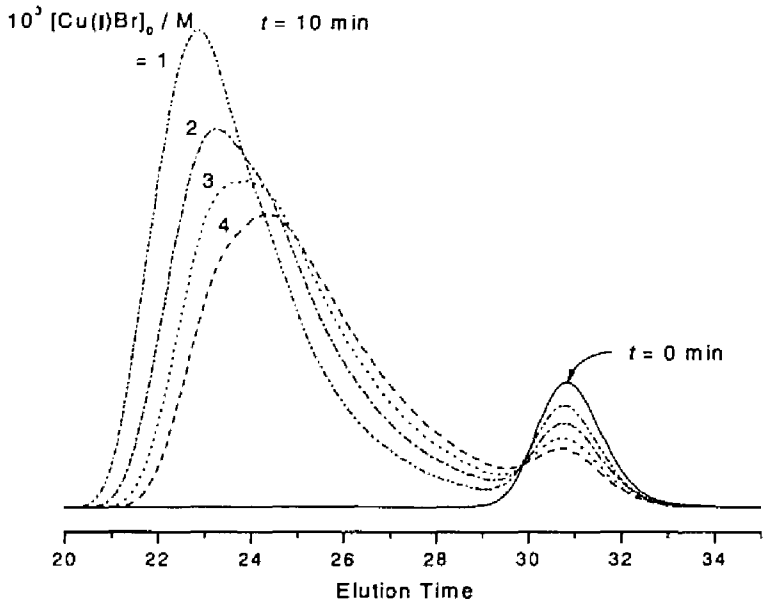

Figure A2-2. GPC charts for the PS-Br (P_0-X)/styrene/BHP mixture with different Cu(I)Br/2L concentrations heated at 110 °C for 10 min: $[P_0\text{-X}]_0$ = 12 mmol L^{-1}; $[BHP]_0$ = 20 mmol L^{-1}; $[Cu(I)Br/2L]_0$ = 1, 2, 3, and 4 mmol L^{-1}.

Figure A2-2 shows the GPC traces of the reaction mixtures with various concentrations of Cu(I)Br/2L, heated at 110 °C for 10 min. All curves are clearly bimodal with a lower-molecular weight component corresponding to the unactivated adduct P_0-X and a higher-molecular weight one composed of the grown chain P_1-X and other minor species possibly produced by a further activation of P_1-X, decomposition of BHP, and so on. The devolution of the P_0-X concentration with time is shown in Figure A2-3 in a first-order plot. At all examined concentrations of Cu(I)Br/2L, a straight line was obtained. Since P_0-X originally contains about 6 % of potentially inactive species (cf. Figure A2-1), it has been corrected by subtracting $0.06S_0$ from both S_0 and S in eq 4. Clearly, an increase in the concentration of Cu(I)Br/2L makes the slope of the straight line or the value of $k_{1,act}$ larger.

Figure A2-4 shows the plot of thus determined $k_{1,act}$ against $[Cu(I)Br]_0$. The data points form a straight line passing through the origin, and $k_{2,act}$ can be estimated to be 0.45 L mol^{-1} s^{-1} according to eq 3. Here we have assumed that the equilibrium concentration [Cu(I)Br] is equal to the initial one $[Cu(I)Br]_0$. This is justified as follows: the radical concentration is estimated to be ≈ 2.0 x 10^{-8} mol L^{-1} from the plot of $\ln([M]_0/[M])$ vs t (data not shown), where [M] is the monomer concentration. The equilibrium constant K (= [P*][Cu(II)Br_2/2L]/[P-X][Cu(I)Br/2L]) of 3.9 x 10^{-8} estimated by Matyjaszewski et al.[4b] suggests that [Cu(I)Br] is

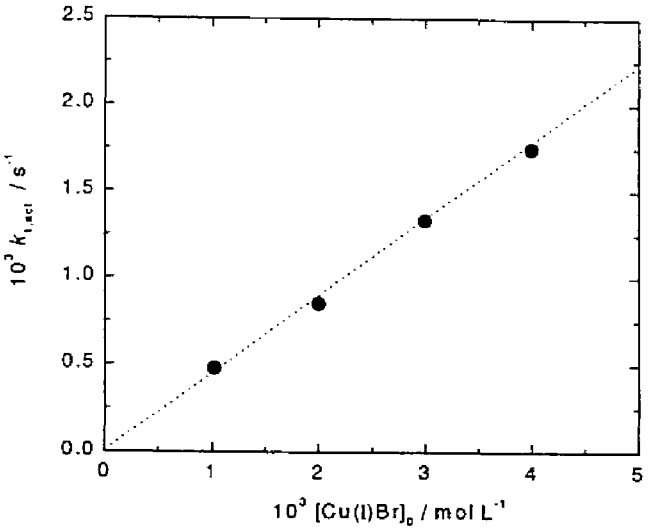

Figure A2-4. Plot of $k_{1,act}$ vs [Cu(I)Br/2L]$_0$: data from Figure A2-3. The slope of the straight line gives: $k_{2,act}$ = 0.45 L mol^{-1} s^{-1}.

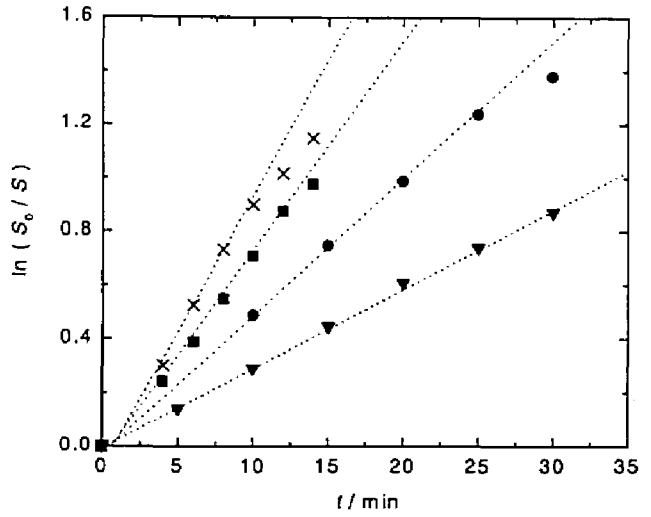

Figure A2-3. Plot of ln(S_0 / S) vs t for the PS-Br activated by cuprous halide complex at 110 °C: [Cu(I)Br/2L]$_0$ = 1 (▼), 2 (●), 3 (■), and 4 (×) mmol L^{-1}.

smaller than the initial value only by approximately 5 %, which is negligibly small compared with other experimental errors. Also importantly, the straight line passing through the origin, given in Figure A2-4, suggests that the degenerative transfer reaction[7] is negligible in this system. Also notably, the above cited value[4b] of the equilibrium constant $K = k_{2,act}/k_{2,deact}$ of 3.9 x 10^{-8} combined with the $k_{2,act}$ value of 0.45 L mol^{-1} s^{-1} gives $k_{2,deact}$ = 1.1 x 10^{-7} L mol^{-1} s^{-1}.

A2-4. Conclusions. The second-order activation rate constant $k_{2,act}$ in cuprous bromide-mediated ATRP at 110 °C was determined by the GPC peak-resolution method to be 0.45 L mol^{-1} s^{-1}. This $k_{2,act}$ value combined with a typical Cu(I)Br concentration of 0.1 mol L^{-1} gives a $k_{1,act}$ value of 0.045 s^{-1}, i.e., a PS-Br adduct is activated once every 22 s. This figure is much smaller than, e.g., the $k_{1,act}^{-1}$ value of 45 min for a PS-TEMPO (2,2,6,6-tetramethylpiperidinyl-1-oxy) adduct at the same temperature,[2b] and explains why the ATRP system provides low-polydispersity polymers *from an earlier stage of polymerization.*[4]

References

(1) For recent reviews, see: (a) Georges, M. K.; Veregin, R. P. N.; Kazmaier, P. M.; Hamer, G. K. *Trends Polym. Sci.* **1994**, *2*, 66. (b) Moad, G.; Solomon, D. H. *The Chemistry of Free Radical Polymerization*; Pergamon: Oxford, U. K., **1995**, p 335. (c) Davis, T. P.; Haddleton, D. M. In *New Methods of Polymer Synthesis*; Ebdon, J. R.; Eastmond, G. C., Eds.; Blackie: Glasgow, U. K., **1995**; Vol. 2, p 1. (d) Matyjaszewski, K.; Gaynor, S.; Greszta, D.; Mardare, D.; Shigemoto, T. *J. Phys. Org. Chem.* **1995**, *8*, 306. (e) Davis, T. P.; Kukulj, D.; Haddleton, D. M.; Maloney, D. R. *Trends Polym. Sci.* **1995**, *3*, 365. (f) Hawker, C. J. *Trends Polym. Sci.* **1996**, *4*, 183. (g) Sawamoto, M.; Kamigaito, M. *Trends Polym. Sci.* **1996**, *4*, 371. (h) Matyjaszewsi, K., Ed. *Controlled Radical Polymerization*; ACS Symposium Series 685; American Chemical Society: Washington, DC, 1998.

(2) (a) Goto, A.; Fukuda, T. *Macromolecules* **1997**, *30*, 5183. (b) Goto, A.; Terauchi, T.; Fukuda, T.; Miyamoto, T. *Macromol. Rapid Commun.* **1997**, *18*, 673. (c) Goto, A.; Ohno, K.; Fukuda, T. *Macromolecules* **1998**, *31*, 2809.

(3) (a) Goto, A.; Fukuda, T. *Macromolecules* **1997**, *30*, 4272. (b) Fukuda, T.; Goto, A. *Macromol. Rapid Commun.* **1997**, *18*, 682: the factor – 2 appearing in eq 4 in ref 3b is a misprint for $C - 2$.

(4) (a) Patten, T. E.; Xia, J.; Abernathy, T.; Matyjaszewski, K. *Science* **1996**, *272*, 866. (b) Matyjaszewski, K.; Patten, T. E.; Xia, J. *J. Am. Chem. Soc.* **1997**, *119*, 674.

(5) Matyjaszewski, K. *Macromol. Symp.* **1996**, *111*, 47.

(6) Greszta, D.; Matyjaszewski, K. *J. Polym. Sci., Part A: Polym. Chem.* **1997**, *35*, 1857.

(7) (a) Matyjaszewski, K.; Gaynor, S.; Wang, J. S. *Macromolecules* **1995**, *28*, 2093. (b) Gaynor, S.; Wang, J. S.; Matyjaszewski, K. *Macromolecules* **1995**, *28*, 8051.

Summary

In **Chapter 1**, a glucose-carrying monomer (2-(methacryloyloxy)ethyl-α-*D*-glucopyranoside, MEGlc) was polymerized by using a lipophilic radical initiator. The obtained amphiphile formed a stable liposome by mixing with *L*-α-dipalmitoylphosphatidylcholine (DPPC) or di(*trans,trans*-2,4-octadecadienoyl)phosphatidylcholine (DDPC, polymerized by UV-irradiation after preparation of liposome), and the interaction of sugar moieties of the amphiphile with a lectin at liquid-lipid and solid-lipid interfaces was investigated by the turbidimetry and the multiple internal reflection fluorescence (MIRF) method, respectively. The rate of binding of the sugar-carrying liposome to the surface modified with the lectin was smaller than the theoretical value for a simple collision and strongly dependent on both weight percent of the sugar lipid in the liposome and the degree of polymerization of MEGlc.

In **Chapter 2**, a galactose-carrying monomer (2-(methacryloyloxy)ethyl-β-*D*-galactopyranoside, MEGal) was polymerized by using a lipophilic radical initiator. The amphiphile obtained formed a liposome by mixing with bis(*trans,trans*-2,4-octadecadienoyl)phosphatidylcholine (DDPC), and the obtained liposome was physically stabilized by the polymerization of DDPC by UV irradiation. The enzymatic treatment of the galactose-carrying liposomes with galactose oxidase resulted in the formation of aldehyde groups on the liposome surface. By the subsequent mixing of the liposome suspension with the amino-group carrying liposome suspension, a rapid increase in turbidity was observed due to the formation of Schiff bases between the aldehyde groups and amino groups at the interface of the liposomes. The rate of turbidity change strongly depended on the degree of polymerization of MEGal, the surface densities of galactose and amino groups on the liposome, the distance from the liposome surface to amino end groups, and the flexibility and deformability of the liposomes.

In **Chapter 3**, a galactose-carrying vinyl monomer (2-(methacryloyloxy)ethyl-β-*D*-galactopyranoside, MEGal) was polymerized by using a lipophilic radical initiator. The obtained amphiphiles (DODA-PMEGal) formed stable liposomes by mixing with phospholipids, and the galactose residues on the liposome surface were effectively recognized and oxidized by galactose oxidase. The affinity (estimated by the $1/K_m$ value) of galactose oxidase for the galactose residues on the liposomes was higher than those for free galactose and MEGal, and dependent on the length of galactose-carrying polymer chains on the liposome

surface and the fluidity of the membranes, whereas not significantly influenced by the surface density of galactose residues on the liposomes. The affinity of galactose oxidase for the galactose-carrying linear polymers, which were prepared by using an ordinary azo-type radical initiator and a chain transfer reagent, was also higher than those for free galactose and MEGal, and dependent on the degree of polymerization of MEGal. The affinity was, however, relatively much smaller than those for DODA-PMEGals incorporated in liposomes.

In **Chapter 4**, the first synthesis of a well-defined glycopolymer by free radical polymerization was described. *N*-(*p*-vinylbenzyl)-[*O*-*β*-*D*-galactopyranosyl-(1→4)]-*D*-gluconamide (VLA), a styrene derivative with an oligosaccharide moiety, was polymerized in *N,N*-dimethylformamide solution at 90 °C by the nitroxide-mediated free radical polymerization technique. Acetylated VLA gave polymers with a molecular weight from about 2000 to 40000, an M_w/M_n ratio of about 1.1 in all cases, and a conversion of up to about 90 %, where M_w and M_n are the weight- and number-average molecular weights. Indispensable for this success were (1) the use of di-*tert*-butyl nitroxide (DBN) rather than other nitroxides like TEMPO, (2) the acetylation of VLA, and (3) the use of a radical initiator DCP (dicumyl peroxide) as an accelerator. DBN provided a well-controlled polymerization of VLA at 90 °C (VLA becomes unstable at higher temperatures, e.g., > 120 °C). The acetylation effectively prevented the chain transfer that leads to dead polymers and broad polydispersities. DCP remarkably accelerated the rate of polymerization (the rate of chain extension), which otherwise was impractically slow, without causing any appreciable broadening of polydispersity.

In **Chapter 5**, controlled free radical polymerization of a sugar-carrying acrylate, 3-*O*-acryloyl-1,2:5,6-di-*O*-isopropylidene-α-*D*-glucofuranoside (AIpGlc), was achieved in *p*-xylene at 100 °C by using a di-*tert*-butyl nitroxide (DBN)-based alkoxyamine as an initiator and dicumyl peroxide (DCP) as an accelerator. The polymerization gave low-polydispersity ($1.2 < M_w/M_n < 1.6$) polymers with predicted molecular weights. The same approach with a DBN-capped polystyrene (PS-DBN) as an initiator afforded block copolymers of the type PS-*b*-PAIpGlc. The acidolysis of the homopolymers and block copolymers gave well-defined glucose-carrying polymers PAGlc and PS-*b*-PAGlc, respectively. These amphiphilic PS-*b*-PAGlc block copolymers were observed to exhibit microdomain surface morphologies, which differed for different copolymer compositions. This success opens up a novel route to the synthesis of well-defined sugar-carrying polymers of various architectures.

In **Chapter 6**, controlled free radical polymerization of sugar-carrying methacrylate, 3-*O*-methacryloyl-1,2:5,6-di-*O*-isopropylidene-*D*-glucofuranose (MAIpGlc) was achieved by the atom transfer radical polymerization (ATRP) technique with an alkyl halide/copper-complex system in veratrole at 80 °C. The time-conversion first-order plot was linear and the number-average molecular weight increased in direct proportion to the ratio of the monomer conversion to the initial initiator concentration, providing PMAIpGlc with a low polydispersity. The sequential addition of the two monomers styrene (S) and MAIpGlc afforded a block copolymer of the type PS-*b*-PMAIpGlc. The acidolysis of the homo- and block copolymers gave well-defined glucose-carrying water-soluble polymers PMAGlc and PS-*b*-PMAGlc, respectively. The amphiphilic PS-*b*-PMAGlc block copolymer exhibited a microdomain surface morphology with spherical PS domains in a PMAGlc matrix.

In **Chapter 7**, controlled free radical polymerization of *N*-(*p*-vinylbenzyl)-2,3,5,6-tetra-*O*-acetyl-4-*O*-(2,3,4,6-tetra-*O*-acetyl-*β*-*D*-galactopyranosyl)-*D*-gluconamide (Ac-VLA) was achieved by the nitroxide-mediated free radical polymerization technique with a lipophilic alkoxyamine "initiator" with a dioctadecyl group in 1,2-dichloroethane at 90 °C. The polymerization proceeded in a "living" fashion, providing Ac-VLA polymers with a low-polydispersity. The hydrolysis of the polymers gave well-defined glycopolymer-carrying amphiphiles, viz., artificial "glycolipids", the mixing of which with a phospholipid gave a stable liposome. The galactose residues on the liposome were confirmed to be specifically and effectively recognized by a lectin (RCA).

In **Appendix**, kinetics of thermal decomposition of a polymer-nitroxyl adduct and kinetics of the activation process in an atom transfer radical polymerization were described.

List of Publications

Chapter 1.

(1) Sugar-Containing Lipids Prepared by Using a Lipophilic Radical Initiator: Interfacial Recognition by Lectin As Studied by Using the Multiple Internal Fluorescence Reflection Method.
Kitano, H.; **Ohno, K.** *Langmuir* **1994**, *10*, 4131–4135.

Chapter 2.

(2) Galactose-Containing Amphiphiles Prepared with a Lipophilic Radical Initiator: Association Processes between Liposomes Triggered by Enzymatic Reaction.
Ohno, K.; Sohda, K.; Kosaka, A.; Kitano, H. *Bioconjugate Chem.* **1995**, *6*, 361–366.

Chapter 3.

(3) Catalytic Properties of Galactose Oxidase to Liposome-Forming Amphiphiles Which Have Many Pendent Galactose Residues
Ohno, K.; Kitano, H. *Bioconjugate Chem.* **1998**, *9*, 548–554.

Chapter 4.

(4) Synthesis of a Well-Defined Glycopolymer by Nitroxide-Controlled Free Radical Polymerization
Ohno, K.; Tsuji, Y.; Miyamoto, T.; Fukuda, T.; Goto, M.; Kobayashi, K.; Akaike, T. *Macromolecules* **1998**, *31*, 1064–1069.

Chapter 5.

(5) Nitroxide-Controlled Free Radical Polymerization of a Sugar-Carrying Acryloyl Monomer
Ohno, K.; Izu, Y.; Yamamoto, S.; Miyamoto, T.; Fukuda, T. *Macromol. Chem. Phys.*, submitted.

Chapter 6.

(6) Synthesis of a Well-Defined Glycopolymer by Atom Transfer Radical Polymerization
Ohno, K.; Tsujii, Y.; Fukuda, T. *J. Polym. Sci., Part A: Polym. Chem.* **1998**, *36*, 2473–2481.

Chapter 7.

(7) Free Radical Polymerization of a Sugar Residue-Carrying Styryl Monomer with a Lipophilic Alkoxyamine Initiator: Synthesis of a Well-Defined Novel Glycolipid
Ohno, K.; Fukuda, T.; Kitano, H. *Macromol. Chem. Phys.* **1998**, *199*, 2193–2197.

Other associated publications.

(8) Interfacial Recognition of Sugars by Novel Boronic Acid-Carrying Amphiphiles Prepared with a Lipophilic Radical Initiator
Kitano, H.; Kuwayama, M.; Kanayama, N.; **Ohno, K.** *Langmuir* **1998**, *14*, 165–170.

(9) Mechanism and Kinetics of Nitroxide-Controlled Free Radical Polymerization. Thermal Decomposition of 2,2,6,6-Tetramethyl-1-polystyroxypiperidines
Ohno, K.; Tsujii, Y.; Fukuda, T. *Macromolecules* **1997**, *30*, 2503–2506.

(10) Nitroxide-Controlled Free Radical Polymerization of *p-tert*-Butoxystyrene. Kinetics and Applications
Ohno, K.; Ejaz, M.; Fukuda, T.; Miyamoto, T.; Shimizu, Y. *Macromol. Chem. Phys.* **1998**, *199*, 291–297.

(11) Kinetics Study on the Activation Process in an Atom Transfer Radical Polymerization
Ohno, K.; Goto, A.; Fukuda, T.; Xia, J.; Matyjaszewski, K. *Macromolecules* **1998**, *31*, 2699–2701.

(12) Synthesis of a Well-Defined Anthracene-Labeled Polystyrene by Atom Transfer Radical Polymerization
Ohno, K.; Fujimoto, K.; Tsujii, Y.; Fukuda, T. *Polymer* **1999**, *40*, 759–763.

(13) Mechanisms and Kinetics of Nitroxide-Controlled Free Radical Polymerization
Fukuda, T.; Terauchi, T.; Goto, A.; **Ohno, K.**; Tsujii, Y.; Miyamoto, T.; Kobatake, S.; Yamada, B. *Macromolecules* **1996**, *29*, 6393–6398.

(14) Mechanism and Kinetics of Nitroxide-Controlled Free Radical Polymerization
Fukuda, T.; Goto, A.; **Ohno, K.**; Tsujii, Y. In *"Controlled Free Radical Polymerization"*; Matyjaszewski, K., Ed.: American Chemical Society: Washington, DC, 1998; Chapter 11.

(15) Mechanism and Kinetics of Iodide-Medicated Polymerization of Styrene
Goto, A.; **Ohno, K.**; Fukuda, T. *Macromolecules* **1998**, *31*, 2809–2814.

(16) Controlled Graft Polymerization of Methyl Methacrylate on Silicon Substrate by the Combined Use of the Langmuir-Blodgett and Atom Transfer Radical Polymerization Techiniques
Ejaz, M.; Yamamoto, S.; **Ohno, K.**; Tsujii, Y.; Fukuda, T. *Macromolecules* **1998**, *31*, 5934–5936.

(17) Synthesis of Novel Types of Polymers by Living Radical Polymerization Techniques
Ohno, K.; Fukuda, T. *Polymer Applications* **1998**, *47*, 419–425.

Acknowledgements

The present investigations were carried out at the Department of Chemical and Biochemical Engineering, Toyama University in the period from 1993 to 1996, and at the Institute for Chemical Research, Kyoto University in the period from 1996 to 1998.

The author would like to express his sincere gratitude: to Professor Takeaki Miyamoto for his continuous comments and encouragement throughout this work; to Professor Hiromi Kitano for his invaluable guidance, criticisms and encouragement.

Grateful acknowledgement is due to Associate Professor Takeshi Fukuda for his enthusiastic guidance, valuable discussion and encouragement. The author is sincerely grateful to Dr. Yoshinobu Tsujii for his helpful and valuable discussions and comments.

The author wishes to express his appreciation: to Drs. Nobuo Donkai and Masahiko Minoda for their useful suggestions; to all of his colleagues in Professor Miyamoto's Laboratory and Professor Kitano's Laboratory for their kind help.

Finally, the author wishes to express his heartfelt thanks to his mother, Chieko Ohno and his brother, Hiroki Ohno for their continuous encouragement.

November, 1998

Kohji Ohno